5-2015

Investigating Polymer based Scaffolds for Urinary Bladder Tissue Engineering

Srikanth Sivaraman
Clemson University, sri.rules@gmail.com

Follow this and additional works at: https://tigerprints.clemson.edu/all_dissertations

Part of the Polymer Science Commons

INVESTIGATING POLYMER BASED SCAFFOLDS FOR URINARY BLADDER
TISSUE ENGINEERING

A Dissertation
Presented to
the Graduate School of
Clemson University

In Partial Fulfillment
of the Requirements for the Degree
Doctor of Philosophy
Bioengineering

by
Srikanth Sivaraman
May 2015

Accepted by:
Dr. Jiro Nagatomi, Committee Chair
Dr. Ken Webb
Dr. Naren Vyavahare
Dr. J Todd Purves

ABSTRACT

The urinary bladder is a musculomembranous sac which functions as a short term reservoir for the urine produced in the kidneys. Various diseases including congenital malformations (e.g., myelomeningocele) and postnatal diseases (e.g., bladder cancer) of the lower urinary tract affect approximately 400 million people worldwide. Current surgical treatments for these disorders rely on the use of autologous intestinal segments and xenografts such as small intestinal submucosa, which suffer from various complications including mechanical mismatch and graft shrinkage. Tissue engineering approaches have been explored where the urinary bladder has been successfully engineered in-vitro and implanted in humans by Atala and colleagues who reported successful outcomes implanting collagen-PGA based tissue engineered neo-bladders in both dogs and humans. However, Phase II clinical trials of the same approach by Tengion Inc. using the autologous cell-seeded collagen-PGA/PLGA scaffold for patients suffering from neuropathic bladders demonstrated multiple adverse events such as bowel obstruction and bladder rupture, without improving capacity or compliance which resulted in discontinuation of the study. Although the exact reason for this failure is still unknown, flaws in scaffold mechanical properties and design as well as the use of autologous cells from the diseased bladder may need to be reevaluated. Also, a recent comprehensive review of bladder tissue engineering studies suggests that the technology needs further improvement and evaluation through animal models of bladder dysfunction. Therefore, the objective of this doctoral dissertation was to characterize a viable bladder tissue scaffold (patch) which mimics the mechanical properties of the bladder, maintains the phenotype

of the BSMC seeded in it and finally, tested *in vivo* in a dysfunctional bladder model to evaluate its true efficacy.

In pursuit of this goal, firstly we explored the use of composite hydrogel blends composed of Tetronic (BASF) 1107-acrylate (T1107A) in combination with extracellular matrix (ECM) moieties collagen and hyaluronic acid seeded with bladder smooth muscle cells (BSMC). The results of in vitro experiments demonstrated that the composite hydrogel system provided an environment for bladder smooth muscle cells to adhere, migrate and secrete ECM, thereby increasing the construct's overall strength and stiffness.

Second, we characterized various biodegradable elastomers as scaffolds for bladder tissue engineering since the mechanical properties of our cell-seeded composite hydrogels were limited after two weeks of culture. The comparison of mechanical behaviors of these elastomeric scaffolds demonstrated that the PCUU scaffolds mimicked urinary bladder mechanics more closely than PGS-PCL and PEUU. The PCUU scaffolds exhibit relatively high compliance under low forces and are able to withstand stress corresponding to 100 kPa (super physiological peak stress experienced by urinary bladders *in vivo*) and thus, possess the strength and stiffness necessary to be used as a urinary bladder tissue engineering scaffold. The PCUU scaffolds also showed cyto-compatibility as well as increased porosity with increasing stretch indicating its ability to aid in infiltration of smooth muscle cells.

Thirdly, the BSMC-seeded PCUU scaffold was subjected to uniaxial mechanical stretch mimicking bladder cycling using our custom-made bioreactor under standard cell

culture conditions (37 °C, humidified, 5% CO2 / 95% air). When subjected to uniform and continuous uniaxial stretch (1.25-1.75), the BSMC-seeded PCUU scaffolds did not undergo permanent deformation in spite of high stretch and indicated its suitability to be used *in vivo*. We demonstrated that coating the PCUU scaffolds with fibronectin and gelatin using the layer-by-layer method enhanced BSMC adhesion and infiltration into the scaffold, which was necessary for continued adhesion of the BSMC under mechanical stretch. The study has completed calibration of the custom bioreactor for future studies to characterize the *in vitro* response of BSMC seeded on PCUU scaffolds to conditions mimicking bladder cycling.

Finally, we attempted at implanting the PCUU scaffolds onto a bladder outlet obstruction (BOO) rat model to create a clinically informative study. The BOO bladders tend to exhibit overactive bladder symptoms with high pressure and voiding frequency and, if untreated, could often lead to death of the rats due to vesicoureteral reflex. The PCUU augmentation led to the enhanced survival of the rats (66.66%) and increased bladder capacity and voiding volume with time, indicating that the high-pressure bladder symptom was alleviated. The histological analysis of the explanted scaffold indicated some smooth muscle cell and connective tissue infiltration, but also calcium deposits. We hypothesize that ECM-coating and pre-seeding PCUU scaffolds with cells can aid in promoting faster scaffold integration into the host bladder. Due to inherent tendency of stone formation in rat models, future studies may switch to using dysfunctional bladder models of larger animal like pigs. However, the present study is one of the first to analyze

a synthetic bladder scaffold using a bladder dysfunction model in rats for application in urinary bladder tissue engineering.

In summary, the present study characterized composite hydrogel and elastomeric scaffolds for bladder tissue engineering applications. Based on the results of *in vitro* mechanical characterization and cell culture studies, we concluded that PCUU scaffolds was most relevant scaffold for bladder tissue engineering among the ones we examined. For the first time, we used an established rat model for studying bladder dysfunction (BOO) to evaluate the effect of augmentation of the bladder with PCUU scaffolds on bladder capacity and voiding volume. The knowledge gained in the present study will work towards future improvement of bladder tissue engineering technology to ultimately aide in the treatment of bladder disorders.

ACKNOWLEDGEMENTS

TABLE OF CONTENTS

Chapter 1: Introduction and Background

Chapter 2: Rationale and Specific Aims

Chapter 3: Tetronic®-based Composite Hydrogel scaffolds seeded with Rat-Bladder

Smooth Muscle Cells for Urinary Bladder Tissue Engineering Applications

Table of Contents (Continued) Page

Table of Contents (Continued)   Page

LIST OF FIGURES

LIST OF TABLES

Chapter 1

INTRODUCTION AND BACKGROUND

Urinary Bladder Anatomy

The urinary bladder is a hollow, distensible musculomembranous sac that lies in the pelvic cavity just posterior to the symphysis pubis (1, 2). It functions as a short-term reservoir for the urine produced by the kidneys. Under normal conditions, the human bladder has a capacity to store approximately 500 ml of urine although progressive sensation of fullness and desire to void are experienced when the volume reaches around 300ml. As it fills the bladder expands up to fifteen times its contracted size assuming an ovoid shape. During voluntary micturition, smooth muscle of the bladder contracts while sphincter muscles of the urethra relax to allow releasing of the content.

The bladder wall tissue is composed of four distinct layers, namely the urothelium, lamina propria, detrusor, and serosal layer (Figure 1-1). The mean bladder wall thickness measured from the urothelium to serosa in adult humans is approximately 3.3 ± 1.1 mm for males and 3.0 ± 1 mm for females, respectively (3). The unique features of the bladder, the large capacity and high compliance, are due to the highly specialized properties of the urothelial lining and the smooth muscle wall of the bladder (4).

Urothelium

The urothelium is a specialized type of epithelium called the transitional epithelium. The cells in the layer have the ability to slide past one another and the number of cell layers decreases as the volume of the urinary bladder increases (2). The

urothelium plays a major role in maintaining the composition of urine akin to that generated by the kidneys. This is achieved via four unique features of the urothelium. First, the tissue offers a minimum surface area to urine for passive permeability of substances between blood and lumen. Second, the passive permeability of the tight junction between cells and apical cell membrane to electrolytes and non-electrolytes is also very low. Third, hormonally regulated absorptive system of the urothelium regulates sodium absorption to counter the passive movement of sodium from blood to urine. Last, all of these permeability properties of the urothelium are unaffected by most substances found in blood or urine, and, thus, the composition of urine stays constant (5).
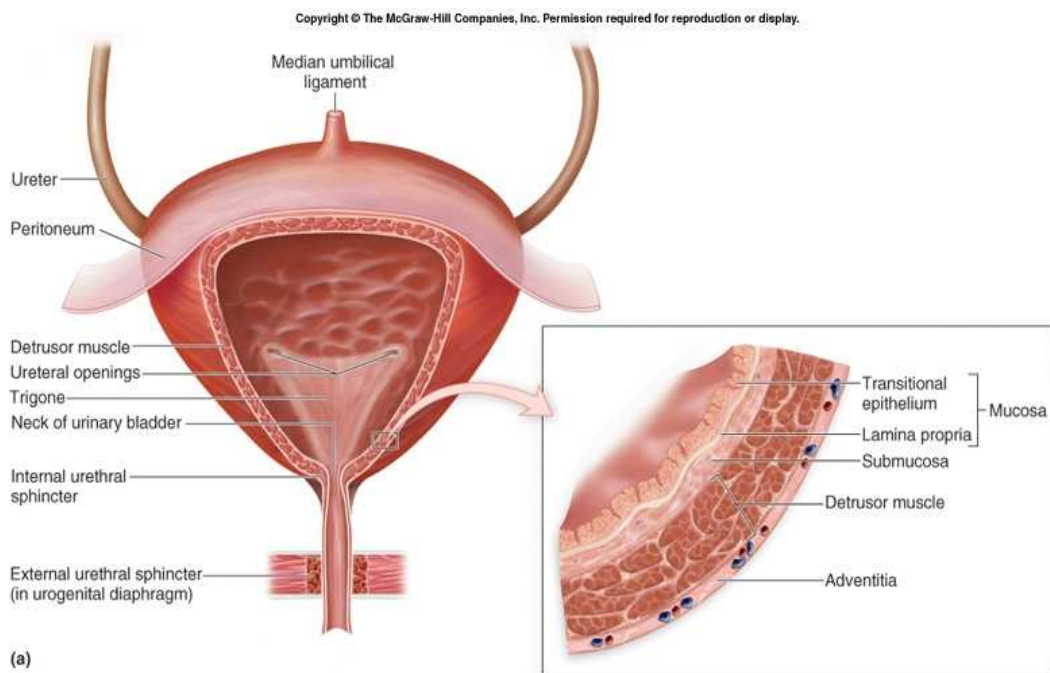
Figure 1-1: Tissue layers of the urinary bladder.

Lamina Propria

Lamina propria is a collagenous connective tissue (4) that functions to maintain the shape of bladder wall and to limit its overall compliance (ratio of maximum volume divided by pressure). This layer is approximately 1.3 mm thick in humans and supports various cell types, and the entire bundle of capillary network is embedded in it (4). The lamina propria is composed mainly of dense irregular connective tissue, fibroblasts, and a thin smooth muscle muscularis mucosa (6) .

Detrusor and Serosal Layers

The detrusor muscle layer plays a major role in the voiding of urine by contraction (7). Detrusor wall thickness in humans is approximately 1.4 mm for males and 1.2 mm for females (8). This layer is mainly composed of coarse bundles of smooth muscle fibers (9), (10). The muscle fibers form branching, interlacing bundles loosely arranged into inner longitudinal, middle circular, and outer longitudinal layers(11) . However, in the upper aspect of the bladder, these layers are clearly not separable, and any one fiber can travel between each of the layers, change orientation, and branch into longitudinal and circular fibers. This meshwork of detrusor muscle is ideally suited for emptying the spherical bladder (11). The individual smooth muscle fibers in these bundles run parallel to one another and are generally 1-2 μm in diameter. The muscle bundles have a diameter of 50–150 μm and the interfascicular space between the bundles is usually between 20-50 μm. Within the interfascicular space, capillaries and larger blood vessels are observed (9).The detrusor layer is surrounded by the serosal layer,

which is a dense layer of fine collagen fibrils that are straight and uniform and are not interspersed with blood vessels (4, 9).

Pathological Conditions of the Urinary Bladder Requiring Repair and Reconstruction

Approximately 400 million people worldwide are affected by various diseases of the urinary bladder that require repair and reconstruction (12). This figure includes, but is not limited to, congenital malformations of the lower urinary tract such as bladder exstrophy (part of the bladder is present outside the body and the pelvic bones are separated), myelomeningocele (spine does not close before birth), or posterior urethral valves (obstructing membrane in the posterior male urethra)(13). Additionally, postnatally acquired diseases such as chronic interstitial cystitis (characterized by frequent and painful urination and/or pain in the bladder and pelvic region), neurogenic bladder (characterized by difficulty in storing or voiding urine), bladder fibrosis and cancer (among the 10 most common cancers) amount to critical need of surgical replacement and repair (12).

Current treatments to congenital malfunctions and bladder fibrosis involve surgical augmentation of the bladder, which often requires a second surgery to reconstruct surrounding bones and soft tissues (11, 14-17) . In contrast, the neurogenic bladders may be initially treated with medicines to activate or relax the bladders, or through exercise to strengthen the pelvic muscles (18-20). However, if the problem becomes severe the neurogenic bladders are emptied by intermittent or permanent

catheterization and surgical approaches such as artificial sphincter, sling surgery, or electrical stimulation of the sacral nerve may be adopted (18-20). Similarly, interstitial cystitis is treated mainly via medication, and surgical interventions (e.g., supratrigonal cystectomy and cystourethrectomy) are reserved as a last resort (21). Bladder cancer, on the other hand, is routinely treated surgically with a variety of techniques such as partial or radical cystectomy in combination with radiation therapy, chemo therapy, immunotherapy depending on the patient and the stage of the disease (22, 23), (24, 25).

While a number of urological complications are surgically treated, conventional modes of treatment for bladder repair suffer from several limitations. One of the common risks for treatment of urinary bladder disorders are urinary tract infections and incontinence (14-21). Apart from that, many treatment methods suffer from specific risks: sexual dysfunction in the case of surgery for exstrophy (16, 17); meningitis, hydrocephalus and loss of bladder control in the case of surgery of myelomeningocele (15); renal failure and vesicoureteral reflex in the case of posterior urethral valve treatment (14); and chronic urine leakage and kidney damage in the case of neurogenic bladders (18-20). Treatment for bladder cancer also can lead to the risk of anemia, swelling of the ureters and urethral strictures (22-26).

Current Approaches in Bladder Repair

Currently, materials used in surgical repair to treat various complications of the urinary bladder include autografts, allografts and xenografts, which have exhibited varying successes and problems as reviewed in the following sections.

Use of Autologous Tissues in Cystoplasty

Cystoplasty is one of the most common approaches to treat patients who lack adequate bladder capacity or detrusor compliance. Abnormal compliance or decreased bladder capacity may manifest as debilitating urgency, frequency, incontinence, recurrent urinary tract infections (UTIs), pyelonephritis, or progressive renal insufficiency. For many patients, augmentation cystoplasty can provide a safe functional reservoir that allows for urinary continence and prevention of upper tract deterioration (27). These problematic bladders have been conventionally treated using segments of autologous natural tissue such as omentum, peritoneum, ureters and most commonly, a portion of the large intestine (enterocystoplasty) (28). The procedure aims to improve bladder capacity in severely contracted bladders with compliant and vascularized tissues (4). However, enterocystoplasty has been known to generate various long-term complications that include mucus production by the bowel epithelium, stone formation, bacteriuria, metabolic disturbances, malignancy, and intestinal complications (4, 26). These complications of enterocystoplasty may result from the fact that, the intestinal epithelium is neither structurally, nor physiologically adapted to prolonged exposure to urine (29).

Since the side effects of enterocystoplasty were considered due to the interaction of urine with the bowel mucosa, numerous animal model studies have been performed to expose the raw muscle surface to urine after the removal of the bowel epithelium and examined the effects of de-epithelialization (4). However, contrary to expectations, the results of these studies provided evidence of graft shrinkage and fibrosis, severe inflammation, infection, and ischemia (30) all of which underscored the importance of

epithelial tissue. Although complete elimination of these problems was not achieved, two major studies using a porcine model have demonstrated so far that fibrosis and shrinkage of the implanted grafts were minimized by covering the augmenting graft with autologous human urothelium (31, 32). The first study used autologous urothelial cells isolated at hemicystectomy and sprayed onto demucosalised colon, which was then incorporated into the remaining bladder. After 6 weeks, the presence of uroplakin-positive urothelium was observed on top of a bladder or colonic smooth muscle submucosa and no inflammation was described (31). In another study, in vitro–propagated autologous urothelial cells were implanted onto a vascularised, de-epithelialized uterine tissue used as the augmenting segment in a "composite cystoplasty" (32). However, there was evidence of stromal inflammation within both augmented and native segments along with incomplete urothelialisation leading to poor urinary barrier properties. Based on these findings, the authors hypothesized that implanting "differentiated" urothelium would lead to rapid establishment of an effective urinary barrier and would provide the stroma with immediate protection form urine-mediated damage (32). However, enterocystoplasty as a technique still suffers from problems such as substantial graft shrinkage, and, thus, alternatives are being sought to replace this technique.

Another approach of bladder repair using the patient's own tissue is ureterocystoplasty, which exploits the use of urothelium derived either from a grossly dilated ureter or from the bladder itself after excising the overlying detrusor muscle (33). While it is a clinically proven concept and the use of autologous urothelial tissues can

eliminate many, if not all, of the complications associated with enterocystoplasty, this approach is confined to a small minority of patients with gross ureteric dilatation. Moreover, studies have demonstrated that it is not suited to small or trabeculated bladders, which are commonly encountered in neuropathic dysfunction (33), (29). These shortcomings of the currently available techniques of cystoplasty have led clinicians and researchers to turn to alternative biomaterials (e.g., free tissue grafts and decellularized matrices) for bladder repair.

Free Tissue Graft

A free tissue graft is a section of tissue detached from its blood supply, moved to another part of the body, and reattached by microsurgery to a new blood supply (34). This is unlike cystoplasty described above, which retain its own blood supply during transfer to site of repair. A number of attempts have been made to incorporate various types of free human tissues including muscle flaps, split skin grafts, placenta, peritoneum, and dural membrane into the bladder in the form of patches (4). The results to date have been mixed, ranging from graft contraction and stone formation to hair growth on grafts derived from skin (4).

Muscle Flap as Bladder Wall Substitute

An animal model study compared rectus abdominis and musculo-peritoneal (rectus abdominis with overlying peritoneum) flaps used as urinary bladder wall substitutes in rats (35).The quality of urothelium and smooth muscle layer regenerated

with the detrusor myectomy (incorporation of skeletal muscle) was similar in both groups at the end of six and ninety days indicating that the rectus abdominis muscle alone sufficed as a matrix for the bladder wall. Although both cases presented urolithiasis, this was attributed to the non-absorbable sutures used in the surgery and to the rat model which is prone to stone formation.

The efficacy of detrusor myectomy was also demonstrated by another study using a canine model of hematuria and stranguria, which revealed that when the rectus abdominis muscle flap was surgically sutured to the defective bladder; the dog maintained normal health and showed no signs of urinary incontinence even after a period of two and a half years (36). Neither caliculi nor stricture or scarring was visible in the abdominal radiographs (36). Though the study was based on only one specimen, the study shows promise and further research to confirm these findings would aid in the use of rectus abdominis muscle flap for bladder repair purposes.

hAM

The Human amniotic membrane (hAM) is an avascular tissue that forms the inner layer of the fetal membranes (37). Since hAM is normally disposed of after parturition it can be readily available for research use with few ethical concerns. To determine the efficacy, bladder augmentation in rats using hAM was performed and the results were compared after 3 and 6 months post-operatively (37). Rats that received partial cystectomy with primary closure without an implant served as the control. The authors reported that the hAM-reconstructed bladder wall displayed all three major (mucosal,

9

muscular, and serosal) layers of the bladder wall as well as nerve fibers although nerve and smooth muscle bundles were sparser and smaller compared to control groups. In addition, very few inflammatory cells were observed after 3 months, suggesting the absence of rejection. While no obvious graft shrinkage was observed, bladder calculi were found in 8 of the 18 rats (44%) in the hAM group at 6 months (37). When tested in vitro, regenerated bladder strips exhibited noticeable contractile responses to a muscarinic receptor agonist and to electrical field stimulation. The contractile responses by hAM bladder strips were, however, very low compared to those of the control bladder strips even after six months indicating immature tissue development. Although hAM exhibits a number of positive features, the use of hAM as a bladder tissue substitute is very limited since it cannot be mass-produced or obtained in an off-the shelf manner for all cases.

Decellularized Matrices

SIS

Decellularized xenogeneic or allogeneic matrices prepared from the submucosa of small intestine and bladders have been tested in the surgical treatment of the urinary bladder and other tissues (29). Small intestinal submucosa (SIS) is a collagenous membrane derived from porcine small intestines (Figure 1-2) which was first described by Badylak et al. (38).The tunica mucosa, serosa and tunica muscularis are mechanically removed from the inner and outer surfaces of the intestinal wall to leave a 0.1-mm collagen-rich membrane largely composed of the submucosal layer (39). The early

studies demonstrated that, when incorporated in the urinary bladder of rats, SIS allowed not only rapid cellular encroachment and infiltration, but also vascularization and re-innervation (40). SIS degrades completely in the body within a period of four to eight weeks and its byproducts are excreted via the urine (41). Although the bladder repairing approach using SIS allowed post-surgical regeneration of tissue that exhibited all three layers of the normal bladder (41), several unwanted outcomes have been noted. For example, when implanted in dogs the regenerated bladders often exhibited a higher collagen to muscle ratio than normal bladders and its long-term clinical implications have not been fully understood (41).These SIS-based bladder grafts have also shown fibrosis and reduced smooth muscle contraction (29). Moreover, the regenerative potential of SIS was dependent on the age of the donor and the portion of the intestine from which the SIS matrices are derived (4). An animal study provided evidence that SIS derived from pigs older than 3 years old exhibited consistent bladder regenerative results compared to SIS derived from younger pigs (42). In addition, the same study revealed that bladder regeneration is more reproducible with SIS from distal segments than from proximal segments of the ileum (42).While these studies have provided valuable information and demonstrated the feasibility of decellularized matrices as a bladder repair material, these limitations have prevented SIS from being considered as an ideal implant to aid in effective bladder regeneration and remodeling.

Figure 1-2: A sheet of small intestinal submucosal scaffold.

BAM

Bladder acellular matrix graft (BAM) is another type of decellularized tissue matrix which has shown to support regeneration of the bladder in vivo. Following partial cystectomy and after 22 weeks of implantation, the BAM-augmented bladder exhibited urothelial and muscle layers with reinnervation and revascularization in porcine models (43). Histological analysis of excised BAM revealed that four major components of the extracellular matrix, type I and type IV collagen, elastin, laminin, and fibronectin were present in the matrix (44), (43) and similar results were in canine and murine models(4). Although many of the results have been positive, it has been reported that BAM also exhibit problems seen with SIS, namely, lithogenesis, graft shrinkage, and incomplete and disorganized smooth muscle infiltration (4). Moreover, despite the stringent decellularization process (with a series of hypotonic buffer solutions and various detergents), remnants of cellular components have been identified within BAM (45) , which may lead to an immunogenic reaction when implanted into the body. Thus, further

improvement in processing and pre-treatment may be necessary for BAM to be used successfully in bladder tissue regeneration.

Current Research in Bladder Tissue Engineering

Because of the various complications associated with auto-, allo-, and xeno-grafts, the alternative approaches are being sought in the direction of tissue engineering. This involves seeding appropriate autologous cells onto scaffolds to form live, implantable tissue constructs. The biomaterials used for scaffolds may be either synthetic polymers or naturally occurring materials. While synthetic polymer allows for controlling various parameters such as mechanical properties and pore architecture, natural biomaterials have many inherent advantages which include the presence of native growth factors, a naturally occurring architecture, and the presence of ubiquitous extracellular elements (45).The following subsections will review the current research in the field of bladder tissue engineering.

Clinical Success of Bladder Tissue Engineering

Since the advent of the term and concepts of tissue engineering in the early 1990's, the bladder has been one of the few organs that have been synthesized in vitro and successfully implanted. Atala and colleagues were the first group to report such seminal work on tissue engineered neo-bladders in both dogs and humans (13, 46). The biomaterial used for the scaffolds was polyglycolic acid (PGA) coated with poly-DL-lactide-co-glycolide 50:50 (PLGA) and the implant was wrapped with the hosts'

omentum (a fatty tissue layer under the peritoneum) in both cases (13, 46). Briefly, after a trigone-sparing cystectomy, one group of beagle dogs underwent closure without a reconstructive procedure; the second group underwent reconstruction with cell free scaffolds, and the third group received scaffolds seeded with autologous urothelial cells on the luminal surface and smooth muscle cells on the exterior surface. The results of this animal study clearly showed structural and functional differences among the three experimental groups 11 weeks post-surgery (46). The animals that received no implant gained a minimal increase while the non-seeded bladders exhibited a slight increase in reservoir volume over time. Although these non-seeded scaffolds developed an intact urothelial layer, the smooth muscle layer was deficient and fibrotic resulting in low compliance (46). In contrast, the cell-seeded neo-bladders exhibited capacities and compliance greater than the pre-cystectomy level (46). The retrieved tissues displayed a normal cellular organization, consisting of a trilayer of urothelium, submucosa, and muscle with innervation (46).

The group then investigated tissue engineered bladder augmentation in humans with end-stage bladder diseases needing cystoplasty (13). The study involved seven patients suffering from myelomeningocele, aged 4-19 years with high pressure or poorly compliant bladders. Urothelial and smooth muscle cells were obtained from a bladder biopsy from each patient and expanded in culture for seven weeks prior to seeding. The neo-bladder recipients were categorized based on three types of constructs; a homogenous decellularized bladder submucosa scaffold, a cell seeded collagen matrix

implant wrapped with omentum, and a collagen-PGA composite implant wrapped with omentum (Figure 1-3).
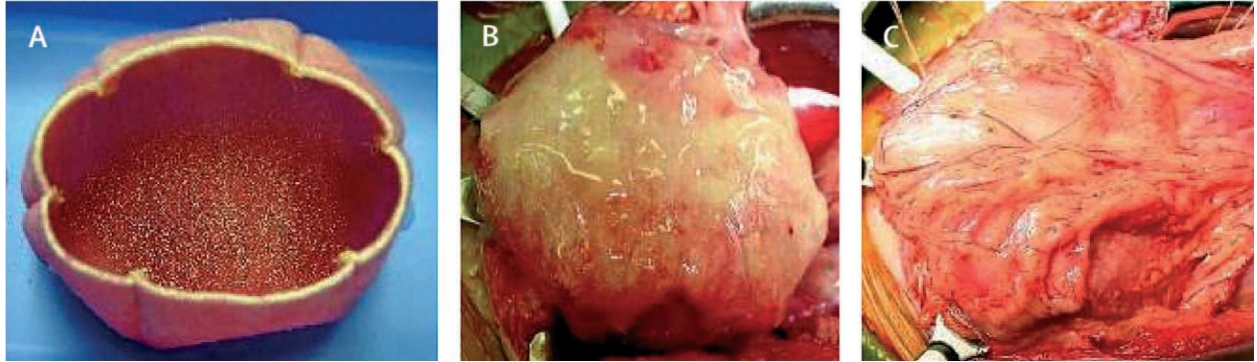
Figure 1-3: Construction of engineered bladder. Scaffold seeded with cells (B) engineered bladder anastomosed to native bladder with running 4–0 polyglycolic sutures (C) Implant covered with fibrin glue and omentum.

While all three types of bladders displayed low intravesical pressure (below 40 cm H_2O) and stable renal functions post-operatively, the collagen-PGA composite scaffolds with omentum wrapped exhibited the greatest bladder capacity and compliance (13). Moreover, immunohistochemical analyses of biopsy tissues revealed that smooth muscle and urothelial cells within the regenerated bladder constructs were phenotypically normal.
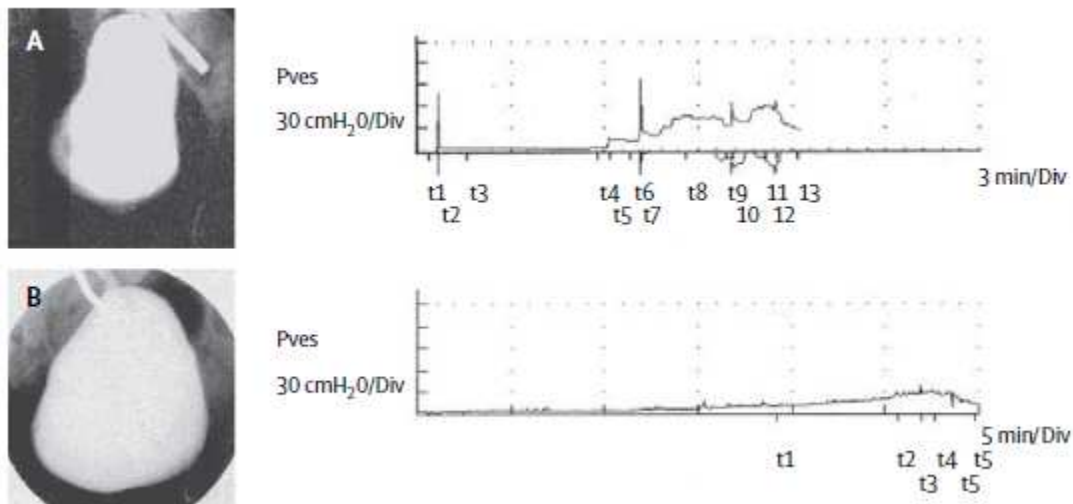
Figure 1-4: Cystograms and urodynamic findings in a patient with a collagen-PGA scaffold engineered bladder (A) Preoperative and (B) 10-month postoperative

The results of this seminal study demonstrated that the abnormally high bladder pressure before the operation clearly improved 10 months after implantation of the neo-bladder that was composed of cell-seeded collagen-PGA scaffold and the patient's omentum (Figure 1-4). Although these studies demonstrated the feasibility of bladder tissue engineering, several issues are still unresolved. For example, the success of the bladder augmentation was limited and seems to depend on the presence of omentum, which may or may not be available in all patients needing bladder replacement. Also, Studies by Eberli et al. have shown that Collagen-PGA composite scaffolds possessed twice the stiffness (Young's modulus ~0.001 MPa) compared to native bladder tissue (Young's modulus ~0.002MPa) (47).

In-Vitro Cell Studies of Cell-Biomaterial Interactions

Although initial trials of bladder tissue engineering have met with some success, a number of basic scientific questions remain unanswered. For example, the choice and designs of scaffold materials are known to influence the behavior of seeded cells, which must be carefully examined and controlled prior to implantation of the engineered tissue constructs. The following subsections review the current in vitro work on cell-biomaterial interactions.

Bladder Cell Interactions with Polyesters

To date, a number of synthetic polymers have been studied as potential scaffold materials for engineering of the urinary bladder. The advantages of these synthetic materials are that they can be manufactured rapidly in a large scale and can be processed to obtain desired levels of strength, microstructure, and degradation rate. In addition, some of the synthetic polymers (e.g., poly lactic acid (PLA), poly glycolic acid (PGA), poly (lactic-co-glycolic acid) (PLGA) and poly caprolactone (PCL)) have been approved by the US food and drug administration (FDA) for use in medical devices, and thus, do not require additional regulatory compliance assessments prior to use in clinical applications.
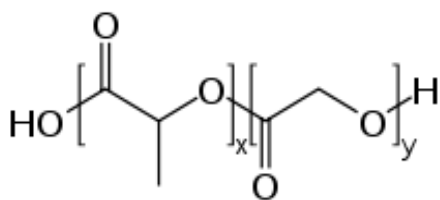
Figure 1-5: Basic structure of poly (lactic-co-glycolic acid) (PLGA). In this figure; 'X' represents the number of units of lactic acid and 'y' represents the number of units of glycolic acid.

Applicability of these polyesters to bladder tissue engineering was assessed by examining the influence of physical properties of PCL (Figure 1-6) and PLGA (Figure 1-5) films on the growth of normal human urothelial (NHU) and bladder SMC in vitro (48) ,(49). More specifically, two types (high and low elastic moduli) of PLGA and PCL films were compared with standard tissue culture plastic (control). The cell growth of both NHU and SMC on the low modulus PLGA films was greater than that on the high modulus films at 24, 48, and 72 hour time points. A similar trend was observed for the SMC growth on PCL films; a greater number of cells were present on lower modulus films at 72 hour and 7 day time points (48). Together, these results demonstrate that the elastic modulus of the scaffold material is a critical parameter for the proliferative response by the bladder cells seeded.
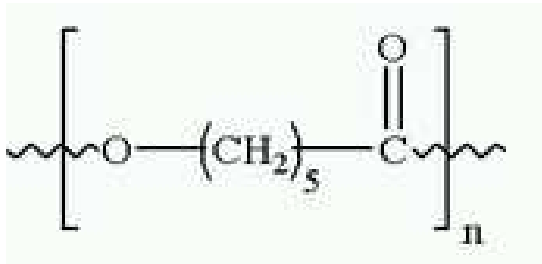
Figure 1-6: Basic structure of polycaprolactone (PCL)

The effect of mechanical properties of polyester scaffolds was further investigated in a 3-D environment by culturing human urinary tract stromal cells on PLGA and PCL foams prepared by emulsion freeze-drying (49). The stromal cells on PCL scaffolds exhibited a 4.4-fold higher attachment and 2.4-fold higher rate of proliferation compared to the stromal cells cultured on PLGA scaffolds after a period of seven days. Since the storage modulus of PCL (2MPa) is half of that of PLGA and is closer to the storage moduli value for native bladder tissue (0.25 MPa (50)) (49), the authors concluded that cell attachment and proliferation were enhanced by the high compliance nature of PCL (49). Thus, based on the results from these 2D and 3D studies, the PCL may be a better candidate material than PLGA in bladder tissue engineering applications although a number of other parameters have yet to be examined.

Bladder Cell Interactions with SIS

To demonstrate the efficacy of SIS in use for bladder augmentation, Kropp and colleagues performed a series of studies using cell-seeded and non-seeded SIS (42), (39, 51). Specifically, SIS was evaluated in-vitro after seeding it with human urothelial and smooth muscle cells (passages between 2 and 8) at a density of 1×10^5 cells per cm^2 in

five different configurations (39). The culture configurations that were evaluated were (1) urothelial cells seeded alone on the mucosal surface of SIS, (2) smooth muscle cells seeded alone on the mucosal surface, (3) layered co-culture of smooth muscle cells seeded on the mucosal surface followed by urothelial cells 1 hour later, (4) sandwich co-culture of smooth muscle cells seeded on the serosal surface followed by seeding of urothelial cells on the mucosal surface 24 hours later, and (5) mixed co-culture of urothelial cells and smooth muscle cells seeded together on the mucosal surface. Four weeks after cell seeding, it was seen that a layered and sandwich co-cultures exhibited smooth muscle cell invasion of SIS, organized cell sorting, and formation of well-defined urothelium, which were not seen with cultures of smooth muscle or urothelial cells alone (39).The mixed co-culture exhibited no evidence of cell sorting either, though it exhibited smooth muscle penetration of SIS matrix (39). Their results suggest that establishment of cell-to-cell communications between identical cell types (i.e., SMC-SMC, urothelial-urothelial) seeded as separate layers may be a requisite for formation of distinct layers in neo-bladders engineered with SIS.

Stem Cell Differentiation into SMC on PEG Hydrogel Scaffolds

Hydrogels are a class of highly hydrated polymer materials (water content > 30% by weight) which are composed of hydrophilic polymer chains. The major advantages of using hydrogels are that they can be processed under relatively mild conditions (general absence of toxic chemicals in synthesis) and have structural and mechanical properties similar to the ECM (52). One of the common hydrogels used in soft tissue engineering

applications is polyethylene glycol (PEG), which is prepared by polymerization

of ethylene oxide and is commercially available over a wide range of molecular weights

from 300 Da to 10,000 kDa (52), (53). Since PEG undergoes limited metabolism in the

body, only PEGs with molecular weight less than 50 kDa are considered in tissue

engineering application as they can be completely eliminated from the body (via the liver

and kidney)(54). PEG has many advantageous characteristics which are essential for

tissue engineering application. They are hydrolytically non-degradable polymers with

excellent solubility in water and many other organic solvents. Melting points of the

different PEG derivatives are dependent on the molecular weight of the chain and this

property can be exploited to manipulate the mechanical properties of polymers applied at

room temperature (Figure 1-7). PEG can form highly hydrated polymer coils on the

biomaterials surface which can effectively be used to repel proteins. This property can be

used to from inert polymer surfaces and non-fouling coatings to prevent bacterial growth

or cellular adhesion on biomaterial surfaces. The terminal functional groups of PEG can

be co-polymerized with various polymers and this property can also be used to

manipulate its degradability (54).
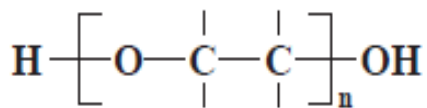
Figure 1-7: Structure of poly (ethylene glycol) (PEG).

Toward bladder tissue engineering applications, the differentiation of human

mesenchymal stem cells (MSC) cultured on 3D PEG hydrogel scaffolds into SMC-like

cells was examined by Adelow and colleagues (55). More specifically, PEG hydrogel

was modified with an adhesive peptide, arginine-glycine-aspartic acid (RGD) for stem

cell attachment and matrix metalloproteinase- (MMP-) degradable peptides for enzymatic

degradation of the matrix for cell infiltration. The human MSC from bone marrow

(300,000 cells per scaffold with 2.3 cm diameter) were seeded on the hydrogel scaffolds

Cell viability, spreading, and proliferation as well as key functional marker expression

were assessed at various time points up to 21 days after hydrogel formation. The authors

reported that both MSC and SMC within the 3D hydrogel exhibited the elongated,

spindle-like morphology indicative of the contractile phenotype after two weeks in

culture. The resulting cells in the 3D PEG hydrogels exhibited up-regulation of markers

associated with the less synthetic, but more contractile phenotype of smooth muscle cells,

and increased cell proliferation compared to cells grown in 2-D culture (55). These

results demonstrated that strategic functional regulation of bladder SMC can be achieved

using PEG hydrogel, which may serve as ideal scaffolds to regenerate bladder tissue.

Application of Nanotechnology to Bladder Tissue Engineering

Among the limitations with use of synthetic materials in bladder tissue

engineering is the mechanical property mismatch between the polymers and tissues as

well as the lack of biological recognition of polymer surface by the host cells. To address

these issues, application of nanotechnology has been proposed as it has been shown to

promote cell growth and tissue development through appropriate designing of the inner

architecture of the scaffolds (45). For example, several groups (56-58) have studied nano-structured synthetic materials as bladder tissue replacements and demonstrated that increased surface roughness (at the nanometer and submicron levels) improved the adsorption of select proteins important for bladder cell functions. In theory, the surfaces of these nanomaterials offer a favorable environment for cell growth as they mimic the natural environment of the bladder. This is because it has been reported that the extracellular matrix proteins in bladder tissue are nanodimensional (28). This idea was tested in an in vitro study that examined human smooth muscle cell function on PLGA, PCL, and polyurethane (PU) films with nanodimensional surface features in a range of 50–100 nm (created using chemical etching techniques via NaOH and HNO$_3$ soaking)(56). In comparison with the cells cultured on micron or submicron surfaces, bladder smooth muscle cells cultured on nanosurfaces exhibited greater elastin synthesis and collagen production indicating that the difference in surface textures indeed influenced bladder cell behavior (56). This was further confirmed by a study using 3D nanotextured PLGA and PU scaffolds, which also demonstrated greater elastin and collagen production by bladder smooth muscle cells compared to conventional nanosmooth polymers (57).

However, these results with bladder smooth muscle cells did not agree completely with other in vitro studies using rat PC12 adrenal medulla cells, which demonstrated that nanometer surface features alone did not influence cell proliferation, unless serum proteins are present in the cell culture media (59), (60). Taken together and applying this principle to bladder SMC, it can be hypothesized that the adsorption of select soluble

23

proteins to the substrate surface is essential for enhanced bladder smooth muscle cell function (58). To date, however, most of the studies using nano-structured materials have focused on in vitro assessment and not been subjected in vivo testing for regeneration of bladder. Further study, therefore, is needed to evaluate the true efficacy of nanotechnology in bladder tissue engineering.

Effects of Mechanical Force Stimuli on Bladder Tissue Engineering

Since the urinary bladder is subjected to different mechanical forces during filling and emptying, it has been postulated that subjecting bladder cells and cell-seeded scaffolds to relevant mechanical forces in vitro may be beneficial for bladder tissue regeneration. For example, an in-vitro study demonstrated penetration of rat bladder smooth muscle cells in SIS along with de novo synthesis of collagen and elastin by these seeded cells when the matrices were subjected to both chemical and mechanical stimuli for 2 weeks (61). Briefly, the elastin synthesis by SMC seeded on SIS was significantly greater when they were subjected to 15% cyclic stretch at a frequency of 0.1 Hz compared to the cells subjected to stretch at 0.5Hz or maintained under static conditions. In addition, collagen synthesis, cell proliferation, and migration into SIS by SMC were greater when exposed to cyclic stretch in the presence of VEGF (10 ng/ml) compared to that in the absence of VEGF (61). Although application of mechanical force and incorporation of growth factors enhanced the synthetic functions of SMC, their effects on the contractile markers remain unknown. This was addressed by another study that examined the effects of sustained tension on rat bladder SMC in 3D collagen gel culture

(62). More specifically, compared to the cells of no tension control, SMC that were subjected to sustained tension inside the collagen gel exhibited significantly greater expression of α-smooth muscle actin and elongated cell morphology, both of which indicated enhanced contractile phenotype (62). Together, the results of these studies suggest that mechanical and chemical cues may be just as important as scaffold material selection for bladder tissue engineering.

In vivo Animal Studies in Bladder Tissue Engineering
Application of SIS in tissue engineering

Motivated by the success of in-vitro results, further studies were conducted to evaluate the performance of cell-seeded vs. unseeded SIS in vivo (51). Human SMC and urothelial cells were seeded on SIS in a layered co-culture fashion and were implanted subcutaneously in nude mice (unseeded SIS was implanted as control). These grafts were then harvested at 4, 8 and 12 weeks after implantation. Evaluation of cell-seeded grafts at the 4 week time point indicated the presence of relatively fewer viable cells compared to the number of cells originally present at the time of implantation indicating substantial cell death in the initial grafting process (51) . However, the seeded SIS grafts exhibited progressively organized tissue regeneration at subsequent time points compared to unseeded SIS (51). The feasibility of cell-seeded SIS for repairing bladder defects was further investigated in a canine model of subtotal cystectomy (90% partial cystectomy) with a control group which received no augmentation (63). Unlike previous studies with smaller bladder defects, tissue regeneration was not achieved in this study with no

statistically significant difference in bladder capacity, function, or SMC regeneration among the three (seeded SIS, non-seeded SIS, and control) groups. This was mainly due to the inflammation and scarring of the remaining bladder from the cystectomy and the lack of neo-vascularization to the implanted grafts (63). These results suggest that cell-seeded SIS implant may be useful for repairing minor bladder defects, but methods to rapidly establish vascular networks into the implanted tissue would be an important requisite for improving its applicability to repairing of larger bladder defects. The various advantages of SIS including biocompatibility, degradability, and its ability to be used as an "off the shelf" bladder scaffold makes it an attractive option for bladder repair. However, there has not been an effective way to control graft shrinkage or encourage large scale bladder regeneration. Overcoming these barriers, would pave the way for SIS to be used as a scaffold for bladder tissue engineering.

Silk Fibroin Scaffold

Over the past decade, silk fibroin has been investigated as potential scaffold materials for diverse tissue engineering applications such as bone, cartilage, ligament and skin (64) mainly because of its exceptional combination of high tensile strength and elasticity (65) Recently, using a murine model of bladder augmentation, Mauney et al. investigated the utility of gel spun silk fibroin scaffolds in bladder tissue engineering applications. After 70 days of implantation, the tubular shaped, non-cell seeded, silk fibroin scaffolds showed regeneration of smooth muscle and urothelial layers along with evidence of substantial de novo ECM deposition with no signs of scaffold degradation.

Cystometric analyses revealed that the voided urine volume and overall capacity of the augmented bladders were comparable to those of the non-surgical control animals after 70 days. The augmented bladder, however, exhibited a mild, acute inflammatory reaction and high voiding frequency, which was presumably attributed to incomplete urothelial maturation (66). Though silk fibroin has been known to elicit minimal inflammatory response due to its presence in the human body, the absence of scaffold degradation even after 70 days is a matter of concern. Further studies to characterize degradation of the scaffold would help in deciding the fate of the polymer in bladder tissue engineering studies.

Poly (lactic-co-glycolic acid) (PLGA)

Several in vivo studies have been performed to study the efficacy of cell-seeded PLGA scaffolds toward bladder tissue engineering applications. For example, human adipose-derived stem cells (ASC) were seeded on a PLGA scaffold designed to replicate the tissue architecture of the native bladder and cell differentiation was examined in vitro and in vivo in a rat model (67). Specifically, the luminal surface of the construct was made from a thin layer of malleable and non-porous PLGA microfibers, which were tightly woven to keep the urine from permeating the graft yet strong enough to hold solid sutures without tearing. A thicker, 95% porous PLGA sponge was added to the outer surface of the composite to provide a greater surface area for ASC seeding and to aid host cell penetration and vascularization when implanted in adult female Rnu athymic rats. Unseeded PLGA scaffolds and suture closed scaffolds were prepared identically as controls. The authors reported that ASCs differentiated into smooth muscle cells within

the cell-seeded bladder constructs after 12 weeks, which were evidenced by expression of molecular markers such as α-actin, calponin, caldesmon and smooth muscle myosin heavy chain (MHC) (67). In addition, the ASC-seeded bladder constructs maintained viability *in vivo* and exhibited greater *ex vivo* contractility, compliance, and smooth muscle mass compared to the control bladder constructs after 12 weeks of implantation. However, the regenerated bladder in all the animals displayed signs of bladder calculi (67), which must be addressed and avoided in future studies. Moreover, the results that the acellular controls also formed a tissue structure similar to that of ASC-seeded constructs suggest that the contribution of ASC to the regeneration of the bladder has to be carefully evaluated. These results are highly encouraging and demonstrated the potential of PLGA as an appropriate scaffold that support bladder regeneration and induce ASC differentiation into SMC. However, further studies using larger animal models are necessary to demonstrate the true efficacy of the PLGA scaffolds in bladder tissue regeneration.

Collagen Gel Scaffolds

Collagen (especially types1 and 4) is one of the major components of the extracellular matrix (ECM) and contains various cell adhesion domains important for maintaining native phenotype and activity of cells (68). It is readily purified from various animal tissue sources via enzyme treatment and salt/acid extraction; purified collagen products have been approved by the US Food and Drug Administration (FDA) for multiple medical applications (69). Most collagen scaffolds used in bladder tissue

engineering are in the form of hydrogels and studies have shown cell compatibility,

normal urothelium growth, and retention of contractile phenotype of SMC in collagen

gels (70). One of the major problems associated with collagen hydrogels, however, is its

mechanical strength that is not adequate for tissue wall reconstruction. For this reason,

plastic compressed (PC) collagen gels have been proposed as a novel method to improve

the mechanical properties of neo-tissues (71). PC collagen constructs were made by a

simple and fast method and yield controllable mesoscale structures. Briefly, collagen gel

(pre-seeded with SMC and UC) was sandwiched between two nylon meshes placed on

top of a stainless steel mesh and filter paper and loaded with a 50g flat plastic block for 5

min at room temperature (Figure 1-8).
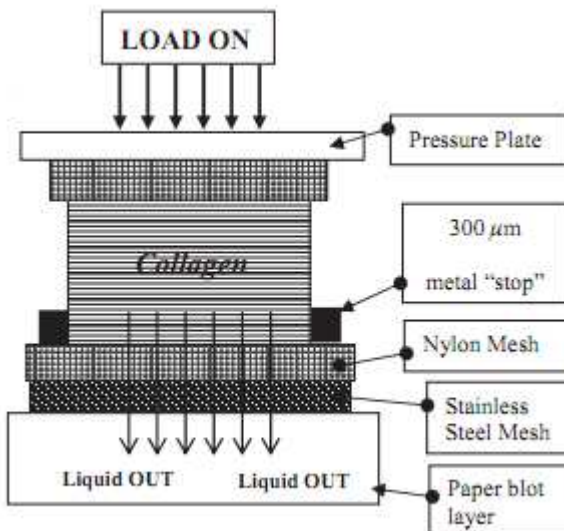
Figure 1-8: Routine assembly for plastic compression of pre-formed collagen gels.

The compression led to the expulsion of over 95% of the water contained within the gel and formation of a 20-40µm thick flat collagen sheet with viable cells inside. Although PC collagen scaffolds supported cell growth for two weeks and exhibited greater tensile properties compared to uncompressed collagen gels, the gels were not strong enough to withstand suturing and handling in ultimate clinical use (69). It was, thus, necessary to improve upon these limitations by combining PC collagen gels with biodegradable synthetic meshes composed of poly (lactic acid-co-ε-caprolactone) (PLAC) (72). PLAC was chosen as it was a slow degrading, elastic polymer and could provide the appropriate mechanical strength. The hybrid scaffolds were prepared by placing PLAC meshes between two layers of neutralized collagen gels, which were then subjected to plastic compression. The scaffolds were subjected to in-vitro analysis to determine cell phenotype, distribution, and proliferation over a period of 14 days. Furthermore, the PC collagen-PLAC hybrid scaffolds were implanted subcutaneously in adult Swiss nude mice for up to 24 weeks to determine their biocompatibility. The results of the in-vitro tests demonstrated that human SMCs and UC's embedded together in the hybrid scaffold proliferated well on the outer surface and interior of the scaffold by 14 days. The specimens supported a maximum force of 33.62 ± 5.69 N before rupture. This force level corresponds to a pressure of 571 cmH$_2$O indicating that the hybrid scaffold strong enough to withstand internal bladder pressures (40-60 cmH$_2$O in adults during bladder contraction) (72). The in-vivo studies provided evidence of neutrophil and macrophage infiltration into the hybrid scaffold as early as 2 days after implantation, which subsided after 28 days indicating a resolution of inflammation. However, a rise in

the presence of immune cells such as macrophages and foreign body giant cells was noted in the PC collagen-PLAC hybrid scaffolds after 24 weeks of subcutaneous implantation. It was speculated that the degradation products of the PLAC mesh caused a rise in inflammation reaction. The in-vivo studies also indicated near absence of SMC and UC activity in the hybrid scaffolds after 28 days (72). Although the in-vitro results were highly promising, the hybrid scaffolds in the current form do not seem to support cell growth and are susceptible to inflammation in vivo. Addressing these long-term, host response issues through strategic designing of polymer materials would certainly increase the utility of the hybrid scaffolds in bladder tissue engineering.

Based on the results of the studies to date, future studies in bladder tissue engineering should specifically focus on two major issues: (1) improving the strength and compliance of the material to support the bladder's main functions to store the urine (while maintaining low pressure) for a considerable period of time, and to withstand internal bladder pressures (40-60 cmH$_2$O in adults during bladder contraction) during voiding; and (2) maintaining the contractile phenotype of the SMC (associated with increased compliance of the smooth muscle layer) in the scaffold so as to prevent fibrosis (associated with synthetic phenotype).

Chapter 2

RATIONALE AND SPECIFIC AIMS

Various diseases including congenital malformations (e.g., myelomeningocele) and postnatal diseases (e.g., bladder cancer) of the lower urinary tract affect approximately 400 million people worldwide (12). Current surgical treatments for these disorders rely on the use of autologous intestinal segments and xenografts such as small intestinal submucosa, which suffer from various complications including mechanical mismatch and graft shrinkage (73). Atala and colleagues reported successful outcomes implanting collagen-PGA based tissue engineered neo-bladders in both dogs and humans (13, 46). However, Phase II clinical trials of the same approach using the autologous cell-seeded collagen-PGA/PLGA scaffold for patients suffering from neuropathic bladders demonstrated multiple adverse events such as bowel obstruction and bladder rupture, without improving capacity or compliance (74) which resulted in discontinuation of the study. Although the exact reason for this failure is still unknown, flaws in scaffold mechanical properties and design as well as the use of autologous cells from the diseased bladder may need to be reevaluated (74). For successful urinary bladder tissue engineering, further studies are necessary. Based on the results of the studies to date, the objective of this doctoral dissertation was to characterize various scaffold biomaterials seeded with bladder smooth muscle cells, which would mimic the mechanical properties of the bladder for tissue engineering applications.

The Specific aims of the present research were as follows:

AIM 1: In vitro characterization of composite hydrogel scaffolds for application in bladder tissue engineering

Approaches: Tetronic (BASF) 1107-acrylate (T1107-A) in combination with ECM moieties, collagen and hyaluronic acid were tested in this application. BSMC were encapsulated in the composite scaffolds and cell morphology, collagen production as well as mechanical properties of the cellular hydrogels constructs were examined.

AIM 2: In vitro characterization of biodegradable elastomers for application in bladder tissue engineering

Approach: Uni-axial and bi-axial tensile tests and pressure-volume tests of the scaffolds were performed to quantify the ability of the scaffolds to withstand tension and pressure. Immuno-staining of the BSMC seeded on scaffolds were also performed to confirm cytocompatibility of the elastomers.

AIM 3: Conditioning of the BSMC seeded scaffold using a custom-made bioreactor

Approach: BSMC seeded on PCUU scaffolds were subjected to sustained tension by our custom-made bioreactor to determine the effect of tension on BSMC.

AIM 4: Pilot *in vivo* study for bladder augmentation in bladder outlet obstruction (BOO) induced rats

Approach: PCUU scaffolds will be augmented into a BOO rat bladder for a period of three weeks to characterize cellular infiltration, bladder capacity and voiding volume.

With the completion of these aims, we expect to advance our knowledge in the field of

bladder tissue engineering specifically related to mechanical characterization of scaffolds

and augmentation of these scaffolds in diseased bladder models.

Chapter 3

TETRONIC®-BASED COMPOSITE HYDROGEL SCAFFOLDS SEEDED WITH

RAT-BLADDER SMOOTH MUSCLE CELLS FOR URINARY BLADDER

TISSUE ENGINEERING APPLICATIONS

Introduction

Bladder augmentation has been conventionally performed using autologous

natural tissue such as a portion of the intestine (enterocystoplasty) (28) to treat patients

who lack sufficient bladder capacity or detrusor compliance (73). However,

enterocystoplasty can generate long-term complications, including mucus production by

bowel epithelium, stone formation, malignancy and bacteriuria (4, 26). Other tissue grafts

such as skeletal muscle flaps (35) and human amniotic membrane (37) have limitations

including lithogenesis and immature smooth-muscle layer development (35, 37).

Researchers have studied other tissue engineering approaches in bladder augmentation

with cell-seeded collagen-PGA/PLGA composite scaffolds (47) small-intestine

submucosa (SIS) (38), (51, 63) and multilaminate matrices derived from silk fibroin (66).

However, these materials exhibited inadequate peak strain, (75) or extensibility (76)

when compared to native bladder tissues (50). For example, the collagen-PGA/PLGA

scaffolds that were used in human clinical studies (13, 74) would exhibit twice the

stiffness (Young's modulus ~0.002 MPa) compared to native bladder tissue (Young's

modulus ~0.001 MPa) (47) and hence, doesn't allow natural distension and contraction

required for normal bladder function. Thus, mechanical mismatch is a major obstacle in designing a scaffold for bladder tissue engineering applications.

Hydrogels have been investigated as scaffold materials because they display low sliding resistance against other tissues and viscoelastic mechanical properties similar to the extracellular matrix (ECM) (52). The mechanical properties of hydrogels can be manipulated based on the cross links formed between polymer chains via chemical bonds and can be designed according to mechanical necessities (52). The high water absorbance and liquid content (> 20 wt %) of hydrogels enables adequate nutrient and waste transport to support encapsulated cells (77). Thus, synthetic and biologically-derived hydrogels are being explored as potential scaffold material for bladder tissue engineering applications. For example, using matrix metalloproteinase (MMP)-sensitive poly (ethylene glycol) (PEG) hydrogels (78), Adelow and colleagues demonstrated that human mesenchymal stem cells (MSC) seeded on these scaffolds differentiated into bladder smooth muscle-like cells after two weeks in culture (55). However, PEG-based scaffolds in general tend to be relatively weak for the mechanical necessities of a number of load-bearing organs including the urinary bladder (79) and have the drawback of post-polymerization swelling. Thus, alternative approaches are needed to improve the strength and stiffness of hydrogel-based bladder grafts.

Tetronics (BASF) are four-armed polyethylene oxide-polypropylene oxide (PEO-PPO) block copolymers comprised of a hydrophobic PPO core domain surrounded by a hydrophilic PEO shell (80). When compared to PEG hydrogels that are prepared only by covalent crosslinking, Tetronic-based hydrogels are prepared by a combination of covalent

and noncovalent cross-linking, leading to improved physical properties. Previously, Sefton and colleagues characterized the semi-synthetic Tetronic T1107-collagen hydrogels (photo-polymerization of T1107-methacrylate in collagen-containing aqueous solutions) and demonstrated that the hydrogel scaffolds exhibited higher storage and loss moduli than pure collagen gels (80). Although in this report human hepatoma HepG2 cells embedded in T1107-collagen were viable, (21) synthetic hydrogels with highly cross-linked networks tend to restrict proliferation and migration of encapsulated cells and delay matrix production in early stages of tissue remodeling (81). To mitigate this, Kutty and colleagues explored addition of hyaluronic acid (HA) to PEG-based hydrogels and demonstrated improvement in spreading and cell proliferation of fibroblasts within the construct (81). The addition of hyaluronidase inhibitors neomycin trisulfate and ascorbic acid-6-palmitate eliminated fibroblast-spreading within HA-containing semi-IPNs, confirming the importance of enzymatic HA degradation in creating localized imperfections leading to fibroblast proliferation. These studies have demonstrated that combination of synthetic moieties such as T1107-methacrylate and PEG-bis-AP with ECM components such as collagen and HA improved overall strength and stiffness of the hydrogel construct and could serve scaffolds for tissue engineered applications. However, little is known about the effect of encapsulated cells on the mechanical properties of these hybrid synthetic-ECM hydrogel scaffolds.

The objective of the present study was to characterize a composite hydrogel scaffold as a matrix material for culture of BSMC in vitro. This is the first study to explore the use of hydrogel blends composed of Tetronic T1107-acrylate (T1107A) in combination

with type I collagen and HA toward applications in urinary bladder tissue engineering. We examined cell morphology and ECM production by BSMC embedded in this composite hydrogel system and the time-course variation in the mechanical behavior of the cell-seeded composite hydrogel constructs.

Materials and Methods

Materials

Free samples of Tetronic T1107 (T1107, MW: 15 kDa, HLB: 18-23) and Irgacure 2959 were obtained from BASF corporation (USA). Acryloyl chloride, Celite 500 fine and 4-methoxyphenol, and hexanes were purchased from Sigma-Aldrich (St.Louis, MO, USA). Toluene (HPLC grade), ethyl ether (anhydrous, BHT stabilized), hexanes (HPLC grade) and anhydrous sodium sulfate were purchased from Fisher Scientific (NJ, USA). Dichloromethane (HPLC grade), triethylamine (TEA), sodium bicarbonate, calcium hydride and $CDCl_3$ were obtained from Acros Organics (NJ, USA). Dichloromethane was dried with calcium hydride and stored over molecular sieves (Grade 514, Type 4A). RPMI 1640 medium and trypsin-EDTA (0.05 %) were obtained from Gibco/Life Technologies (Canada). Fetal Bovine serum (FBS) was obtained from Hyclone (Logan, UT), Collagen type I from MP Biomedicals (Solon, OH, USA) and hyaluronic acid (HA) from Sigma-Aldrich (St.Louis, MO, USA). All chemicals were used as received.

Cell culture

BSMC were isolated from the bladders of adult Sprague-Dawley rats (Female, ~12 weeks old) following our established methods (62). Prior to harvesting of the organs, the rats were euthanized in accordance with the policies of Clemson's Institutional Animal Care and Use Committee based on the Animal Welfare Act. Briefly, using the aseptic technique, the mucosal layer of the bladder was mechanically removed under a dissection microscope, and the rest of the tissue was digested in a solution containing RPMI 1640 medium, 0.1% collagenase (Type II, Worthington, NJ), and 0.2% trypsin-EDTA to dissociate cells from the extracellular matrix. The smooth muscle cells were collected by centrifugation of the tissue digest and then cultured in RPMI medium supplemented with 10% FBS and 1% Pencillin-Streptomycin (P/S) under standard cell-culture conditions (37 °C, humidified, 5% CO_2 / 95% air). The smooth muscle phenotype of these cells was confirmed by immunostaining with mouse monoclonal antibodies for α-smooth muscle actin (1:500 dilution, Sigma-Aldrich, USA) and smooth muscle myosin heavy chain (SM1(1:400 dilution) & SM2(1:500 dilution); Hybridoma Banks, University of Iowa). Fluorescently labeled Alexa Fluor 488 was used as the secondary antibody (Invitrogen, 1:200 dilution). The immunostaining and imaging revealed that the isolated rat bladder SMC clearly expressed both α-smooth muscle actin and SM-MHC (SM1 and SM2) up to six passages. Therefore, only cells up to six passages were used in these experiments.

Synthesis of T-1107 acrylate

T1107-acrlate (T1107A) was prepared by reaction of T1107 terminal hydroxyl groups with acryloyl chloride (82). Briefly, T1107 (30g; 2 nmol) was dehydrated by azeotropic distillation for 2 h with toluene, which was then removed by rotary evaporation (Buchi Rotavapor®, Switzerland). After being cooled to room temperature, the dried T1107 was dissolved in 270 ml dehydrated dichloromethane and mixed with TEA (1.694 ml; 8 mmol). Acryloyl chloride (1.494 ml; 9 mmol) in 30 ml of dry dichloromethane was added drop-wise to this mixture, and the reaction was allowed to continue at 4°C for 24 h. The reactant was filtered through Celite to remove TEA-HCl salt and then concentrated by rotary evaporation to reduce the solvent to one-tenth of its initial volume. The residue obtained was precipitated in 250 ml of cold ethyl ether and 250 ml of hexane, recovered by filtration and dried under vacuum for a few hours. The product was redissolved in 300 ml of dichloromethane and washed with 30 ml of 10% w/v sodium bicarbonate solution until the pH of the solution was neutral. This was followed by water washes (30 ml each) until the pH of the water was neutral and drying with anhydrous sodium sulfate. After the solution was concentrated by rotary evaporation, the residue was precipitated and washed three times with cold ethyl ether (−20 °C). The final product was recovered by filtration, dried for 48 h in a vacuum desiccator and stored at 4°C until use (82). The NMR (Bruker Avance III 300, USA) spectra obtained on the final product was used to determine its acrylation efficiency.

Preparation of composite hydrogel

The T1107A (117.5 mg/ml) powder was added to collagen type I solution (6 mg/ml in 0.02 N acetic acid) and mixed overnight at 4 °C. The collagen-T1107A solution (319 µl) and photo-initiator Irgacure 2959 (I-2959; 7.5 µl, 1:10 dilution in ethanol) were incubated at 4ºC for 30 min with periodic vortexing. The centrifuge tubes containing the hydrogel solution were then brought to room temperature inside the biosafety cabinet; subsequently, hyaluronic acid (HA) (MW=1.5-1.8 MDa; 75-150 µl; 1:100 dilution in H_2O) was added to this solution using a 1000 µl pipette. BSMC ($4x$ 10^6/ml) in 3X RPMI +10% FBS solution were then mixed into the solution to form the final hydrogel solution (0.75mL), composed of 5% T1107A, 0.25% collagen type I, 0.1-0.2% HA, 0.1% I-2959 and ~3x 10^6 cells. The total volume was balanced using 3X RPMI + 10% FBS solution for different concentrations of HA, and the BSMC were omitted in acellular hydrogels. The gel specimens were cast in custom-made Teflon molds (3cmx1cmx0.5cm) with biovyon (Porvair plc, Norfolk, UK) wafers on the ends as anchors (62) and polymerized under UV light for 12 min. The SMC-seeded composite hydrogel constructs were cultured in RPMI medium supplemented with 10% FBS and 1% penicillin-streptomycin for up to14 days.

Quantification of mass swelling ratio of composite hydrogel

Acellular hydrogel specimens were equilibrated in PBS for 24 h to remove unpolymerized monomers and lyophilized. After dry weights (w_d) were recorded, the specimens were soaked in distilled water and allowed to swell for 24 h. Subsequently the

wet weights (w_s) were recorded, and mass swelling ratio, q, was calculated as the ratio of wet to dry weight (w_s / w_d).

Examination of BSMC viability and morphology

BSMC viability inside the composite hydrogels was qualitatively determined with a live/dead viability/cytotoxicity kit (molecular probes, NY, USA). After 4, 7 and 14 days in culture, the composite hydrogels were incubated with 2μM Calcein-AM to stain the living cells and 4μM Ethidium homodimer-1 to stain the dead cells. After 30 min, the constructs were visualized using a laser confocal microscopy (C1Si Confocal; Nikon Ti Eclipse).

To qualitatively determine cell morphology, the BSMC encapsulated in the hydrogel were fixed in paraformaldehyde (1:50 dilution in PBS, P6148, Sigma) at room temperature for 15 min, and the excess aldehyde in the constructs was quenched with 0.1M glycine (T9284, Sigma) for 5 min at the end of the prescribed time periods. The cells were permeabilized with 0.1% triton-X 100 (T9284, Sigma) for 1 min and incubated with rhodamine-phalloidin (1:100 dilution in PBS, R415, Molecular Probes/invitrogen) for 15 min. This was followed by nuclear staining with DAPI (1:100 dilution, D-1306, Molecular probes, Eugene, OR) for 5 min. The hydrogels were then subjected to triplicate PBS washes for 5 min, and the specimens were imaged using laser confocal microscopy (C1Si Confocal; Nikon Ti Eclipse).

Mechanical characterization of composite hydrogel

The mechanical characterization of the composite hydrogels was performed by uniaxial tensile testing using MTS Synergie 100 to quantify peak stress, elastic modulus and peak stretch of the samples. The dog bone-shape hydrogel constructs were subjected to tension under hydrated conditions (PBS at 37ºC) at a rate of 5mm/min until rupture. Average Lagrangian peak stress values were calculated from the load applied to the specimens over continuous time-points divided by the original cross-sectional area of the hydrogel. The stress-stretch relationship was analyzed where stress (τ) was plotted against stretch (λ) (where λ is the stretch ratio of deformed to reference lengths). The elastic modulus (kPa) of the hydrogels was calculated from the linear regions of their respective stress-strain curves. Peak strain was also calculated.

Quantification of collagen synthesis by BSMC

After 7 and 14 days of culture, hydroxyproline assay was performed according to the published method to quantify the collagen synthesized by BSMC (hydroxyproline represents 12% of collagen (w/w)) (83). Acellular hydrogel samples were used as control. Briefly, all hydrogel samples were flash frozen in liquid nitrogen and lyophilized using a freeze dry system (Freezone 4.5, Labconco, USA). The lyophilized samples were then hydrolyzed in 4N NaOH at 120 ºC for 4 hours and neutralized with citric acid (1.4N). Series concentrations (0-50%) of hydroxyproline (100µg/ml) dilutions were prepared as standards. Each of the samples and standards was mixed with 1 ml of chloramine-T and incubated at room temperature for 20 min. This was followed by

addition of p-dimethylaminobenzaldehyde (PDMAB) and additional incubation at 65°C

for 15 min. The light absorbance of samples was measured at λ=550 nm in triplicate

using a universal microplate spectrophotometer (μQuant, Biotek Instruments Inc., USA).

Statistical analysis

     All numerical data were analyzed using the single-factor Analysis of Variance

(ANOVA), followed by a post-hoc test when statistical significance was detected. All

statistical analyses were performed using JMP ANOVA statistical software package

(SAS, NC, USA). Four samples were used for uniaxial mechanical testing and three

samples were used in the hydroxyproline assay.

Results

Synthesis of T-1107 acrylate

     Schematic representation of T1107A synthesis is shown in Figure 3-1. The

percent acrylation efficiency was calculated based on the ratio of the integrals of the PEG

backbone (δ=3.5-3.7) and acrylic peaks (δ=6.15-6.4) (Figure 3-2) as previously shown in

studies done by Cho et al. (84). A yield of 22.5 g of T1107A was obtained from the

original 30g of T1107 used in the synthesis and T1107A having more than 85%

acrylation efficiency was used in the experiments. Efficient removal of unreacted

acryloyl chloride was confirmed by the ratio of acrylate to activated PEG terminal

(δ=4.3) methylene peaks, which closely approximated the theoretical value, 3:2.
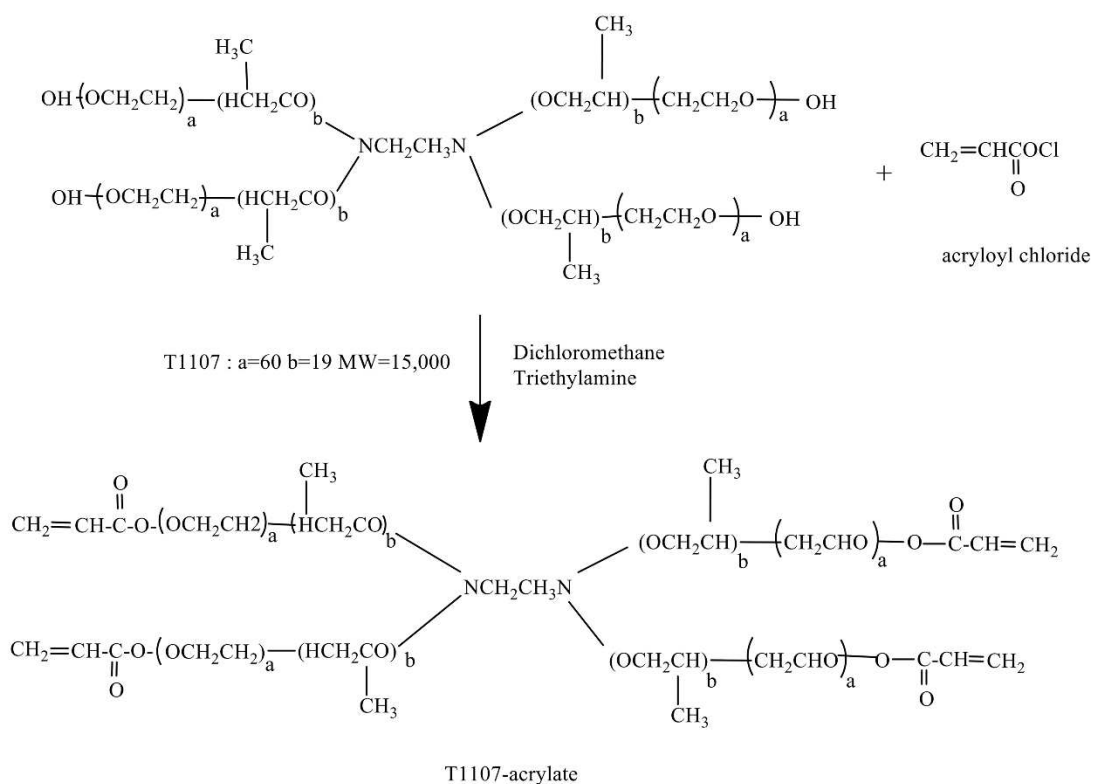
Figure 3-1: Schematic representation of synthesis of T1107A.The formation of acrylate groups on all four arms of T1107, a block copolymer of (a) Polyethylene oxide (PEO) and (b) polypropylene oxide (PPO), is described.
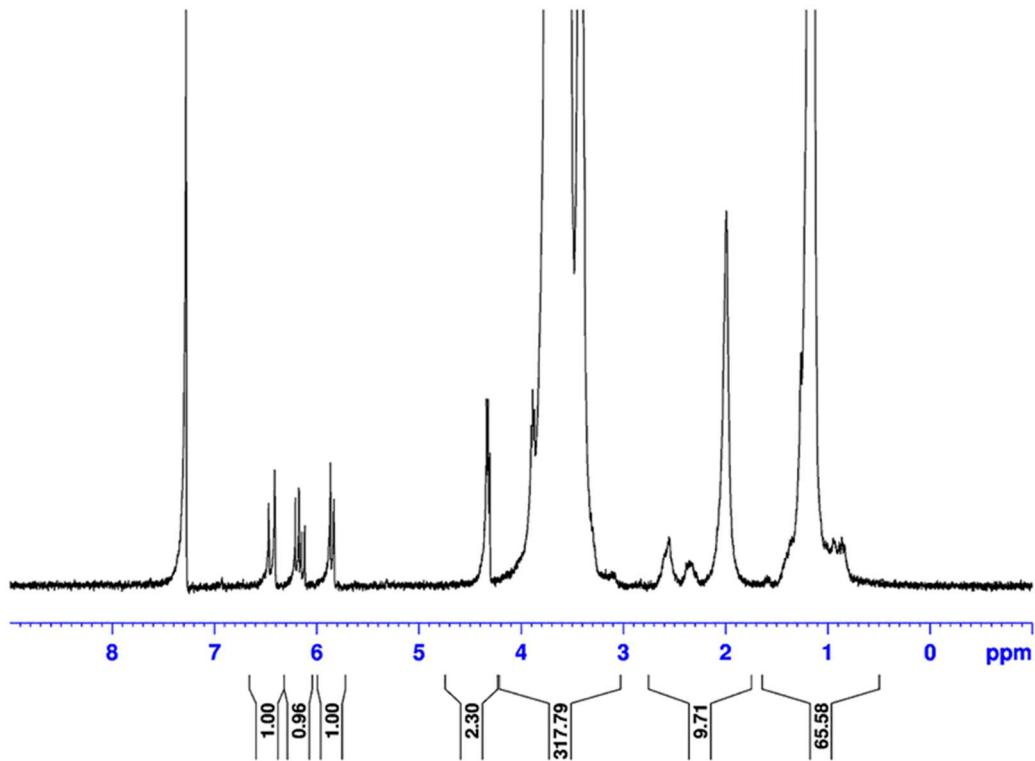
Figure 3-2: Representative ¹H-NMR spectrum of acrylated T1107. Analysis of the

NMR data based on the integrals of the PEG backbone (δ=3.5-3.7) and acrylic peaks

(δ=6.15-6.4). The integrals include δ = 1.1 (a, PPO CH3), 3.4 (a, PPO CH), 3.54 (a, PPO

CH2), 3.65 (a,PEO CH2), 4.32 (-CCH2OC (=O)-), 5.8 and 6.4 (2H, acrylic –CH2),

6.15 (1H, acrylic –CH) ppm.

Mass swelling ratio and mechanical characterization of composite hydrogel scaffold

The ratios of swollen mass to dry mass of acellular composite hydrogel specimens

(Figure 3-3) were similar for the three different concentrations of HA (0.1, 0.15 and

0.2%) used in the hydrogels (Figure 3-4A). In contrast, the results of tensile testing

indicated that higher the concentration of HA, greater the elastic modulus (defined as the

slope of the linear region of the stress/stretch curve) of the composite hydrogels (Figure

3-4B). The formulations containing 0.15 and 0.20% HA exhibited significantly (P<0.01)

greater elastic modulus (stiffness) than the specimens with 0.10% HA content (Figure 3-

4B). Based on this result, we incorporated 0.2% HA in our composite hydrogels for the

rest of our study.
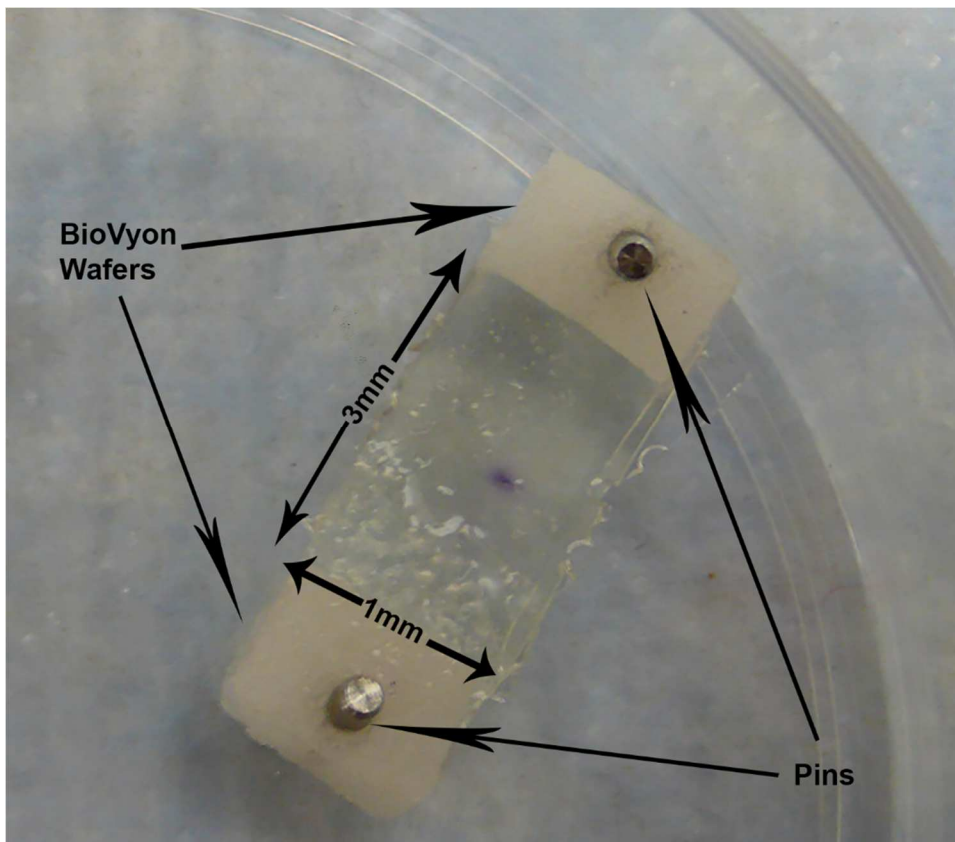
Figure 3-3: Representative image of the acellular composite hydrogel. The composite

hydrogel was obtained by subjecting the gel composition to UV radiation for 12 minutes

between BioVYON wafers which assist as grips during uniaxial tensile testing.
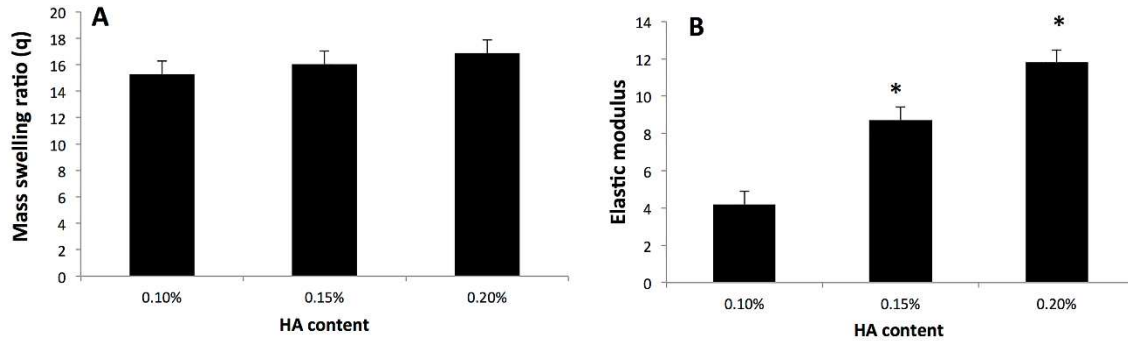
Figure 3-4: Effect of HA content on the mass swelling ratio and elastic modulus of the composite acellular hydrogels. While swelling ratio (A) was unaffected, the elastic modulus (B) increased significantly as concentration of HA in the composite hydrogels increased. Values are mean ± SEM, * $p<0.01$, n=3 per group.

BSMC Cell Viability and Morphology

The live/dead study indicated the presence of viable cells in the scaffold at a magnification of 100X after 4, 7 and 14 days of culture (Figure 3-5). The Rhodamine-phalloidin staining and confocal imaging revealed distribution of BSMC up to a depth of 1.13 mm of the construct, which after 14 days in culture, revealed an increased distribution for a depth of 1.26 mm along with increased BSMC migration towards the surface of the hydrogel scaffolds (Figure 3-6A and 3-6B). When the constructs were viewed at the 600X magnification at the 14 day time-point, the individual BSMC demonstrated a spread cell morphology (Figure 3-6C).
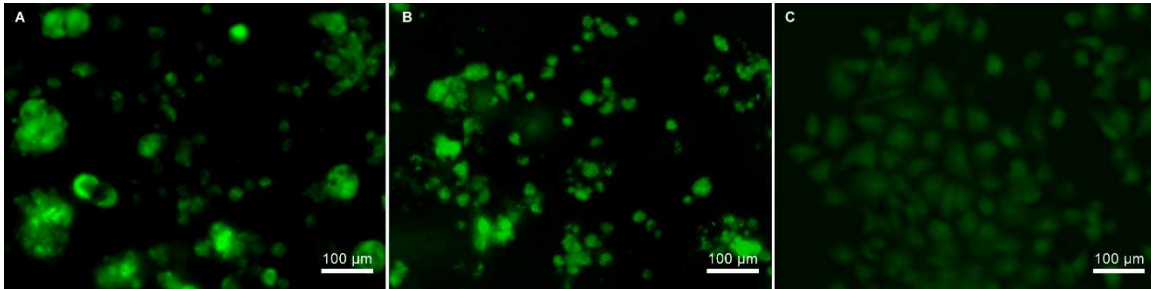
Figure 3-5: Live/Dead staining of BSMC in the composite hydrogel. High viability of BSMC was confirmed by the presence of live (green) cells and the absence of dead (red) cells in the scaffold after 4 (A), 7 (B) and 14 (C) days of cell seeding. In addition, BSMC exhibited spread cell morphology at day 14 (C) (Magnification=100X).
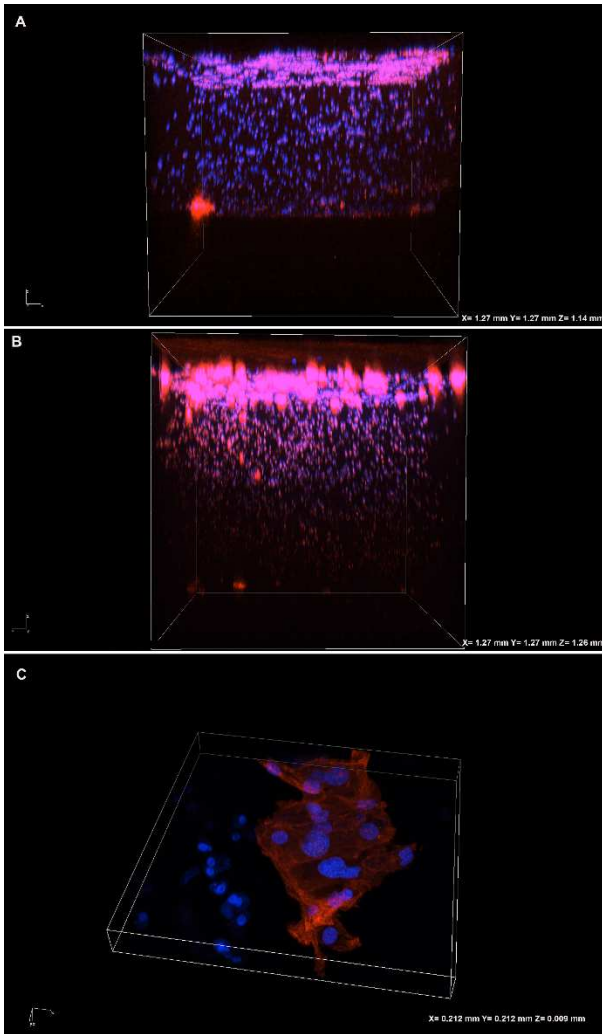
Figure 3-6: Confocal imaging of BSMC in the composite hydrogels. The results

demonstrate BSMC are well distributed at day 4 (A: magnification = 40X), and increased

cell migration towards the surface at day 14 (B: magnification = 40X). The spread

individual bladder smooth muscle cells are also seen at the 14-day culture period (C:

magnification = 600x).

Effects of cell-seeding on mechanical properties of composite hydrogel

When compared to acellular gels (Peak Stress: 4.1 ±1.2 kPa, Elastic modulus (stiffness): 11.8 ±1.1 kPa, Peak Stretch: 1.21±1.23) hydrogels seeded with BSMC (4 X 10^6 cells /mL) exhibited greater values for peak stress, peak stretch, and elastic modulus (Figure 3-7). Among the BSMC-seeded hydrogels, specimens cultured for 14 days exhibited significantly (P<0.05) greater values of peak stress (11.6± 2.2 kPa) and elastic modulus (42.7 ± 4.0 kPa) compared to specimens cultured for 7 days (Peak stress: 5.2±0.6 kPa, Elastic modulus: 19.3±2.8 kPa). When compared to cell-seeded hydrogel specimens cultured 7 days (1.23 ± 0.04), specimens cultured 14 days (1.39±0.12) exhibited peak stretch values with a strong trend of higher value; this was not statistically different due to large variability(Figure 3-7B).
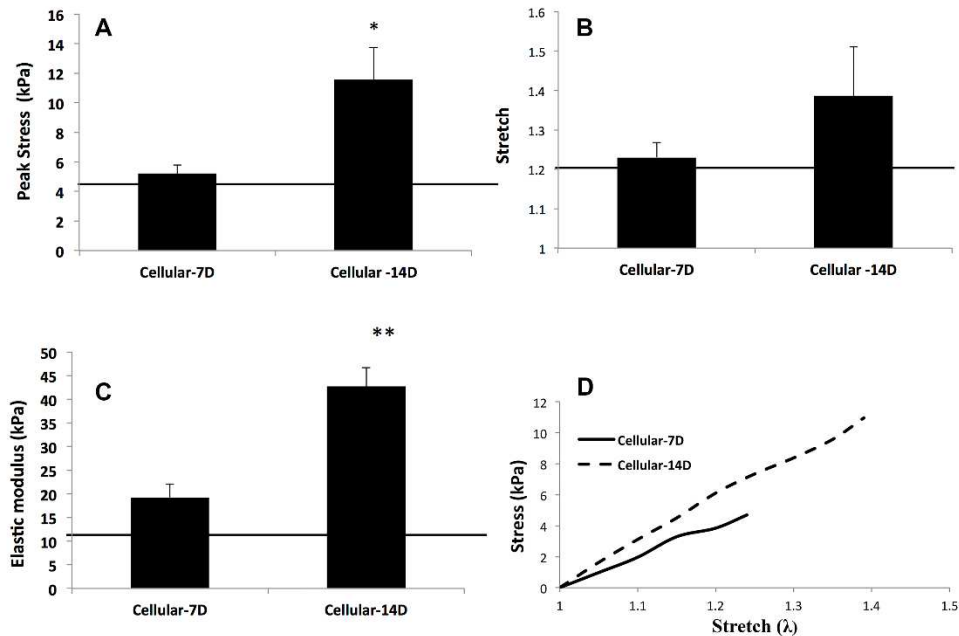
Figure 3-7: Mechanical properties of the composite cellular hydrogels. Specimens were subjected to uniaxial tension at the rate of 5mm/min until failure and average peak

stress (A), peak stretch (B) and elastic modulus (C) were calculated from the stress-stretch relationship (D) of composite cellular hydrogels at the 7 and 14 day time point. The lines across the bar graphs represent the corresponding values for acellular composite hydrogels (0.2% HA). Values are mean ± SEM; analyzed by ANOVA, *p<0.05, **p<0.01, n=4.

Hydroxyproline assay

   The results of the hydroxyproline assay indicated that compared to acellular samples (35.1± 3.1 µg collagen/mg sample mass), the 7-day (48.5 ± 9.6 µg collagen/mg sample mass) and 14-day cellular constructs (61.7 ± 5.9 µg collagen/mg sample mass) contained significantly ($p < 0.05$) greater amounts of collagen (Figure 3-8)
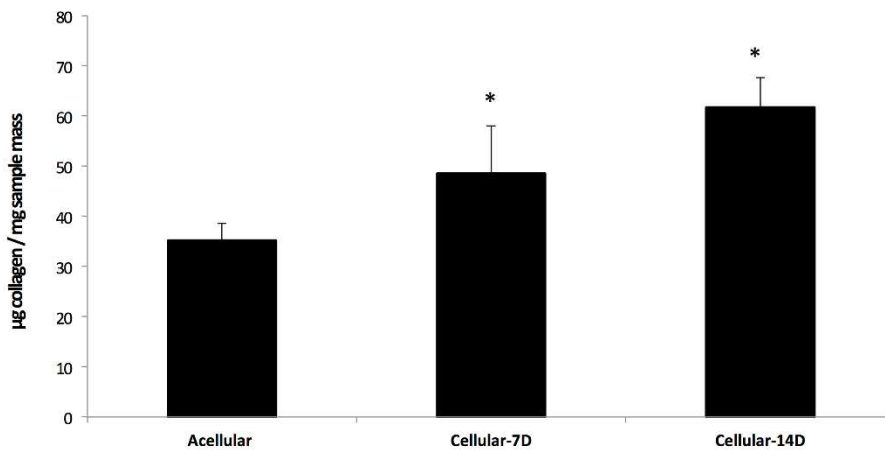
Figure 3-8: Collagen concentration in the composite hydrogels. Results of hydroxyproline assay revealed that cellular specimens contained significantly greater amounts of collagen after 7 and 14 days of culture compared to the acellular specimens. Values are mean ± SEM; *p<0.01, n=3.

Discussion

The long-term goal of the present study is to develop a functional 3D tissue construct for bladder augmentation. In pursuit of this goal, we prepared a composite hydrogel using a blend of Tetronic T1107A, type I collagen, and HA cross-linked to form a semi-IPN scaffold for encapsulation of BSMC. First, to evaluate the impact of HA inclusion on mass swelling ratio and elastic modulus (stiffness) of our composite hydrogel, different concentrations of HA (0.1%, 0.15%, 0.20%) were mixed into the acellular hydrogel constructs. Results show that while the mass swelling ratios of hydrogels with different concentration of HA were nearly identical, the elastic moduli increased with increasing concentration of HA (Figure 3-4). These results are in agreement with the report by Kutty et al., which demonstrated that in PEG-bis-AP/HA semi-IPNs, increasing concentration of HA from 0.06% to 0.18% caused a minimal increase in volumetric swelling ratio and a significant increase in elastic modulus relative to controls without HA (81). The lack of any change in the mass swelling ratio indicates that the inclusion of HA in our composite scaffold did not affect the density of the construct's crosslinks and consequently, did not affect swelling. These results are in contrast with a previous study, which demonstrated that in collagen-HA semi-interpenetrating network hydrogels, inclusion of increasing concentrations of HA led to a corresponding decrease in the swelling ratio (85). This was because the HA chains in the collagen-HA semi-interpenetrating network hydrogels were cross-linked into the composition, causing stiffer gels (86). In the present study, the HA molecules were not cross-linked, and they merely entangled with the main Tetronic network inside the

53

composite hydrogels. Thus, increasing HA weight percentage did not cause increased crosslinking and decreased swelling. However, HA solid content, due to its high molecular weight relative to collagen (81), molecularly reinforced the hydrogel (86) and had a significant impact on elastic modulus (stiffness) of the composite scaffold (Figure 4). Previous studies have shown that the elastic modulus of alginate gels is affected by the molecular weight of polysaccharides encapsulated in it (87). HA, one of the longest types of glycosaminoglycans (GAG), led to increased elastic modulus (stiffness) in the composite hydrogel with increasing concentration. This was demonstrated by Kim et al., who showed that higher weight percentage of HA led to increased elastic modulus in MMP-sensitive HA-based hydrogels (88).

In the present study, the BSMC encapsulated in composite hydrogel displayed high cell viability at various time points (Figure 3-5). Moreover, the confocal imaging demonstrated that distribution of BSMC was visible in the scaffold (Figure 3-6). These results are in agreement with previous studies that during a similar culture period, smooth muscle cells seeded in collagen-based hydrogels tended to migrate towards the surface of the constructs (69, 89). The increased BSMC distribution may be due to facilitation of cell spreading and migration by the degradation of HA and localized increases in mesh size of the scaffold, as previously reported with fibroblasts encapsulated in HA-containing PEG-based semi-IPN hydrogels (81). Though BSMC at 4 and 7 days exhibited the round morphology of the synthetic phenotype of smooth muscle cells (Figure 3-5A and 3-5B), the BSMC at the 14day time-point exhibited a more spread morphology (Figure 3-5C and 3-6C).

54

In mechanical testing, the hydrogel scaffolds increased in strength and elastic modulus (stiffness) when seeded with BSMC and cultured for up to 14 days. Compared to the acellular hydrogels, the mechanical properties (peak stress, peak strain and elastic modulus) of the cellular hydrogels were significantly greater. The average peak stress and elastic modulus of the BSMC-seeded composite hydrogels were significantly ($p < 0.05$) higher 14 days after cell seeding than specimens tested 7 days after BSMC seeding. We hypothesized that the increase in strength and elastic modulus (stiffness) of the cellular constructs was due to *de novo* ECM synthesis by BSMC, and we quantified the amount of collagen within the cell-seeded composite hydrogel specimens using hydroxyproline assay (90). Collagen (especially types 1 and 3) is the major protein of the urinary bladder ECM and contains various cell-adhesion domains important for maintaining native phenotype and cellular activity (91). Since the 7-day and 14-day cellular constructs contained significantly ($p < 0.05$) greater amounts of collagen per specimen mass than the acellular composite hydrogel scaffolds (Figure 3-5), we concluded that BSMC deposited the newly synthesized collagen, which led to the increase in strength and stiffness of the gel constructs (Figure 3-4). Although the increased collagen content suggested correlative increases in mechanical strength, the ultimate tensile stress of the BSMC-seeded composite hydrogels in the present study (11.6 ± 2.2 kPa) did not display the level achieved in other studies (89) or an estimated peak physiological stress of the native bladder (~100 kPa) (92). This may be because the two-week end-point used in the present study was too short (89) or chemical stimulation was needed to support crosslinking of newly synthesized collagen fibrils that contributes to the stiffening of the

overall construct (93). For example, Berglund et al. reported that the ultimate tensile stress of endothelial cell-seeded collagen hybrid scaffolds was more than 100kPa at the end of 23 days (94). Tranquillo and colleagues demonstrated that addition of 1or 5 ng/ml of TGF-β1 and 2μg/ml of insulin led to a seven-fold increase in collagen concentration and cross-linking with a three-fold increase in ultimate tensile strength in fibrin gel-based constructs seeded with neonatal vascular smooth muscle cells (95). Thus, to promote cross-linking of the newly synthesized collagen it may be necessary to culture the composite hydrogels for longer time periods of 3-5 weeks and/or in the presence of soluble chemical compounds.

In summary, mechanical mismatch has been a major obstacle in designing a scaffold for bladder tissue engineering applications. The composite hydrogel system in our current study provided a viable environment for bladder smooth muscle cells to survive and reconstruct the scaffold, thereby improving the construct's overall strength and stiffness. Culturing the construct for longer time periods after BSMC seeding and addition of growth factors to the composite hydrogel system would further aid in accurately mimicking the mechanical properties of the bladder wall.

Chapter 4

IN VITRO CHARACTERIZATION OF BIODEGRADABLE ELASTOMERS FOR
APPLICATION IN BLADDER TISSUE ENGINEERING

Introduction

In the previous chapter, we discussed that the mechanical strength and stiffness of
the composite hydrogels after 14 days of BSMC seeding could not mimic the mechanics
of the bladder wall and hence, the present study explored the use of biodegradable
elastomers, namely, polyglycerol sebacate –polycaprolactone (PGS-PCL), poly (ether-
urethane) urea (PEUU), and poly (carbonate-urethane) urea (PCUU) as scaffold materials
for urinary bladder tissue engineering since these materials have previously been shown
to exhibit high extensibility and biocompatibility (96, 97). For example, Sant and
colleagues demonstrated that, compared to electrospun PCL-only (mesh) scaffolds,
electrospun (ES) fibrous PGS-PCL scaffolds supported greater cell attachment and
proliferation of human umbilical vein endothelial cells (HUVECs) and mitral valve
interstitial cells (MVICs) (98, 99). In separate studies, Wagner et al. demonstrated that
ES-PEUU scaffolds simulated the anisotropic mechanical response of vascular tissues
(100, 101) and promoted smooth muscle neo-tissue formation in rats with sub-acute
myocardial infraction (102). Studies on the PCUU scaffold showed that though it
degraded slower than PEUU (when implanted subcutaneously in rats at the end of 8
weeks), it also promoted native smooth muscle infiltration and growth similar to PEUU
(97). In addition to cytocompatibility, PGS-PCL, PEUU and PCUU exhibited high tensile

strength (10-35 MPa) (97) and elongation (400-800%) (97, 103), which are ideal for

applications toward the bladder that demonstrate a peak stress (~ 1.6 MPa) and

elongation of 150-350% depending on regional variations when subjected to uniaxial

tension (7). Therefore, the present study focused on characterization of the mechanical

behavior and the *in vitro* cytocompatibility of these biodegradable elastomers for urinary

bladder tissue engineering applications.

Materials and methods

Materials

All elastomeric scaffolds were kindly donated by collaborators who prepared

them using conventional electrospinning methods with conditions described in previous

reports (96, 101). The PGS-PCL scaffolds (Figure 4-1A) were fabricated in the laboratory

of Dr. Ali Khademhosseini (Wyss Institute for Biologically Inspired Engineering,

Harvard-MIT). Briefly, the PGS and PCL polymers (33 wt. %) were dissolved in a

mixture of ethanol and anhydrous chloroform so that the PGS: PCL weight ratio was kept

constant at 2:1. Electrospinning was carried out at 12.5 kV using a 21G blunt needle and

at a flow rate of 2ml/hr for 30 min. The distance between the needle and the collector

were kept constant at 18 cm (96). For easy removal of the fibers non-adhesive tape was

attached to an aluminum plate to collect them. Scaffolds were stored in a desiccator until

further use (96). PEUU (Figure 4-1B) and wet PCUU (Figure 4-1C) scaffolds were

fabricated in the laboratory of Dr. William Wagner (McGowan Institute of Regenerative

Medicine, University of Pittsburgh). Briefly, PCUU was dissolved in HFIP under

mechanical stirring at either 5 or 12 wt%. The PCUU/PEUU solution and cell culture media (composed of DMEM media supplemented with 10% fetal bovine serum (FBS) and 5% penicillin-streptomycin) was fed at ~0.98-1.2 ml/hour (dependent on ambient relative humidity) using two different syringe pumps (Harvard Apparatus PhD) located at 17 cm and 4.5 cm respectively from the target (mandrel). High voltage generators (Gamma High Voltage Research) were utilized to charge the PCUU/PEUU solution at 12 kV, cell culture medium at 9kV and their target at -7kV. The electrospinning was performed at a rotational speed of ~200 rpm, with a 5cm motor translation pattern, which meant the mandrel translated back and forth at a distance of 5cm, while maintaining minimal scaffold media wetting during fabrication. The approximate fabrication time was about two hours and the PEUU/PCUU scaffold was kept overnight in UV for sterilization before use. There were two versions of PCUU which were fabricated; a normal version and a slightly more compliant version (higher amount of media is added while fabrication).
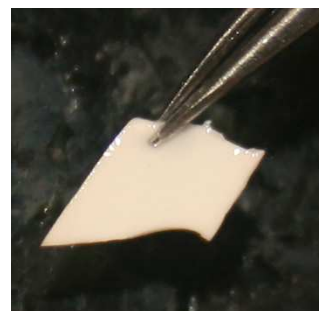
A   B   C

Figure 4-1: **Representative Images of PGS-PCL (A), PEUU (B) and PCUU (C).**The PCUU scaffold(wet) is stored in cell culture media composed of DMEM supplemented with 10% FBS , 10% horse serum and 5% penicillin/streptomycin.

Uniaxial mechanical testing of elastomeric scaffolds

The mechanical testing specimens were prepared according to the ASTM standards D3039/D3039D and subjected to uniaxial tensile loads under hydrated conditions (PBS at 37ºC) at a rate of 18mm/min until rupture (50) using MTS synergie 100. The mechanical behaviors of these materials were analyzed by plotting the calculated values of tension (N/mm) against stretch ratio λ (ratio of deformed to reference lengths) and by comparing the maximum tensions and stretch ratios at failure. Since the thickness of the elastomeric scaffolds (0.1-0.2 mm) was negligible compared to its length and width, tension was quantified instead of stress. As a reference, the physiological peak tension of the bladder in the human body was estimated. Using the Law of Laplace, we calculated for membrane tension in the bladder (M_T) where $M_T = p*R/2$ where p is the internal pressure and R is the radius of the bladder. Stress is then computed by $T = M_T/thickness$. In these equations, the internal radius of the normal bladder (6 mm) , the maximum thickness (0.4 mm), and the peak pressure (75 cmH$_2$O or 7.34 kPa) was based on previous studies and measurements(73, 104). These computations lead us to believe that native urinary bladders *in vivo* undergo a peak physiological tension of approximately 100 kPa.

Biaxial mechanical testing of elastomeric scaffolds

PCUU specimens approximately 6mm X 6mm in size were subjected to biaxial

mechanical testing using the CellScale BioTester (Waterloo, Canada). The BioTester was

fitted with 2.5N load cells and BioRakes^{TM} with 1.0 mm tine spacing. The specimens

were loaded with an initial grip separation of 4.8 mm. After mounting, the grips were

moved to 5.0 mm before the start of the test in order to provide a small amount of

preload. The intended procedure was to test each specimen with increasing equibiaxial

strains until failure i.e. 20% in 20 sec (5mm to 6mm; λ= 1.2), 40% in 40 sec (5mm to

7mm; λ=1.4), 60% in 60 sec (5mm to 8mm; λ=1.6), and 75% in 75 sec (5mm to 8.75mm;

λ= 1.75). The mechanical behaviors of these materials were analyzed by plotting the

calculated values of tension (N/mm) and stress (kPa) at different strain rates. We also

computed the areal strain (= $\lambda_X\lambda_Y$-1) under 100 kPa equibiaxial stress, where λ_X and λ_Y

represent the stretch along the X and Y axes, respectively. The areal strain represents the

change in area between the reference and deformed states under planar biaxial loading.

SEM imaging of PCUU scaffolds

Rectangular PCUU specimens (thickness 0.11 mm) were created according to the

ASTM standards D3039/D3039D with the dimensions 10 X 1 mm. These scaffolds were

affixed to thin aluminum sheets (gauge -0.0084, Amerimax, USA,) under stretched states

at 1.25, 1.5, and 1.75. These samples were then imaged using SU 6600 scanning electron

microscope (Hitachi). The % porosity was determined semi-quantitatively using ImageJ

(NIH, USA).

BSMC seeding on elastomeric scaffolds

The PCUU scaffolds (5 mm × 5 mm) were sterilized by soaking in 70 % ethanol

for at least 1 h and then washed thoroughly with sterile Dulbecco's phosphate buffered

saline (DPBS) before cell seeding. The scaffolds are then soaked overnight in sterile

BSMC culture media composed of RPMI supplemented with 10% FBS and 1%

antibiotic/antimycotic. The culture media were removed just before cell seeding. The

BSMC were suspended in 20-25 µl of BSMC culture media at a final concentration of ~1

× 10^5 cells/scaffold and seeded evenly at 4-5 places on each scaffold (the scaffolds were

neither too wet or too dry while seeding the cells). The cells were allowed to attach to

scaffolds for 1-1.5 h before flooding the culture plate with additional medium. After

incubation under standard cell culture conditions (humidified, 37 °C, 5% CO_2 / 95% air)

overnight, the cell-seeded scaffolds were transferred to new well plates with fresh media

to separate them from the cells attached to the bottom of PDMS wells. BSMC with six

passages or less were used in all experiments.

Characterization of BSMC viability and morphology

BSMC viability on the PCUU scaffold was determined with LIVE/DEAD assay kit

following the manufacturer's instructions (Molecular Probes, NY, USA). After 7 days in

culture, the PCUU scaffolds were rinsed in sterile PBS following removal of media. The

scaffolds were then incubated with 2µM Calcein-AM to stain the living cells and 4µM

Ethidium homodimer-1 to stain the dead cells. After 30 min, the constructs were

visualized using a laser confocal microscopy (C1Si Confocal; Nikon Ti Eclipse). The %

live cells was determined quantitatively using ImageJ (NIH, USA).

To determine cell morphology, the actin filaments of BSMC seeded on the PCUU

scaffolds were stained with rhodamine-phalloidin after seven days in culture. Briefly,

cells were fixed in paraformaldehyde (1:50 dilution in PBS, P6148, Sigma) at room

temperature for 15 min, and the excess aldehyde in the constructs was quenched with

0.1M glycine (T9284, Sigma) for 5 min. The cells were permeabilized with 0.1% triton-

X 100 (T9284, Sigma) for 1 min and incubated with rhodamine-phalloidin (1:100

dilution in PBS, R415, Molecular Probes/invitrogen) for 15 min. This was followed by

nuclear staining with DAPI (1:100 dilution, D-1306, Molecular probes, Eugene, OR).

The PCUU scaffolds were then subjected to triplicate PBS washes for 5 min, and the

specimens were imaged using laser confocal microscopy (C1Si Confocal; Nikon Ti

Eclipse).

Characterization of BSMC marker expression

The smooth muscle phenotype of BSMC on the PCUU scaffolds was examined

by immuno-staining for α-smooth muscle actin and smooth muscle myosin heavy chain

(SM1 & SM2) after 7 days of culture. Briefly, the cells were fixed for 20 min and then

blocked using a solution composed of 2% bovine serum albumin, 3% goat serum,

prepared in PBS. After triplicate washes with PBS, the specimens were incubated with

primary anti-bodies for α-actin (1:500 dilution, Sigma-Aldrich, USA) and smooth muscle

myosin heavy chain (SM1(1:400 dilution) & SM2(1:500 dilution); Hybridoma Banks,

63

University of Iowa) followed by incubation at 4ºC overnight. The cell-seeded PCUU

scaffolds were then incubated with the secondary antibody Alexa-fluor 488 Anti-Mouse

IgG (H+L) overnight, followed by nuclear staining with DAPI for 5 minutes. The cells

were then imaged using laser confocal microscopy (C1Si Confocal; Nikon Ti Eclipse).

Pressure testing of PCUU scaffolds

Rat bladders were obtained frozen from Pel-Freeze biologicals (Rogers, Arizona)

and were thawed overnight at 4º C before use. A small (~2.0 mm diameter) defect was

created using a 18G needle (BD Precision Glide, NJ,USA) on the dome of each bladder

(~10.5 mm X 5.4 mm) on top of a half severed 100 µl pipette tip (VWR, PA, USA)

(Figure 4-2) and an acellular PCUU patch was sutured using nylon 9-0 sutures to cover

the puncture. The augmented bladder specimens were inflated with saline (with color

added using Coomassie blue for visual confirmation of leaks) using the Harvard pump

(Harvard Apparatus, Holliston, MA) at a flow rate of 0.1 ml/min until failure in the saline

bath at 37 ºC. Changes in pressure during testing were recorded via a pressure transducer

and our custom LabVIEW program. Intact rat bladders with no defects were used as the

control.
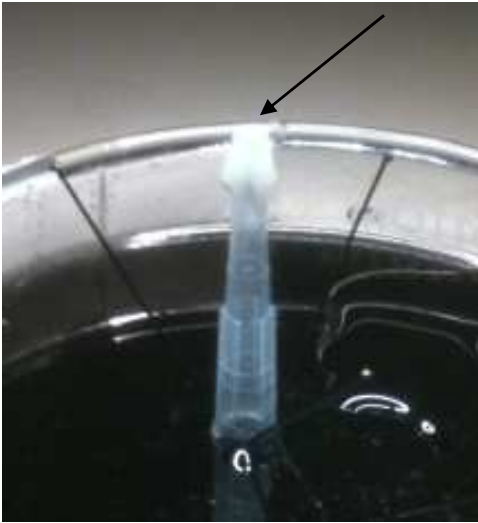
Figure 4-2: Image describing punctured PCUU on top of severed pipette tip. The

arrow denotes the puncture on the rat bladder where the PCUU will be sutured. The

severed pipette tip is held upright using pins on a PDMS bottom petri dish.
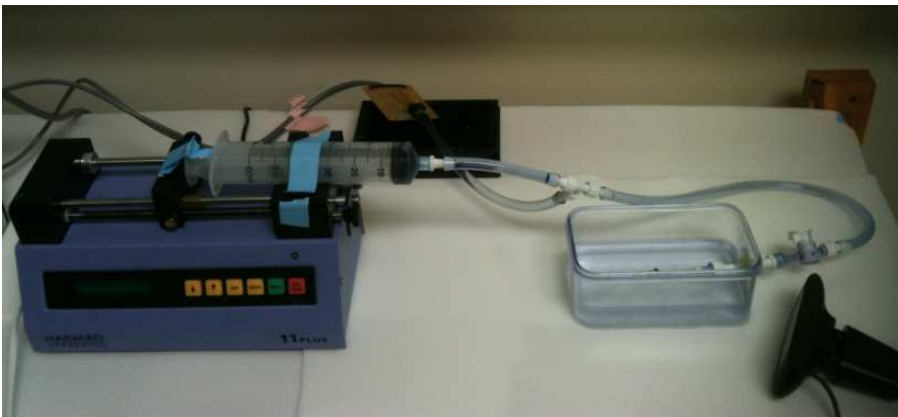
Figure 4-3: Image describing the ex vivo pressure device. The syringe pump injects

colored saline into the PCUU sutured bladder till the patch leaks. The pressure inside the

bladder is monitored by the pressure transducer and LabVIEW program.

Results

Uniaxial mechanical testing of elastomeric scaffolds

The uniaxial tensile testing of the PGS-PCL scaffolds in the present study revealed that although the maximum stretch was 2.15 ± 0.28, the maximum tension at failure was on average 0.072 ± 0.005 N/mm (Figure 3). The uniaxial testing of the PEUU revealed that a maximum tension and stretch ratio at failure were 1.75 ± 0.68 N/mm and 2.47 ± 0.52, respectively (Figure 4- 3C). In contrast, the uniaxial testing of the PCUU scaffolds revealed that not only the maximum tension (0.43±0.029 N/mm) and stretch (2.43± 0.26), but also the overall tension-stretch curve (Figure 4-3) were similar to those of the native bladder reported in the literature (50).

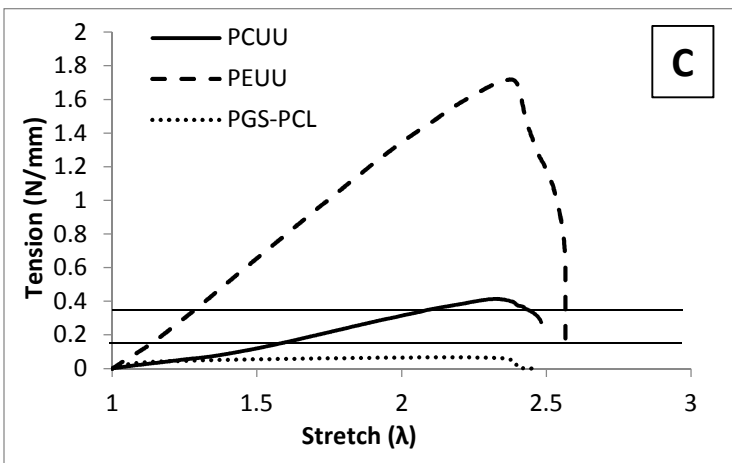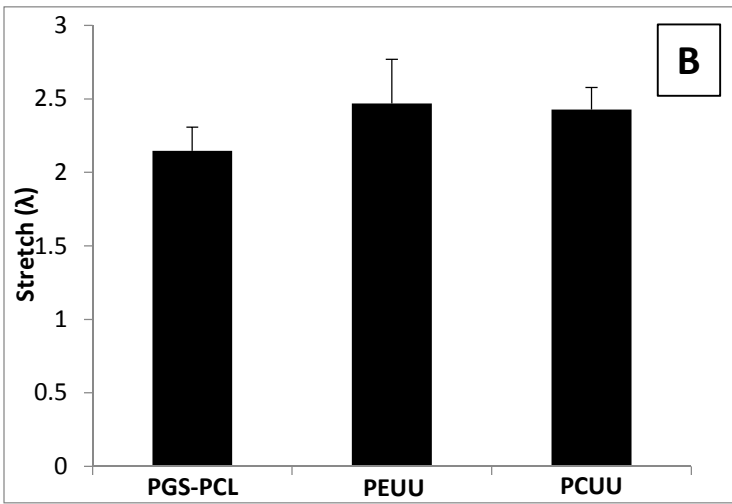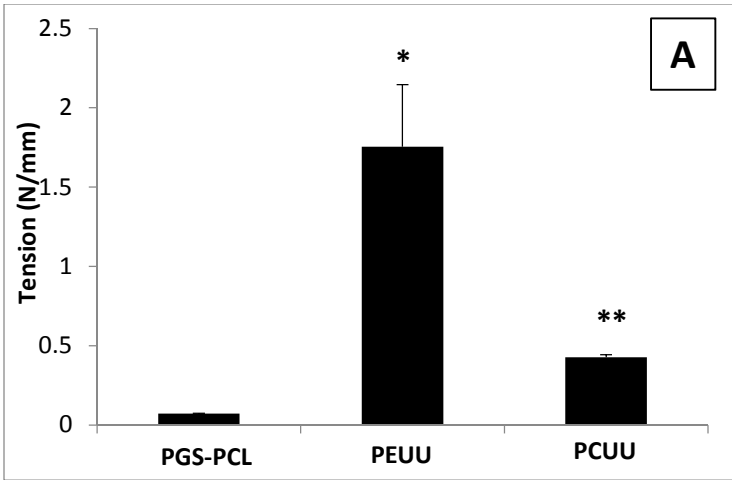**Figure 4-4: Mechanical properties of biodegradable elastomers.** Specimens were subjected to uniaxial tension at the rate of 18 mm/min until failure and average peak tension (A), peak stretch (B) were calculated from the tension-stretch relationship (C) of viscoelastic elastomer scaffolds. The parallel lines across (C) represent the corresponding values for peak physiological tension to which the bladder is subjected in the body varying on thickness (2-4 mm). Values are mean ± SEM; analyzed by ANOVA, *p<0.01, **p<0.05, n=4

Biaxial testing of elastomeric scaffolds

The results indicated different tension-stretch curves for X and Y axes under equibiaxial strains demonstrating anisotropic mechanical behavior of the PCUU scaffolds (normal (**A**) and compliant (**B**)) at all the different strain levels. The normal variants of PCUU required nearly twice the tension to attain the desired stretch values (1.2, 1.4, 1.6 and 1.75) when compared to the compliant variant of PCUU (Figure 4-5). Both samples failed at 75% strain. At a stress of 100 kPa, the areal strain of the PCUU scaffolds were estimated to be 0.13 for sample A and 0.21 for sample B respectively (Figure 4-6).

a   b
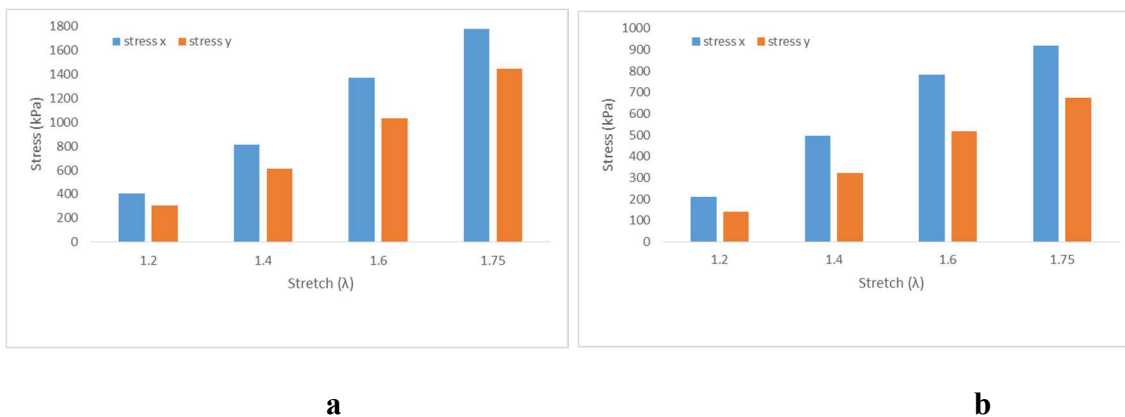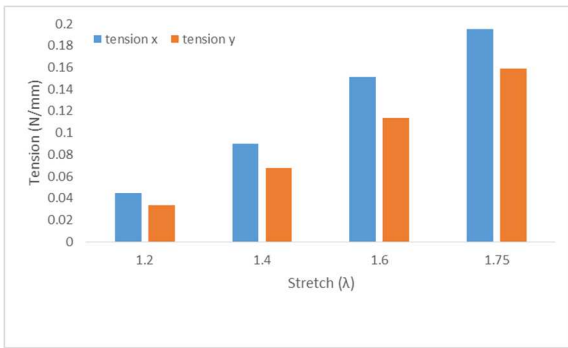
c
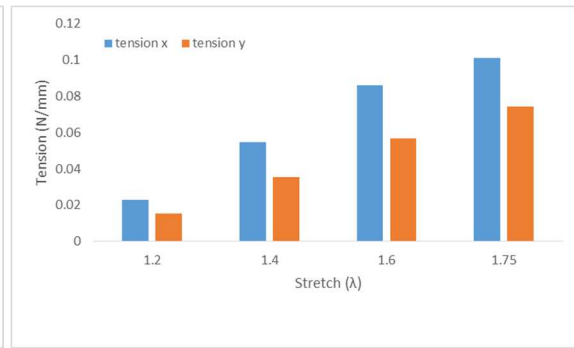
d
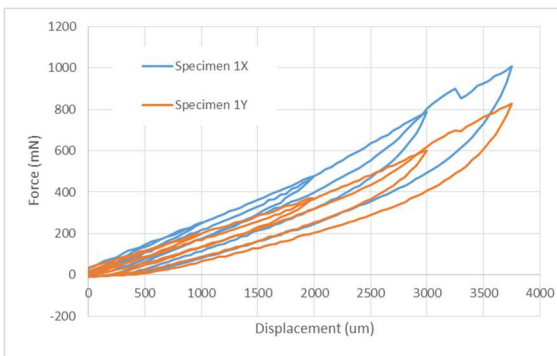
e
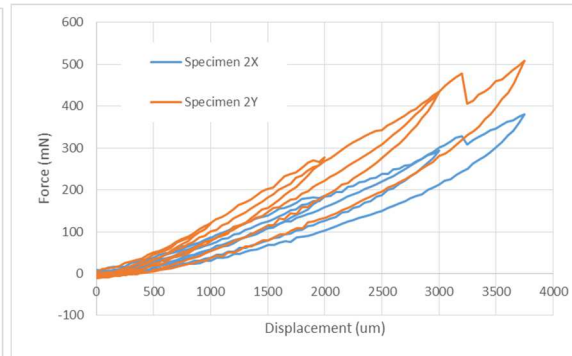
f

Figure 4-5: Biaxial mechanical testing of PCUU. The stress(**a,b**) and tension(**c,d**) values of normal (n=1) and compliant (n=1) PCUU respectively at various stretch values.The Hysteresis curves depicting normal (**e**)(n=1) and compliant (**f**) (n=1) samples of PCUU indicate non-linear viscoelastic behavior at 20 % strain, 40 % strain, 60% strain and 75% strain.
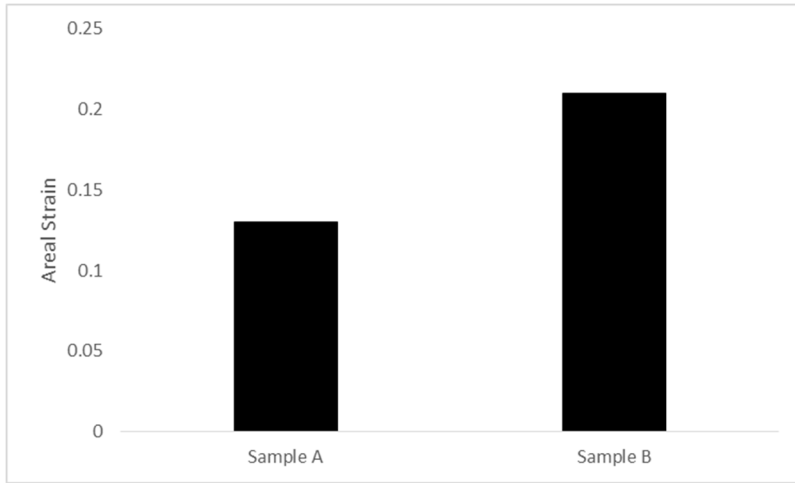
Figure 4-6: Areal Strain of the PCUU samples A (normal) (n=1) and B (compliant) (n=1) at 100 kPa. The compliant version of PCUU was nearly twice as complaint as the normal version of PCUU.

SEM imaging of PCUU scaffolds

The results of the SEM imaging showed that the PCUU scaffolds were porous and the fiber orientation was influenced by the direction and intensity of stretch. The increase in stretch from 0% to 25% led to increase in porosity from 37.6 ± 3.9 % (n=3) to 54.9 ± 1.7% (n=3). The porosity % at 75% stretch was slightly higher at 57.1 ± 2.8% (n=3) (Figure 4-11).

A   B   C
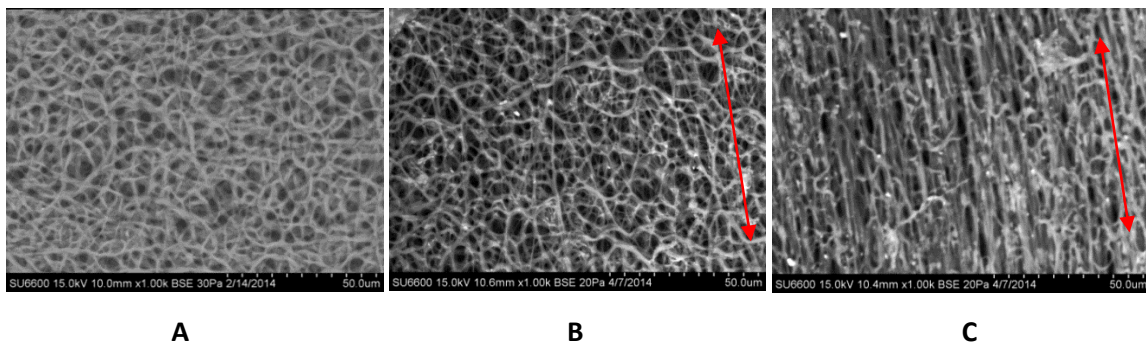
Figure 4-7: SEM images of PCUU at 1000X. PCUU specimen at 0% stretch (A), 25% stretch (B) and at 75% stretch (C). The PCUU fibers align depending on the intensity and direction of stretch (indicated by red arrow) and the % porosity increased nearly 70% from 0% stretch to 25% stretch.

Examination of BSMC viability and morphology on the PCUU scaffolds

The LIVE/DEAD staining of BSMC showed high viability (90.11%) on the PCUU scaffold (Figure 4-7A). Rhodamine-phalloidin and DAPI staining of BSMC demonstrated elongated cell morphology throughout the PCUU surface (Figure 4-7B). The smooth muscle phenotype of BSMC cultured on PCUU scaffolds for 7 days was confirmed by positive staining for uniform expression of α-actin (SMC marker) and SM1 and SM2 (Smooth muscle myosin heavy chain markers) (Figure 8).

A   B
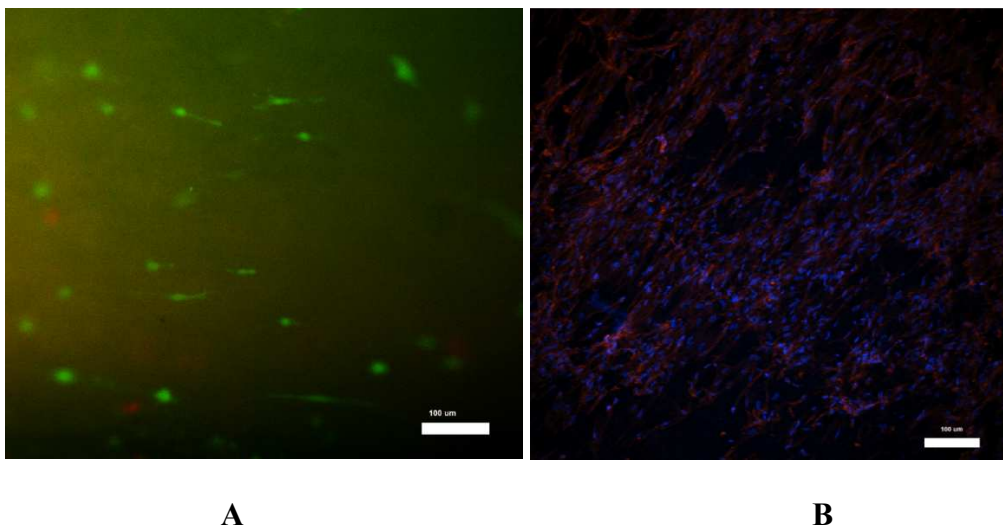
Figure 4-8: Live/dead (A) and Rhodamine –Phalloidin (B) staining of BSMC on PCUU scaffolds at 100X magnification after a 7 day culture-period. High viability of BSMC was confirmed by the presence of 90.11% live (green) cells among the total cells

in the scaffold (A) using imageJ. The Rhodamine-Phalloidin and DAPI results demonstrate F-actin expression in the well distributed and elongated, spindle-like bladder smooth muscle cells (B).
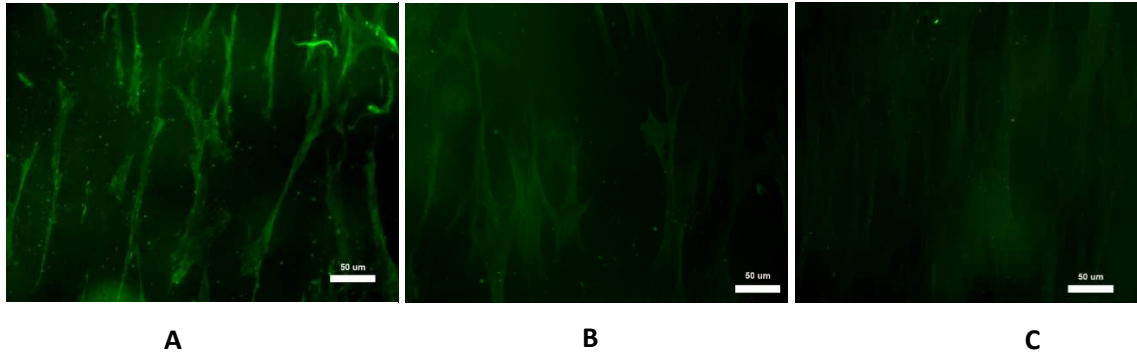
Figure 4-9: Immuno-staining of BSMC on the PCUU scaffold with antibodies for α-actin (A), SM1 (B) and SM2(C) after the 7 day time-point. The Results indicate contractile smooth muscle cell morphology (A) and expression (B & C).

Pressure-volume testing of PCUU scaffolds

The results of the pressure –volume experiment provided evidence that bladders patched with PCUU scaffolds withstood pressure up to 60 cm H_2O (Figure 4-9) after which the defects caused by suturing enlarged leading to leakage of colored saline from the bladder. The control bladders could withstand pressure more than 100cm H_2O after which leakage of saline begins from the bladder at the region of connection with the syringe pump. The pressure volume curve indicted reduction in capacity (also seen in Figure 4-10) and reduced toe region in the sutured bladders compared to the control bladders.
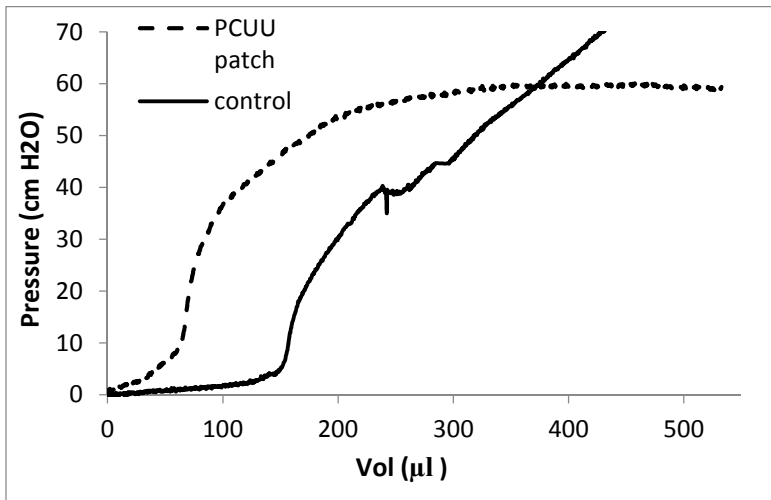
Figure 4-10: Comparison of the pressure-volume relationship of PCUU sutured bladders (n=1) versus native bladders (n=1). The PCUU sutured bladder withstood pressure up to 60 cm H_2O
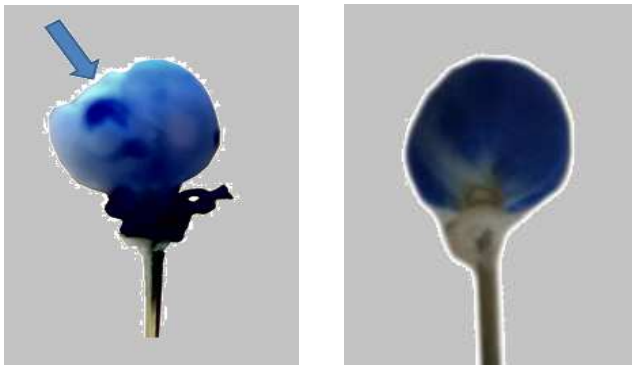
Figure 4-11: Rat bladders at 40 cm H20 with PCUU patch (left) and without PCUU patch (right). Arrow indicates the PCUU patch (~20% the size of the bladder)

Discussion

Previous studies demonstrated that PGS-PCL based scaffolds designed for vascular tissue engineering applications supported cell proliferation and ECM production of human umbilical cord vein endothelial cells and mitral valve interstitial cells (98, 99). Thus, we hypothesized that these scaffolds that are fabricated by combining blends of non-acrylated PGS pre-polymer with biodegradable poly (ε-caprolactone) (PCL) (both approved by FDA) (98) may provide a suitable milieu for bladder tissue engineering. The uniaxial tensile testing of the PGS-PCL scaffolds in the present study revealed that the maximum tension at failure was on average 0.079 N/mm. This was significantly lower than the maximum tension for the normal human bladder 0.2-0.4 N/mm (50) and hence, is unsuitable for bladder tissue engineering purposes due to this mechanical mismatch.

PEUU scaffolds have been used in Lewis rats as patches (1) to promote remodeling and improve function of subacute myocardial infracts, (2) to replace a surgical defect in right ventricles , (3) abdominal aortic wall replacement and have demonstrated smooth muscle tissue regeneration, cellular integration, mechanical reinforcement and minimal inflammation (105-108). Similarly, PCUU scaffolds have been used *in vivo* studies as patches in lewis rats with myocardial infraction and have prevented further deterioration and improved neovascularization and elastin levels. The uniaxial tensile testing results in the present study demonstrated that PEUU scaffolds displayed high stiffness under low forces, unlike the bladder tissue which exhibits a considerable toe region (large deformation under low stress) in its stress-strain curve (50).In contrast, PCUU scaffolds exhibited a non-linear behavior, typical of bladder tissue, displaying relatively high

compliance at low forces and high strength to withstand physiological bladder pressures

(92). Based on these results, subsequent experiments focused on characterization of

PCUU scaffolds.

Although uniaxial tensile testing can provide insightful data, it is not

representative of physiological loading conditions in the urinary bladder, where loading

occurs in all three dimensions. Since the urinary bladder can be biomechanically

characterized as an incompressible thin membrane material due to negligible thickness of

the bladder wall during loading, biaxial mechanical testing would more efficiently mimic

the physiological bladder loading (109). For this reason, we performed preliminary

biaxial testing of acellular PCUU scaffolds with assistance from CellScale technical staff.

The stretch ratio (deformed / original length) of the PCUU scaffolds under equi-biaxial

stress of 100 kPa were estimated to be 1.09 ± 0.03(X-axis) and 1.11 ± 0.04 (Y-axis) for

normal PCUU and 1.14 ± 0.04 (X-axis) and 1.17 ± 0.03(Y-axis) for compliant PCUU,

respectively (Figure 5). These values are in the same range as the biaxial stretch values of

native bladder, which were reported to be 1.09 (X-axis) and 1.10(Y-axis) at 100kPa equi-

biaxial stress (109). The results from these tests demonstrated the anisotropic nature of

the PCUU scaffolds was similar to that of soft tissue organs such as the urinary bladder

under physiological conditions (92), which may be further altered by varying

electrospinning conditions. The results of biaxial testing also provided evidence that both

types of PCUU (normal and compliant) displayed the areal strain under 100 kPa

equibiaxial stress that were slightly lower (normal-0.13, compliant-0.21) (Figure 6) than

that of native rat bladder (~0.28) reported previously by Gloeckner et al (109). It should

be noted, however, that the values reported by Gloeckner et al. were obtained after subjecting the native bladder to pre-conditioning wherein the first nine loading-unloading cycles were performed to stabilize the tissue mechanical responses for reproducibility (109).Thus, the freshly harvested bladder (close to *in vivo* state)would have been stiffer in the absence of preconditioning and would be further closer to the range of the stiffness of the PCUU scaffolds in this experiment.

LIVE/DEAD and rhodamine-phalloidin staining of BSMC indicated high viability (more than 90%) (Figure 6A) and elongated, spindle like morphology of BSMC indicating that the scaffold conditions could support native smooth muscle phenotype (Figure 6B). The immuno-staining results indicated maintenance of contractile smooth muscle cell markers by the BSMC seeded on the surface of PCUU scaffolds at the end of 7 days (Figure 7). Thus, PCUU indicated its cytocompatibility as scaffold to maintain contractile smooth muscle phenotype *in vitro*. The maintenance of contractile phenotype is important for the successful outcome as an engineered tissue because BSMC have a tendency to differentiate into synthetic / proliferative phenotype (19). Synthetic smooth muscle cells produce excessive amount scar tissue that will decrease compliance and eventually reduce functional bladder volume and increase urinary storage pressures (12).

The pressure-volume experiments of the PCUU-sutured bladder were conducted using our custom *ex vivo* pressure device, which was originally used in other studies of our group to determine the adhesive sealing strength in bladder puncture wounds (110). The previous study demonstrated that the maximum pressure the samples could withstand were 225 ±52.9 cmH$_2$O, for whole bladders and up to 100±5.4 cmH$_2$O for adhesive-

sealed ones (110). In the present study, the PCUU sutured bladders could withstand pressure up to 60 cmH$_2$O before saline started to leak from the defects around the sutures, which prevented us from quantifying the rupture pressure. The results of the pressure-volume experiments showed that the PCUU sutured bladders exhibited an elastic region similar to that of the intact bladder, and had a reduced capacity and shorter toe region compared to the control. The PCUU scaffold did not display unusually high stiffness at low forces and withstood peak stress the bladder experiences typically in the human body and thus, indicated its suitability to be used as a urinary bladder scaffold. We discovered, however, that these experiments were extremely difficult to obtain reproducible data because of poor tissue integrity and leaking of saline from the puncture wounds created during suturing. Although we attempted to seal puncture wounds with cyanoacrylate (super glue), this resulted in stiffening of the bladder-scaffold construct and inaccurate pressure-volume reading.

The SEM imaging results showed that the PCUU scaffold is porous and conducive for BSMC to grow and proliferate. The fibers align along the direction of stretch naturally and increase in stretch lead to increase in porosity, which is conducive for BSMC to infiltrate the scaffold under physiological loading conditions. It should be noted, however, that the percent porosity was analyzed semi-quantitatively using the SEM images and image analysis software unlike conventional approaches to measure the physical porosity by mercury intrusion and ethanol displacement techniques (20). Hence, the percent porosity of PCUU scaffolds calculated in the present study (37.6 ± 3.9 % to

57.1± 2.8%) was not directly comparable to % porosity of PCUU (84±4 %) as reported in previous studies by Hasizume et al. (20).

The SEM imaging also revealed that the pore diameter in the PCUU scaffolds is between 5-20 μm across the scaffold. This is lower than the pore size (35-70 μm) typically necessary to promote angiogenesis (111) and hence the current version of PCUU is unsuited for encouraging capillary infiltration into the scaffold *in vivo*. Several studies have shown that time period and depth of vascular ingrowth into the biomaterial implanted may depend on pore size (112). One method to increase pore size would be to increase the amount of media (DMEM +10% Fetal Bovine Serum +10% horse serum + 5% penicillin/streptomycin) electro-sprayed onto the scaffold while it is being electrospun to loosen up the fibers while fabrication. The pore size and % porosity can also be increased by increasing the mandrel translation speed during the electrospinning process. Previous studies have shown that an increase in mandrel translation speed corresponded to a decrease in fiber intersection density and the formation of a more open structure in PEUU scaffolds (107).

In summary, comparison of mechanical behaviors of biodegradable elastomeric scaffolds demonstrated that the PCUU scaffolds mimic urinary bladder mechanics most effectively compared to PGS-PCL and PEUU. The PCUU scaffolds exhibit relatively high compliance under low forces and are able to withstand stress corresponding to 100 kPa and, thus, possess the strength and stiffness necessary to be used for urinary bladder tissue engineering. The PCUU scaffolds also showed cyto-compatibility to maintain the contractile phenotype of BSMC and increased porosity with increasing stretch indicating

its ability to aid in infiltration of smooth muscle cells. Hence, the PCUU scaffolds were selected to be tested in our custom-made bioreactor and *in vivo* studies for further characterization towards bladder tissue engineering applications.

Chapter 5

CUSTOM-MADE BIOREACTOR FOR CONDITIONING OF BSMC SEEDED

PCUU SCAFFOLDS

Introduction

The results reported in Chapter 4 demonstrated that electrospun, wet PCUU

scaffolds exhibit mechanical behavior similar to that of the human bladder and displayed

BSMC cytocompatibility. Moreover, the immuno-staining of the BSMC seeded on top of

the PCUU scaffolds indicated expression of α-actin (early SMC marker) and SM1 and

SM2 (smooth muscle myosin heavy chain contractile phenotype marker) (Figure 4-6).

However, there is tendency of functional contractile bladder smooth muscle cells in

culture to de-differentiate into a synthetic, proliferative smooth muscle phenotype (55).

Previous work by our group demonstrated that when exposed to sustained tension, BSMC

seeded in collagen gels expressed a significantly greater level of contractile phenotypic

marker proteins (a-SMA and SM22) and a more elongated and spindle shaped

morphology compared to BSMC seeded in collagen gels without tension (62). Based on

these results, the goal of the present study was to examine the effect of controlled tension

loading conditions on the BSMC on the PCUU scaffold.

A number of studies have investigated the effect of mechanical forces by

bioreactors on cells seeded on bladder scaffolds. Human smooth muscle cells on a

flexcell device (FX-3000 , Flexcell International) were exposed to simulated bladder

filling and voiding of a five year old child via step-by-step elongation and relaxation (1%

increase every 5 min 12 s during a period of 104 min) for a period of 10 days (113).

However, this step-wise loading did not resemble physiological bladder filling and

emptying and hence, led to reduction in cell growth. A slight improvement in cell growth

was achieved by the coating of the ECM protein laminin. Thus, the study indicated that

coating scaffolds with ECM proteins like laminin and then subjecting it to physiological

bladder tension would aid in the maintenance of BSMC viability and growth.

Our custom made bioreactor was designed to expose cells on scaffolds to various

loading conditions to mimic bladder cycling, the process of sequential expansion and

contraction, characterized by the filling, storage and evacuation of urine in the bladder

(114). Our bioreactor has the ability to subject the scaffold to continuous pre-determined

stretch, maintain the stretch for a fixed time-period and ramp down to the pre-load length

similar to the filling, storage and evacuation of urine in the body, mimicking cycling.

Cycling, triggered by the production of urine, begins *in utero* and is important in the

anatomic and physiologic development of the normal bladder (114). BSMC in the body

rely upon mechanical stimuli as feedback (mostly coming from the supporting matrix) for

replication (7). Hence, stretch mimicking physiological conditions *in vivo* will aid in

promoting BSMC proliferation and growth.

Previous bladder tissue engineering studies using bioreactors have been limited to

subjecting the scaffolds to no more than 25% stretch (115), although the urinary bladder

under physiological conditions expands to more than 100% during filling (116). To

address this issue, the present study attempted to expose BSMC-seeded PCUU subjected

to 25-75% stretch using our custom-made bioreactor. To aid in the continued attachment

of BSMC onto the scaffold during mechanical loading, the PCUU scaffolds were coated with gelatin and fibronectin to provide cell –adhesion sites to form PCUU[FN-G] scaffolds. We performed two experiments to characterize the cytocompatibility and effectiveness of the PCUU[FN-G]. First we characterized BSMC morphology inside PCUU[FN-G], using histology on 7 and 21 day time –periods after cell seeding, to determine the extent of cell penetration. We then characterized the cell morphology and phenotype of BSMC subjected to stretch (1.25 for three hours) 7 days after cell seeding.

Materials and methods

BSMC seeding on PCUU

The PCUU scaffolds are placed in scaffold shaped defects on polydimethylsiloxane (PDMS) films formed on glass dishes. The PCUU scaffolds (~2 mm × 20 mm) were sterilized by soaking in 70 % ethanol for at least 1 hr and then washed thoroughly with sterile Dulbecco's phosphate buffered saline (DPBS) before cell seeding. The scaffolds are then soaked overnight in BSMC culture media composed of RPMI supplemented with 10% FBS and 1% antibiotic/antimycotic. The BSMC was suspended in 20-25 μl of BSMC culture media at a final concentration of ~1×10^5 cells/scaffold and seeded evenly at 4-5 places on each scaffold (the scaffolds were neither too wet or too dry while seeding the cells). The cells were allowed to attach to scaffolds for 1-1.5 h before flooding the culture plate with additional medium. After incubation under standard cell culture conditions (humidified, 37 °C, 5% CO_2 / 95% air) overnight, the cell-seeded scaffolds were transferred to new well plates with fresh media to separate

82

them from the cells attached to the bottom of PDMS wells. BSMC after three passages were seeded on PCUU scaffolds for immuno-staining experiments.

Bioreactor

The tension-controlled bioreactor was previously designed and assembled by members of Nagatomi lab to expose hydrogel-based 3D cell culture constructs to prescribed tensions in vitro. Briefly, it consists of two channels capable of subjecting specimens (~ 2 X 20 mm) to uniaxial tensile loading with a stepper motor (Haydon Kerk Motion Solutions, Waterbury, CT) and load cell (LCL-113, Omega) on each end of both channels. The stepper motor is controlled by a driver circuit through custom LabVIEW (National Instruments) program allowing for precise control of linear displacement, which simulates bladder filling in vivo. The LabVIEW program controls the uniaxial displacement via five major input parameters: loading rate, unloading rate, number of cycles, time target and desired stretch. The bioreactor is designed to operate in cell incubator conditions of 37°C and 5% CO_2 and device components can be sterilized by UV radiation.

A   **B**
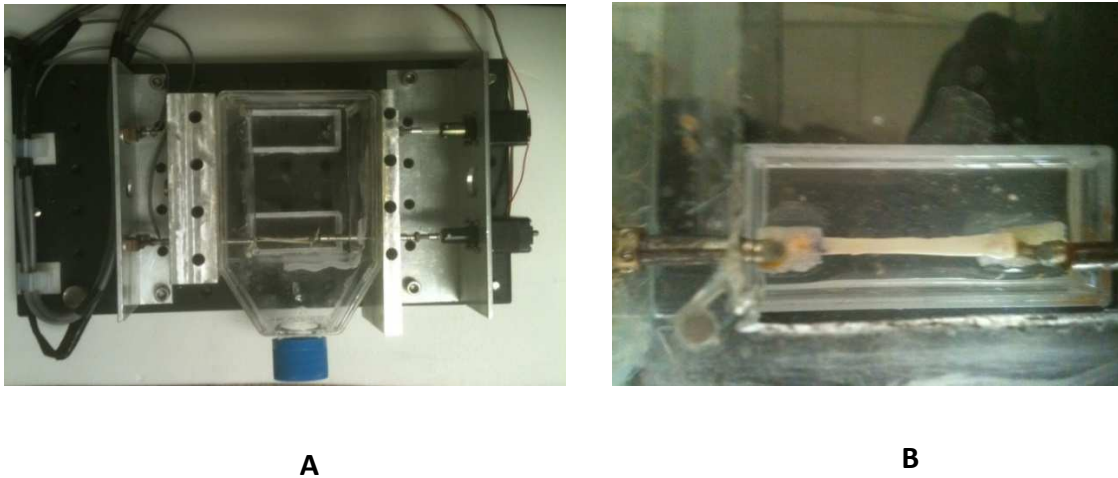
Fig 5-1: Custom made bioreactor (A) subjecting the PCUU scaffold (B) to stretch.
The Bioreactor subjected the PCUU scaffold to 25% stretch for one cycle (3 hours) in cell culture media.

Coating of PCUU scaffolds with Fibronectin-Gelatin films

Layer by layer (LBL) technique by alternate immersion of scaffolds into FN and gelatin solutions was used to form controlled nanometer-sized thin films on each PCUU fiber. Due to interactions with α5β1 integrin receptors on the cell surfaces, LBL preparation of FN-G films were intended to provide adhesive polymer scaffolds for cells without serious disruption of surface structure. Briefly, the PCUU scaffolds were immersed in 0.04 mg/ml fibronectin (FN) (Mw = 4.6×10^5, Sigma-Aldrich) and 0.04 mg/ml gelatin (G) in 50 mM Tris-HCl (pH = 7.4) for 2 min each for the preparation of FN-G films on the scaffolds. After each procedure, the PCUU was washed with 50 mM Tris-HCl (T) (pH =

7.4 after one min. After twenty one steps of immersion, (FN/G) $_{10}$ FN films were prepared onto the scaffold to form PCUU^{FN-G} scaffolds.

Stretch Experiments:

PCUU scaffolds (thickness: 0.1~0.2 mm) were prepared with dimensions ~ 2 X 20 mm and seeded with BSMC at a concentration of 3 X 10^5 cells/ scaffold. Cell-seeded PCUU scaffolds were cultured in RPMI supplemented with 10% FBS and AB/AM for 7 days and then mounted in the bioreactor. Each specimen was subjected to a uniaxial loading over three hours which included one hour of ramping up, one hour of maintaining the maximum stretch (1.25, 1.5, or 1.75), and one hour of ramping down to the pre-load length (Figure 5-2). Each cycle was designed to mimic the gradual stretching the bladder wall tissue during filling followed by voiding (117). However, gradual ramping down, instead of simulated voiding phase was used to avoid cell detachment from the scaffold due to sudden change in the length. The maximum stretch was determined based on the values for bladder filling reported in the literature (116).
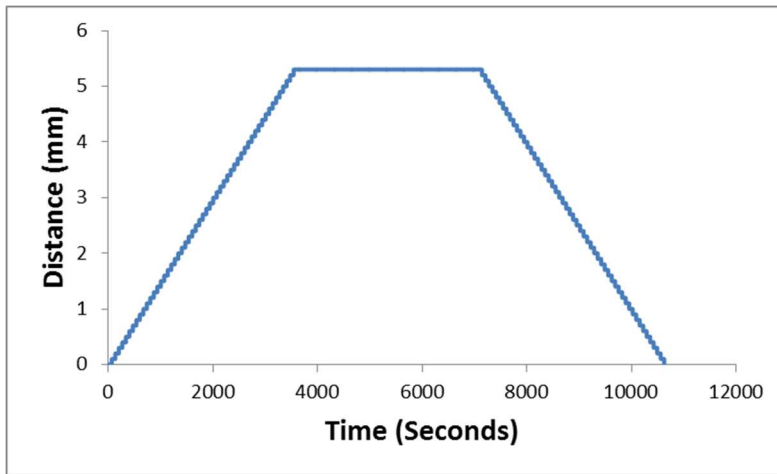
Figure 5-2: Representation of PCUU specimen subjected to 75% stretch for one cycle using the LabVIEW program. The cycle consists of 1 hour of ramping up, one hour of maintaining the maximum stretch (1.75), and one hour of ramping down to the pre-load length

Immuno-staining of BSMC seeded PCUU Scaffolds

The BSMC in the PCUU[FN-G] scaffolds was examined by immuno-staining for a smooth muscle cell phenotypic marker smoothelin. Briefly, the PCUU[FN-G] scaffolds were fixed for 20 min and then blocked using a solution composed of 2% bovine serum albumin, 3% goat serum, prepared in PBS. After triplicate washes with PBS, the PCUU[FN-G] specimens were incubated with primary anti-bodies for mouse smoothelin (1:100 dilution, Thermo scientific, USA) and then incubated at 4ºC overnight. The PCUU[FN-G] scaffolds were

then incubated with the secondary antibody Alexa-fluor 488 Anti-Mouse IgG (H+L) overnight, followed by nuclear staining with DAPI for 5 minutes.

Histological examination

The fixed samples were embedded in Richard Allen Scientific™ NEG 50™ (Frozen section medium, Thermo Scientific, USA) and frozen using Freeze Spray (Chemtronics, GA, USA). Serial sections were generated at thicknesses of 8 μm on a Microm HM505 N cryostat for conventional histology. The specimens were then imaged using laser confocal microscopy (C1Si Confocal; Nikon Ti Eclipse).

Results and Discussion

Stretch Experiments

Initially in all stretch experiments, the BSMC detached from the PCUU scaffolds after subjection to 25%, 50% and 75% stretch. We hypothesized that the PBS wash after sterilization was not enough to promote BSMC spreading and infiltration. Thus, the PCUU scaffolds were seeded with BSMC after 1 day in RPMI 1640 + 10% FBS + 1% AB/AM for ECM protein absorption onto the constructs. The Soaking of scaffolds in serum containing medium helped cells adhere better (Figure 5-3) to the PCUU construct. However, this did not prevent cells from lifting off the PCUU scaffold once it was subjected to stretch. Based on these results, we proceeded to use the layer by layer method to coat the scaffold with gelatin and fibronectin to assist in BSMC adhesion during the stretch cycle. The layer by layer coating of the PCUU constructs in previous

studies of our laboratory demonstrated that the protein coating did not affect the surface structure of the PCUU scaffolds by SEM imaging where uncoated PCUU scaffolds had the same fiber diameter as the PCUU^{FN-G} scaffolds. The cells continued to adhere to the PCUU^{FN-G} after 25% stretch for one cycle (Figure 5-5).
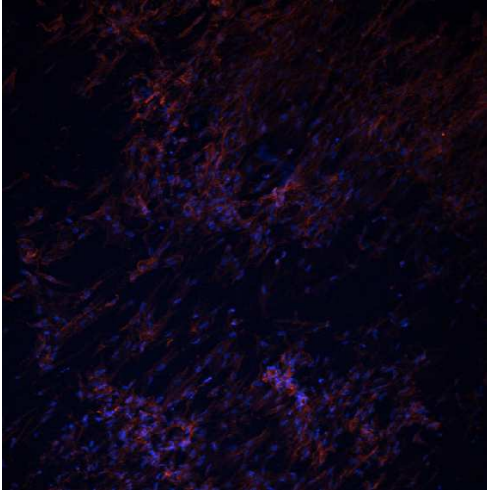
Figure 5-3: Cell adhesion on PCUU scaffolds soaked in cell culture media. The presence of RGD proteins in RPMI 1640 aided in cell adhesion throughout the scaffold.

Immuno-staining and histological examination of BSMC in the PCUU scaffolds

The BSMC infiltration into PCUU^{FN-G} scaffolds increased substantially from the 7 day to 21 day time-point as seen in figure 5-3. The BSMC were present only on the surface on day 7, but infiltrated uniformly up to ~ 50 µm and up to 60-70 µm into the scaffold in some regions on day 21.

<div align="center">A   B</div>
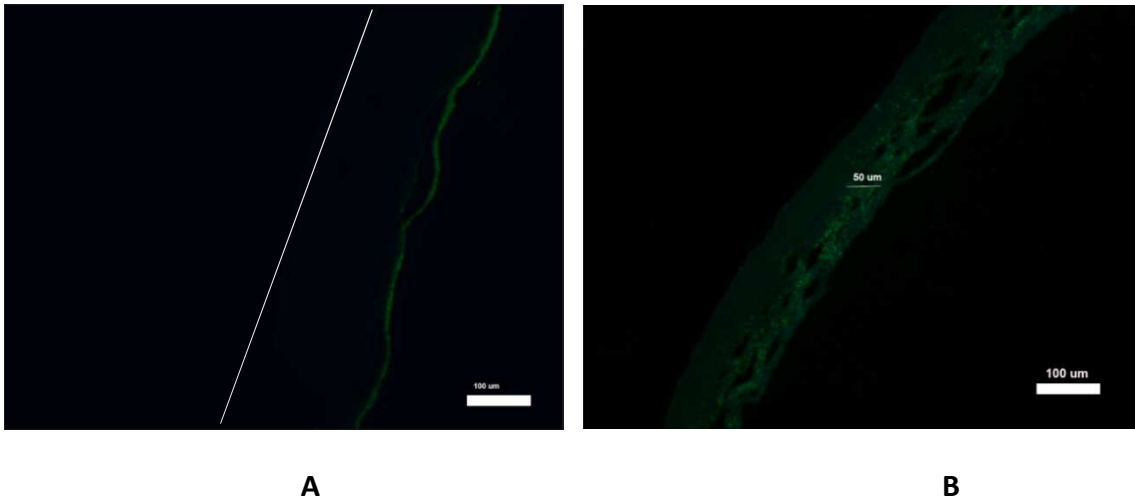
Figure 5-4: Cell infiltration in static PCUU^{FN-G} scaffolds. The penetration of BSMC was deeper inside the PCUU^{FN-G} section after 21 days (B) compared to the 7-day (A) time-point.The acellular surface (bottom) of the PCUU^{FN-G} scaffolds after 7 days is denoted by the white line.

The thickness of the detrusor smooth muscle layer in the human body is ~1.3 mm (73) and hence, based on the rate of BSMC infiltration seen in figure 5-4 (~60 μm in 14 days) , it would theoretically take 303 days for BSMC to actually infiltrate a clinically relevant scaffold implanted to replace the detrusor *in vivo*. Thus, to accelerate cell infiltration inside the PCUU $^{FN-G}$, different techniques need to be adopted. Electrospraying BSMC during electrospinning of PCUU can be done to form highly cellularized PCUU scaffolds, which would drastically reduce the culture time-period prior to implantion *in vivo*.This Cell microintegrated technology has been tested in PEUU scaffolds previously to form conduits for blood vessel replacement and has

demonstrated vascular SMC viability and cytocompatibility(101) after a four day time-point after cell spraying (101). Another technique which we could adopt to create clinically relevant PCUU scaffolds would be to culture BSMC on multiple thin PCUU sheets stacked one on another. This technique was used in studies by Srouji et al. where they nourished human bone marrow-derived mesenchymal stem cells seeded individually on thirty electrospun scaffolds (composed of PCL and collagen to form a stack), cultured in a dynamic flow bioreactor (118) and showed massive cell proliferation and distribution inside the scaffolds. Thus, theoretically following this method, we could stack 10-11 BSMC seeded PCUU sheets, culture the stack in a perfusion bioreactor system which could give us a completely cellularized construct in a period of four weeks which would eventually be implanted *in vivo*.

The stretch experiment demonstrated the continued presence of BSMC in PCUU^{FN-G} scaffolds after 25% stretch for 3 hours. The morphology and distribution of BSMC seeded on the surface resembled the control scaffold (figure 4B) unlike the occurrence of BSMC detachment previously.

A

B
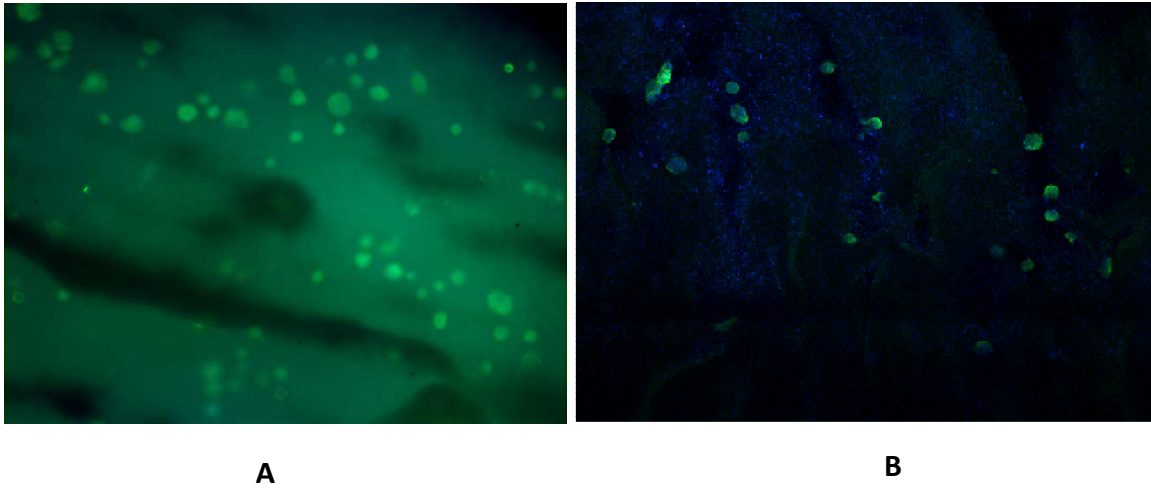
Figure 5-5: Immuno-staining of BSMC on the PCUU^{FN-G} scaffold with antibodies for smoothelin. The PCUU^{FN-G} scaffolds were seeded with BSMC for 1 week and consequently subjected to one cycle of 25% stretch for 3 hours before immunostaining are represented in figure A. The PCUU^{FN-G} Scaffolds which are not subjected to stretch are used as controls (B).

The results of the present study provided evidence that our custom-made bioreactor could generate accurate linear displacement on a polymer sample for a given time-period. The novelty of the tension-controlled bioreactor device is the ability to adjust linear displacement based on the current force monitored by the load cell for a desired number of cycles though automated functionality. The device could also be used with a displacement control mode to subject the scaffold to a prescribed maximum stretch. In the present study, the BSMC seeded PCUU^{FN-G} scaffold was exposed to a stretch as high as 1.25 without cell detachment. However, the BSMC displayed a round

morphology and sparse distribution due to the low cell seeding concentration (Figure 5-5). Based on our rhodamine-phalloidin staining of BSMC on PCUU surface (Figure 4-5) we could estimate that cell seeding at more than (2×10^6 cells/cm^2) could lead to the creation of cell bundles. Thus, future studies will need to use a higher cell concentration to increase cell-cell communication and faster cell infiltration throughout the PCUU^{FN-G} scaffold. Further studies could also focus on the bio-reactor being operated for longer time-periods and multiple cycles.

Chapter 6

IN VIVO STUDIES EXAMINING ACELLULAR PCUU SCAFFOLDS IN

BLADDER AUGMENTATION

Introduction

Previously, Atala and colleagues reported successful outcomes of implanting tissue engineered neo-bladders in both dogs and humans (13, 46). The scaffolds made of polyglycolic acid (PGA) coated with poly-DL-lactide-co-glycolide 50:50 (PLGA) were seeded with autologous urothelial cells on the luminal surface and smooth muscle cells on the exterior surface and cultured for 32 ± 2.8 days. Following implantation in beagle dogs, the neo-bladder was wrapped with the hosts' omentum for vascularisation (13, 46). The cell-seeded neo-bladders exhibited capacities and compliance greater than the pre-cystectomy level of the patients' bladders eleven months post-surgery and the retrieved tissues displayed a normal cellular organization, consisting of a trilayer of urothelium, submucosa, and muscle with innervation (46). Based on the success in the pre-clinical study using dogs, a similar approach for bladder augmentation with engineered neo-tissue was tested in humans with myelomeningocele needing cystoplasty (13). Among the types of scaffolds tested, collagen-PGA composite scaffolds with omentum wrapped exhibited the greatest bladder capacity and compliance. The abnormally high bladder pressure before the operation clearly improved 10 months after implantation of the neo-bladder (13). In addition, immunohistochemical analyses of biopsy tissues revealed that smooth muscle and urothelial cells within the regenerated bladder constructs were

phenotypically normal (13). The success of the bladder augmentation was limited and seemed to depend on the presence of omentum, which may or may not be available in all patients needing bladder replacement. Recent phase II clinical trials by Tengion® was performed using the autologous cell-seeded collagen-PGA/PLGA to establish the safety and efficacy of the regenerative biodegradable scaffold for use in bladder augmentation scaffold for patients (74). Ten patients between age-groups 3 to 21 years with medically refractory neurogenic bladders were selected for the trial and were monitored for a period of 36 months. The results demonstrated that compliance improved in 4 patients at 12 months and in 5 patients at 36 months, although the difference was not clinically or statistically significant. There was no clinical or statistical improvement in bladder capacity at 12 or 36 months in any patient (74). Adverse events occurred in all patients, and most were easily treated. Two patients had low cell growth following bladder biopsy, of whom one withdrew from the study and one underwent a second biopsy. Serious adverse events of bowel obstruction and/or bladder rupture occurred in 4 patients. These multiple adverse events without improving capacity or compliance resulted in discontinuation of the study (74).

A recent, comprehensive review of twenty eight bladder tissue engineering studies by Sloff M and group concluded that though pre-clinical studies using healthy animals showed promising outcomes, subsequent clinical trials could not replicate the results revealing dissimilar outcomes in different clinical/disease backgrounds (119). In addition, the analysis showed that the proliferation and differentiation capacity of isolated UCs and SMCs from diseased patients was diminished and altered compared to healthy

94

individuals. Thus, to correctly predict the effect of tissue engineering for bladder augmentation, animal models with dysfunctional bladders have to be evaluated. Hence, our goal in the present study was to develop a clinically applicable animal model for evaluation of engineered bladder tissue. Thus, in collaboration with Drs. Todd Purves and Monty Hughes, Department of Urology, Medical University of South Carolina, we conducted a pilot study to augment the bladder with a PCUU patch using a rat model of bladder outlet obstruction (BOO). Bladder outlet obstruction (BOO) is a well-known bladder dysfunction model induced by benign prostatic hyperplasia or urethral stricture (120). When there is mild-to-moderate BOO and conservative treatments fail to protect the upper urinary tract, the only remaining treatment option is surgical reconstruction of the bladder. To date, the BOO model is the most prominent model for bladder dysfunction, and other pathologic models are still in early stages of development (120). BOO is one of the most common problems in elderly males. It is caused by collagen deposition in the bladder as a result of various pathological processes. Eventually, this collagen deposition results in bladder fibrosis and induces a flaccid, noncompliant bladder. Bladder fibrosis adversely affects the composition of the bladder wall by reducing the smooth muscle component, resulting in low bladder compliance (120). Due to the limitation with resources and surgeon time, only three animals have been studied to date. During the 21-day implantation period, voiding volume and bladder capacity were calculated at every 7 day time-period by gavaging the rat with H_2O and quantitating the voids in a custom made metabolic cage and weighing scale. Following sacrifice of the

animal, histology and immuno-histochemistry were performed to characterize cell infiltration and calcium deposition.

Materials and methods

Bladder surgery and PCUU implantation

Creation of bladder outlet obstruction and the augmentation surgery were performed by Dr. Todd Purves of Medical University of South Carolina following a established protocol. Briefly, for all BOO rats a sterile, lubricated catheter (P50 tubing; O.D. 1 mm) was inserted transurethrally, the end cauterized and the tubing secured to the inguinal region using 5-0 PGA suture material. The abdominal cavity was then opened longitudinally and the urethra identified. 5-0 silk suture material was then passed around the urethra and tied securely to produce the BOO or tied loosely for Sham BOO animals. The inguinal stich was then cut and the catheter removed. After a period of 10 days, the animals are then anesthetized by intra-peritoneal injection of ketamine hydrochloride (90 mg/kg) and xylazine (10 mg/kg) and then shaved to expose the surgical site using a midline abdominal incision above the pubic bone. A 1 cm-long incision was made at the dome of the bladder using surgical scissors to create a defect and a square piece (1 cm x 1 cm) of PCUU scaffold was sutured using a non-absorbable 8-0 nylon suture (n=1) and absorbable 7-0 Vicryl Sutures (n=2) (Figure 6-1).

Figure 6-1: *in vivo* acellular PCUU implantation. A 1x1cm PCUU patch is sutured onto the day 10 BOO bladder.

Monitoring voiding volume and bladder capacity

At the end of prescribed time-periods (Days 1,7,14, and 21) after PCUU implantation, the rat voiding volume and bladder capacity was studied by placing the rat in a custom made metabolic cage (23 x 15 x 23 cm) with a wire mesh bottom above a scale (mettler toledo, Columbus, Ohio) (Figure 6-2). To ensure that the rat would void recordable volumes of urine during the experiment conducted in day time, the animal was gavaged with 500 µl of drinking water prior to being placed into the cage. The reading of the scale was continuously monitored by a computer with special software (MED-CMG software, Catamount Research and Development, St. Albans, VT)) which registered the time and volume of urine voided by the rat. After the urine voids were recorded on each

day (discounting fecal voiding), the rat was returned to the animal facility. The voiding

volume and bladder capacity of Sham BOO rats (BOO rats without bladder defect

creation and scaffold implantation) , control rats (normal rats with no procedure) , PCUU

day 0 rats (rats with 10 day BOO before defect creation and scaffold implantation) were

also measured by Dr. Monty Hughes, Department of Urology, Medical University of

South Carolina.
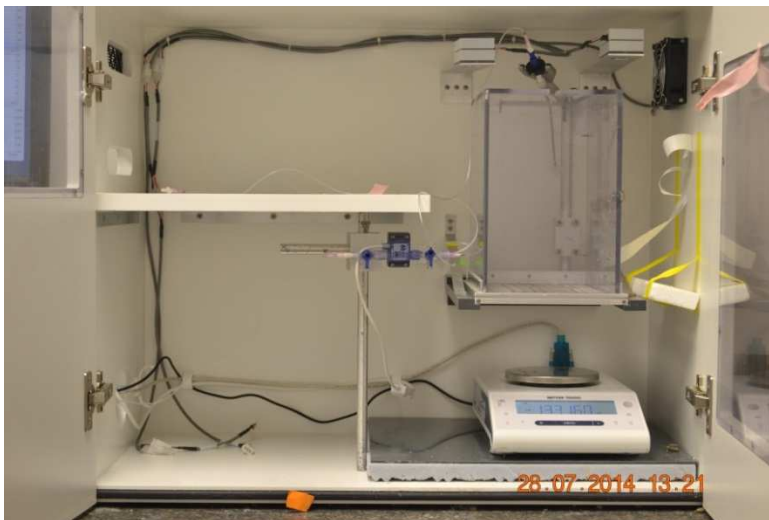

Figure 6-2 : Monitoring voiding volume and bladder capacity. The image describes

the custom-made metabolic cage with a wire mesh bottom placed above a monitoring

scale.

Histological analysis of explanted tissues

At the end of three week time period after implantation, the rat was euthanized

using isoflurane (Piramal Healthcare , Andhra Pradesh , India) and the whole bladder was

harvested. The bladder was then cut in half horizontally and the bladder half with the patch was placed in neutral buffer saline (NBF) for fixing.The bladder was inverted to expose the region of the patch , which was cut into four parts for histological and immunohistochemical analysis. Bladder tissue from control rats (without surgery) and sham BOO rats (BOO rats without PCUU patch) were also examined. The BSMC in the PCUU scaffolds was examined by immuno-staining for α-actin and smoothelin. Briefly, the PCUU scaffolds were fixed for 20 min and then blocked using a solution composed of 2% bovine serum albumin, 3% goat serum, prepared in PBS. After triplicate washes with PBS, the PCUU specimens were incubated with primary anti-bodies for mouse smoothelin (1:100 dilution, Thermo scientific, USA) and α-actin (1:100 dilution, Sigma-Aldrich, USA) and then incubated at 4ºC overnight. The PCUU scaffolds were then incubated with the secondary antibody Alexa-fluor 488 Anti-Mouse IgG (H+L) overnight, followed by nuclear staining with DAPI for 5 minutes. To create frozen histological sections the fixed samples were embedded in Richard Allen Scientific[TM] NEG 50[TM] (Frozen section medium, Thermo Scientific, USA) and frozen using Freeze Spray (Chemtronics, GA, USA). Serial sections were generated at thicknesses of 8 μm on a Microm HM505 N cryostat for conventional histology on glass slides. Other speciments were stained with Hematoxylin and Eosin (H& E), Masson's Trichrome and alizarain red based on standard protocols after obtaining frozen sections on glass slides. All the staining techniques were performed using well established protocols for frozen sections. Briefly, the H& E stain consists of hemotoxyin which is a basic dye (positively charged) which stains the nuclei blue and Eosin which is a acidic dye (negatively charged) which

stains the cytoplasm and other tissue elements in various shades of pink. The Masson's

trichrome staining is used mainly for the detection of collagen fibers which is stained

blue, nuclei which is stained black and muscle,cytoplasm and keratin which is stained

red. The alizarain red stains the calcium deposits in the scaffold in an orange-red color.

Results

Monitoring Voiding volume and bladder capacity

The results of the present study provided evidence that the mean voiding volume

remained similar on day 0 (639.43 ± 239.48 µl) (n=3), day 1 (635.21 ± 391 µl) (n=3) and

day 7 (638.64 ± 413.33 µl) (n=3) followed by a increase on day 14 (815.65 ± 210.45

µl)(n=2) and day 21 (968.75 ± 592.83 µl) (n=2). The control rats had a mean voiding

volume of 871.87 ± 166.14 µl (n=2) and the sham BOO rats had a mean voiding volume

526.9 ± 318.15 µl (n=5). The time span for 8 voids was 8308 ±5359 seconds on day 1,

followed by a decrease on day 7 (7612 ± 700 seconds), leading to a gradual increase on

day 14 (9973±1453 seconds) and day 21 (10,130±10533 seconds) surpassing the time

span of day 1. The control rats did not void more than 4 times 1.5-3 hours after gavaging

and the sham rat took 3963.625 ± 755.72 seconds for 8 voids(n=2), with the remaining

two rats not voiding more than 6 times even after 2.5 hours. The maximum voiding

(bladder capacity) followed a slightly different pattern as the mean voiding volume where

similar values were obtained on day 1 (maximum: 1506 µl, minimum: 313 µl) and day 7

(maximum:1576µl, minimum : 226 µl) followed by a decrease on day 14

(maximum:1167 µl, minimum: 505µl) and a subsequent increase (maximum:1997 µl,

minimum: 230 µl) on day 21 (Table 1).the maximum and minimum voiding values of control and sham BOO rats were (maximum: 1163 µl, minimum: 595 µl) and (maximum: 1414 µl, minimum : 200 µl) respectively (Figure 6-3).

Sample	Number of specimens	Maximum Capacity (µl)	Average voiding volume (µl)
Control	2	1163	871.88 ± 166.14
Sham BOO	4	1414	526.9 ± 318.15
PCUU Day 0	3	1371	639.43 ± 239.28
PCUU Day 1	3	1622	635.21 ± 390.55
PCUU Day 7	3	1576	638.64 ± 413.33
PCUU Day 14	2	1167	815.65 ± 210.45
PCUU Day 21	2	1997	968.75 ± 592.83

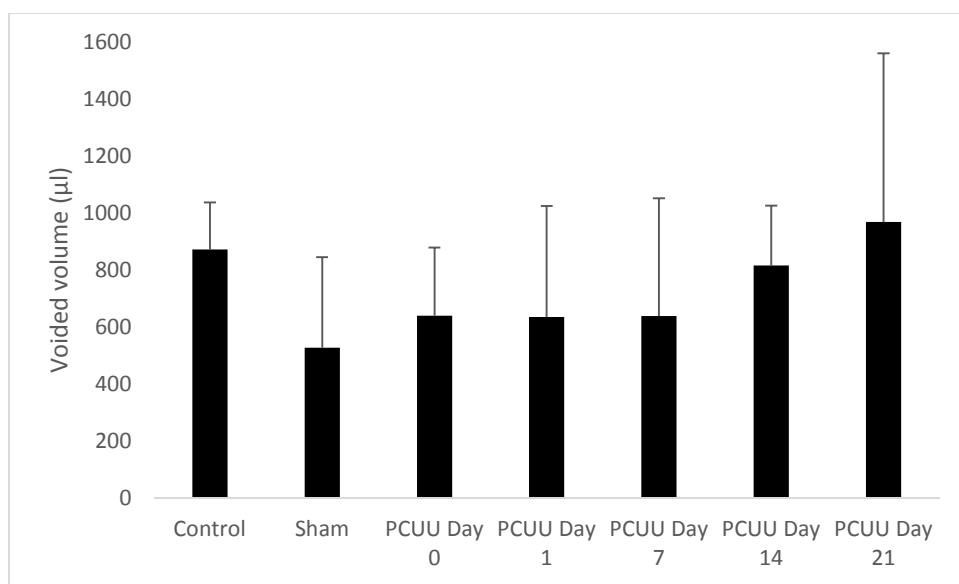**Table 6-1: Measurement of micturition for various samples tested.**

Figure 6-3: Measurement of micturition values. The voiding volume on urine voided by rats for different samples. Values are mean ± SEM; n=2 for control bladders, PCUU Day 14 and 21; n=4 for sham BOO rats; n=3 for PCUU Day 0, 7 and 14.

Morphology and histological analysis

The implanted PCUU scaffold was visible on inspection of the exterior of the augmented bladder upon harvest (Figure 6-4A). Caliculi were clearly visible throughout the inner lumen of the bladder (Figure 6-4B). The PCUU scaffold remained intact for the 21 day period and based on its white color clearly distinguishable from surrounding tissue inside the bladder lumen . H&E stained sections of the explanted PCUU scaffold revealed smooth muscle cell infiltration indicated by eosin (pink) for the cytoplasm of muscle cells and connective tissue cells or fibroblasts indicated by a light purple

(haemotoxylin) for cell nuclei (Figure 5A). Unlike the control explant (figure 5B and 5H), the sham BOO explant (Figure 5C and 5I) indicated the presence of possibly immune cells indicated by the black dots in the muscle layer. The intense red color of Alizarin Red staining indicated that the PCUU specimen was infiltrated with calcium deposits (Figure 5D) which was nearly absent in the control and sham specimens (Figure 5E and 5F). The masson's trichrome staining indicated an acute inflammation in the PCUU explant indicated by the presence of nuclei (black) representing fibroblast and macrophages in the scaffold (Figure 5G). The immuno-staining for α-actin and DAPI indicate presence of cells throughout the scaffold (Figure 5K) and infiltration of smooth muscle cells limited to the surface of the scaffold in contact with bladder tissue was demonstrated by immuno-staining for smoothelin and DAPI (Figure 5N).The negative control specimen with no primary antibody (α-actin and smoothelin) proved the absence of non-specific binding of the α-actin and smoothelin antibodies and indicated only the presence of DAPI staining (Figure 5P). The control and sham BOO explants demonstrate the presence of smooth muscle cells throughout the sections when stained for α-actin (Figure 5L and 5M) and smoothelin (Figure 5N and 5O) respectively.
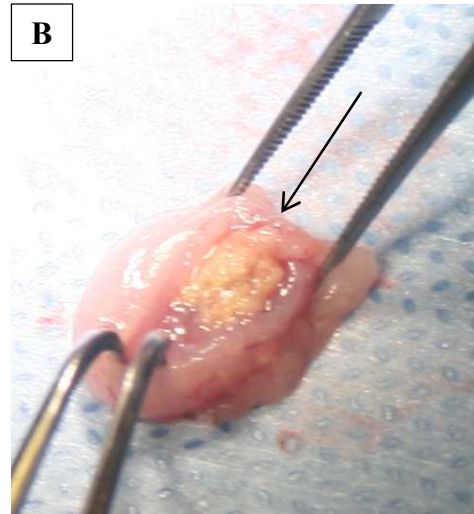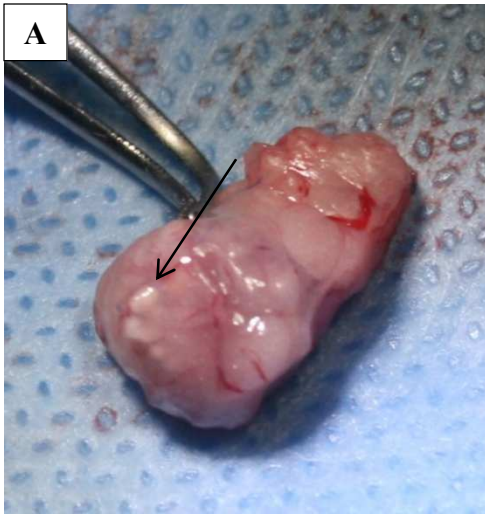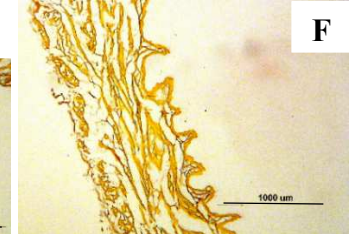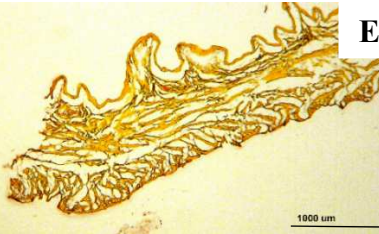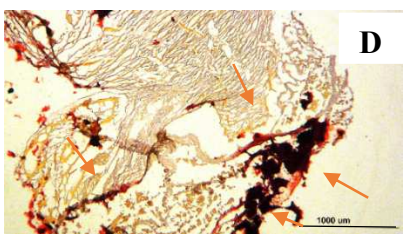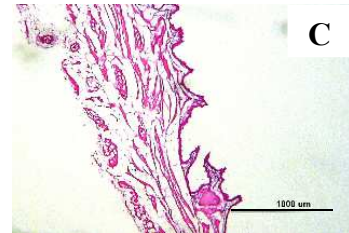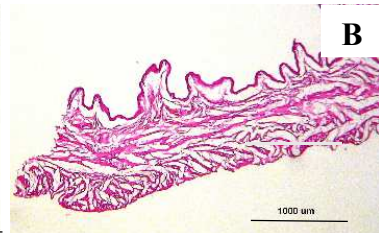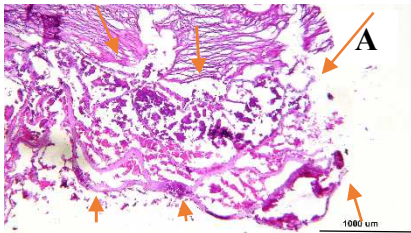
Figure 6-4 : Augmented Bladder removal after 21 days. The presence of the PCUU

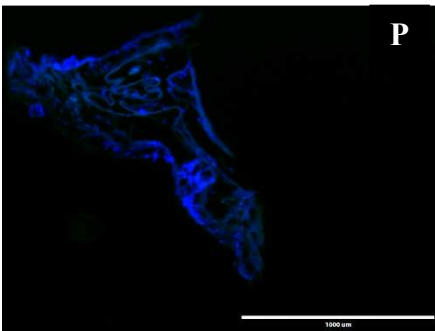scaffold (**A**) and calcium depositions (**B**) is indicated by the black arrow.
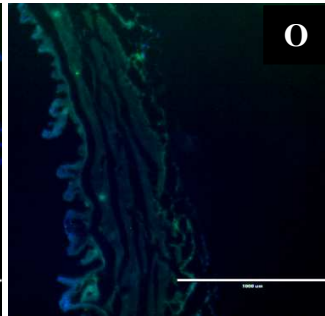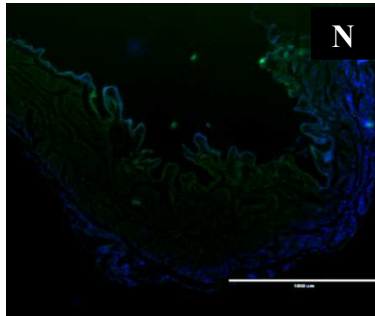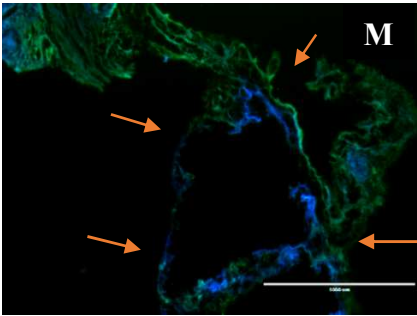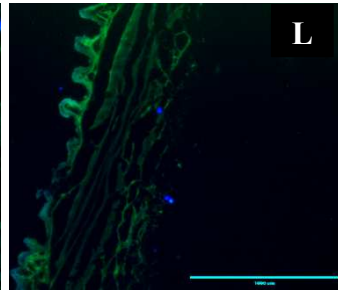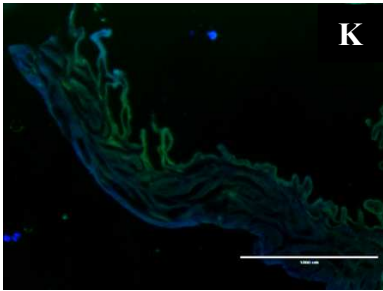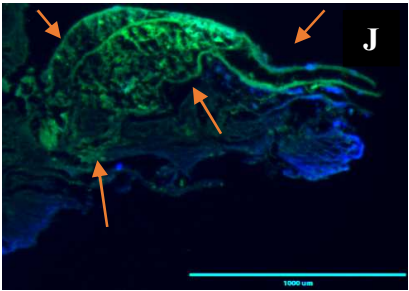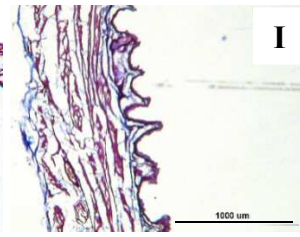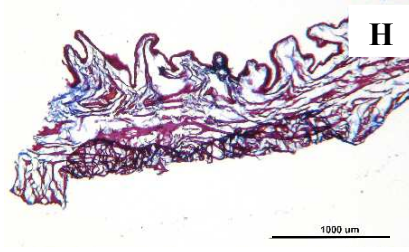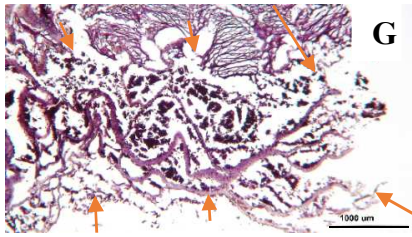
Figure 6-5: H& E staining of PCUU scaffold (A), control bladder (B) and sham BOO bladder (C) tissue sections, Alizarin red staining of PCUU scaffold (D) control bladder (E) and sham BOO bladder (F) tissue sections and Masson's Trichrome staining of PCUU scaffold (G) , control bladder (H) and sham bladder (I) tissue sections at 40X magnification.Immuno-staining for α-actin and DAPI on the PCUU scaffold (J), control bladder (K) and sham bladder (L) tissue sections , Immuno-staining for Smoothelin and DAPI on the PCUU scaffold (M), control bladder (N) and sham BOO bladder (O) tissue sections along with PCUU scaffold with no primary antibody (P) at 40X magnification. The PCUU scaffolds demonstrated scattered pink (eosin) staining indicating cytoplasm in muscle cells and a light purple (haemotoxylin) indicating nuclei of connective tissue or fibroblasts**.** The Masson's trichrome staining indicated red (muscle) , blue (collagen) and nuclei (black) .The PCUU scaffolds demonstrated the orange-red coloration indicating calcium deposits.The PCUU scaffold , control and sham bladder demonstrated the presence of cellular cytoskeleton (green) and nuclei (blue) in the sections. The absence of primary antibody showed only DAPI staining indicating that the green coloration was not non-specific binding. The orange arrows indicate the PCUU explant attached to rat bladder tissue.

Discussion

Although the sample size was limited to two successful animals, the present pilot study of *in vivo* bladder augmentation provided a large amount of valuable information, which could not have been gained from *in vitro* studies alone. First, it demonstrated that

augmentation of the bladder with a PCUU scaffold led to extension of the BOO rats

survival (66 % survival rate was observed 31 days after BOO), which otherwise is limited

to 1 - 2 weeks. Second, the rat BOO model provided a platform of bladder dysfunction

for which functional changes could be monitored. In addition, we found that the BOO-

induced hypertrophy of the bladder made it easier for augmentation.

BOO bladders are overactive bladders typically charcterized by high bladder

pressure and low urine flow rate usually accompanied by small voided volume of urine.

In our study, PCUU day 1 was characterized by bloody voids due to surgical insult to

tissue followed by healing by day 7. However,the voiding volume measurements

demonstrated that mean voiding volume and bladder capacity increased with time and

was highest for the PCUU day 21 compared to the mean voiding volume and bladder

capacity for PCUU day 1, control and sham BOO (Table 1). In rats, bladder tissue

engineering leads to a larger bladder volume after treatment due to the high regenerative

capacity of the rat bladder, in that even after subtotal cystectomy without augmentation,

the bladder volume recovers completely (119). However, Eberli et al. have reported that

canine BSMC and urothelial-seeded collagen-PGA scaffold implanted subcutaneously in

athymic mice demonstrated a scaffold tissue shrinkage at the 4 week time point compared

to the 2 week time point (47). The volume reduction is attributed to the degradation of

PGA-fiber loops with time (47). Contrary to their report, the PCUU scaffold in our study

did not result in shrinking within the three-week time period. Also, the scaffold did not

lead to scar tissue formation at the end of three weeks.

The results of histological analysis provided evidence that cell infiltration after 3 weeks of implantation was limited to smooth muscle cells near the edge of the PCUU construct and other connective tissue cells, fibroblasts sparsely populating the rest of the scaffold. This was further confirmed by the immuno-staining of specimens where presence of cell nuclei and α-actin throughout the scaffold and smoothelin on the extremities of the scaffold were observed. The relatively slow smooth muscle cell infiltration into the PCUU would potentially lead to slower integration into the host tissue. To improve the rate of smooth muscle regeneration in the scaffold, it may be beneficial to pre-seed PCUU scaffolds with BSMC before implanting onto rat bladders. Previous studies by Zhang et al. have demonstrated that human BSMC- and urothelial-seeded SIS scaffolds displayed progressively organized tissue regeneration compared to acellular SIS scaffolds (51) when implanted in nude mice. However, in diseased bladders there is a lack of healthy, accessible cell source within the human population. The autologous BSMC also have a prolonged cell expansion time (67). Hence, several studies are focusing on the use of adipose derived stem cells (ADSC) instead of autologous cells. Studies by Jack et al. have shown the ability of ADSC to differentiate into functional and contractile smooth muscle cells after 12 weeks of implantation when seeded in adult female Rnu athymic rats (67). However, the regenerated bladders in the study by Jack et al. displayed signs of bladder caliculi (67) similar to the calcium deposits seen in the PCUU scaffold implantation of the present study. The cause of stone formation on scaffolds in the bladder is only partially understood at this point. Studies by Seth and colleagues have shown that silk-based scaffolds implanted in rat bladders for a period of

10 weeks also exhibited the presence of calculi (121), but the extent of bladder calculi formation was dependent on the processing method used for silk scaffold construction. On the scaffolds fabricated by solvent-casting/salt-leaching method in combination with silk film, casting stones formed in lesser frequency and smaller diameter than those fabricated by gel spinning technique. In addition, they demonstrated that the more compliant the silk scaffolds were, the lower the percentage of calcium stone formation was displayed (121). However, when we compared the most compliant version of their silk scaffold (maximum elongation 197±4 % (121)) to our PCUU scaffold (maximum elongation 243±26 %), it appears that mechanics of PCUU may not be the cause for caliculi formation in the present study. Another possible reason for the formation of caliculi was the use of non-absorbable sutures, which we used in the first rat for implanting PCUU. However, similar calcium depositions were found when we used absorbable sutures for surgery in two other rats. Thus, in our case, the formation of calcium stones would be motivated by the substantial insult to the bladder tissue while suturing (causing bloody voids within the first week) leading to bladders inability to empty itself fully. Although the formation of caliculi can also be considered as inherent drawbacks of augmentation cystoplasty in rat models (121), the rat model has several advantages which include low cost of purchase and maintenance and rapid regeneration of the bladder upon surgery. However, to gain more clinically relevant data and FDA approval of the bladder tissue engineering scaffold, it is necessary to conduct large animal testing as the bladders of large animals such as pigs resemble the mechanics (ultimate tensile strength and elastic modulus) and ECM composition (Higher density of

type III collagen and lower density of type I collagen) of human bladders (50). In addition, in dogs and pigs, normal bladder capacities are reached after augmentation unlike rats and rabbits where surgery leads to larger bladder volume and bladder stones (119).Thus, future *in vivo* studies should focus on developing a pig BOO model to evaluate the PCUU technology and further advance bladder tissue engineering .

Chapter 7

Conclusions

7.1 Tetronic-based Composite Hydrogel scaffolds seeded with Bladder Smooth Muscle Cells for Urinary Bladder Tissue Engineering Applications

In the present study, we explored tetronic-based composite hydrogel scaffolds seeded with BSMC for urinary bladder tissue engineering applications. The results of in vitro experiments demonstrated that the composite hydrogel system provided an environment for bladder smooth muscle cells to adhere, migrate and secrete ECM, thereby increasing the construct's overall strength and stiffness. To date, however, BSMC-seeded composite hydrogel at the end of the two-week culture is still weaker and more compliant compared to the native urinary bladder tissue (122). We hypothesize that culturing the construct for longer time periods after BSMC seeding and addition of growth factors to the composite hydrogel system would further aid in increasing the strength and stiffness of the composite hydrogel scaffold. Overall, this was the first study to explore the use of hydrogel blends composed of Tetronic T1107-acrylate (T1107A) in combination with type I collagen and HA towards applications in urinary bladder tissue engineering (122).

7.2 *In vitro* characterization of biodegradable elastomers for application in bladder tissue engineering

We characterized various biodegradable elastomers as scaffolds for bladder tissue engineering since the mechanical properties of our cell-seeded composite hydrogels were limited after two weeks of culture. The comparison of mechanical behaviors of these elastomeric scaffolds demonstrated that the PCUU scaffolds mimicked urinary bladder mechanics compared to PGS-PCL and PEUU. The PCUU scaffolds exhibit relatively high compliance under low forces and are able to withstand stress corresponding to 100 kPa (super physiological peak stress experienced by urinary bladders *in vivo*) and thus, possess the strength and stiffness necessary to be used as a urinary bladder tissue engineering scaffold. The PCUU scaffolds also showed cyto-compatibility as well as increased porosity with increasing stretch indicating its ability to aid in infiltration of smooth muscle cells. Based on these findings, PCUU scaffolds were selected for subsequent studies using our custom-made bioreactor and an *in vivo* rat model for further characterization toward bladder tissue engineering applications.

7.3 Custom-made Bioreactor for conditioning of BSMC seeded PCUU scaffolds

The BSMC seeded PCUU scaffold was subjected to uniaxial mechanical stretch mimicking bladder cycling using our custom made bioreactor under standard cell culture conditions (37 °C, humidified, 5% CO_2 / 95% air). The BSMC seeded PCUU scaffolds when subjected to uniform and continuous stretch (1.25-1.75) uni-axially did not undergo failure in spite of high stretch and indicated its suitability to be used *in vivo*. Our study could enhance BSMC adhesion and infiltration into the PCUU scaffold with time by

112

coating the scaffolds with proteins (fibronectin and gelatin) using the layer by layer method (113) and could demonstrate the continued adhesion of the BSMC after a cycle of stretch (1.25). Future experiments, can characterize the BSMC seeded PCUU in multiple cycles and higher values of stretch (closer to maximum physiological stretch). Overall, the study tried to characterize PCUU in conditions mimicking bladder cycling and indicated its suitability for *in vivo* experimentation.

7.4 *In vivo* study examining PCUU scaffolds in bladder augmentation

Despite early promises of bladder tissue engineering, a recent report of unsuccessful clinical trials (74) suggests that the technology needs further improvement and evaluation through animal models of bladder dysfunction (119). Thus, our in *vivo* study was an attempt at implanting electrospun fibrous PCUU scaffolds onto a bladder outlet obstruction (BOO) rat model to create a clinically informative study. The BOO bladders tend to exhibit overactive bladder symptoms with high pressure and voiding frequency and, if untreated, can often lead to death of the rats due to vesicoureteral reflex. The PCUU implantation led to the enhanced survival of the rats (66.66%) and increased bladder capacity and voiding volume with time, indicating that the high pressure bladder symptom was alleviated. The histological analysis of the explanted scaffold indicated some smooth muscle cell and connective tissue infiltration, but also calcium deposits. We hypothesize that ECM-coating and pre-seeding PCUU scaffolds with cells can aid in promoting faster scaffold integration into the host bladder. Due to inherent tendency of stone formation in rat models, future studies may switch to using dysfunctional bladder

models of larger animal like pigs. However, the present study is one of the first to analyze a synthetic bladder scaffold using a bladder dysfunction model in rats for application in urinary bladder tissue engineering.

7.5 Summary

The present study characterized composite hydrogel and elastomeric scaffolds for bladder tissue engineering applications. Based on the results of *in vitro* mechanical characterization and cell culture studies, we concluded that PCUU scaffolds were the most ideal among the ones we examined. For the first time, we used an established rat model for studying bladder dysfunction (BOO) to evaluate the effect of augmentation of the bladder with PCUU scaffolds on bladder capacity and voiding volume. However, further research as recommended below is necessary to advance our understanding of PCUU scaffolds to ultimately aide in the treatment of bladder disorders.

7.6 Limitations of the Present Study and Future Project Recommendations

o Limitation: The BSMC seeded composite hydrogels do not possess the strength and stiffness of the native urinary bladder

    o Recommended solution: The strength and stiffness of the composite hydrogels may be improved by promoting cross-linking of the newly synthesized collagen by culturing the composite hydrogels for longer time

periods and/or in the presence of soluble chemical compounds such as insulin and TGF-β1.

- o Limitation: The investigation of the effect of stretch on BSMC-seeded PCUU^{FN-G} scaffolds using our custom made bioreactor was limited to results from 25% stretch conditions due to extensive cell expansion time required to obtain rat BSMC

  - o Recommended solution: Adipose derived stem cells (ADSC) and other adult stem cells can be used as an alternate cell source as it is multipotent, easy to procure, vastly available and has been shown to differentiate into smooth muscle cells.

- o Limitation: The cell infiltration into the PCUU scaffolds after 3 weeks of implantation was limited to smooth muscle cells near the edge of the PCUU construct and fibroblasts sparsely populating the rest of the scaffold.

  - o Recommended solution: Pre-seeding PCUU^{FN-G} scaffolds with ADSC/BSMC before implantation will help in reducing fibroblast ingrowth and the neo-smooth muscle tissue would aid in integrating with smooth muscle layer of host animal

- o Limitation: The presence of calcium deposits in the PCUU scaffold because of the propensity of the rat bladders to form caliculi

  - o Recommended solution: Although caliculi formation is an inherent problem with the rat model when implanted with a scaffold, some steps can be taken to further minimize it. As reported in the study by Seth et al., increasing the

compliance of PCUU $^{FN-G}$ scaffolds further may reduce caliculi formation after implantation(6). This can be achieved by increasing the media added to the pre-electrospun PCUU mix. As an added benefit, the increased compliance will further bring down the mechanical mismatch with the native bladder and lead to more efficient removal of urine from the bladder. Moreover, pre-seeding PCUU^{FN-G} scaffolds with ADSC/BSMC can form a neo-smooth muscle layer before the scaffold is implanted into the body and may integrate more efficiently into the bladder and help reduce stone formation. The caliculi formation can also be reduced by various anti-calcification treatments. Future experiments can be performed in the PCUU sutured bladders where disodiumethylenediaminetetraacetic acid (EDTA) can be loaded in PLGA nanoparticle pellets and placed periadventitially to minimize caliculi formation as shown in studies by Lei et al. where controlled release of EDTA led to regression of elastin specific calcification in the aorta (123).

REFERENCES

1. Gray H, Howden R. Anatomy, descriptive and applied. Longmans, Green; 1916.

2. Seeley R, Stephens T, Tate P, editors. Anatomy & Physiology. fifth ed. Mcgraw-Hill Higher Education; 2000.

3. Hakenberg OW., LinneC, Manseck A, and Wirth MP. Bladder wall thickness in normal adults and men with mild lower urinary tract symptoms and benign prostatic enlargement. Neurourol Urodyn. 2000;19(5):585-93.

4. Turner AM, Subramaniam R, Thomas DFM, Southgate J. Bladder Tissue Engineering. Tissue Engineering using ceramics and polymers. 2007:445-459.

5. Lewis SA. Everything you wanted to know about the bladder epithelium but were afraid to ask. American journal of Physiology.Renal Physiology. 2000(6).

6. Deveaud CM, Macarak EJ, Kucich U, Ewalt DH, Abrams WR, and Howard PS. Molecular analysis of collagens in bladder fibrosis. J Urol. 1998;160(4):1518.

7. Korossis S, Bolland F, Ingham E, Fisher J, Kearney J, and Southgate J. Tissue Engineering of the Urinary Bladder: Considering Structure-Function Relationships and the Role of Mechanotransduction. Review. Tissue Engineering. 2006;12(4):635-44.

8. Oelke M, Hafner K, Jonas U, Ubbink D, de la Rosette J, and Wijkstra H. Ultrasound measurement of detrusor wall thickness in healthy adults. Neurourol Urodyn. 2006;25(4):308-17.

9. Koenig F, Gonzalez S, White WM, Lein M, and Rajadhyaksha M. Near-infrared confocal laser scanning microscopy of bladder tissue in vivo. Urology. 1999(53):853.

10. Shier D, Butler J, Lewis R, editors. Hole's Human Anatomy & Physiology. 11th ed. New York: Mcgraw-Hill Higher Education; 2007.

11. Brook JD, editor. Campbell-Walsh Urology. 9th ed. Saunders, an imprint of Elvesier; 2007.

12. Adelöw CAM, Frey P. Synthetic Hydrogel Matrices for Guided Bladder Tissue Regeneration. . 2007 July;140.

13. Atala A, Bauer SB, Soker S, Yoo JJ, Retik AB. Tissue-engineered autologous bladders for patients needing cystoplasty. The Lancet. 2006;367(9518):1241.

14. Warren J, Pike JG, Leonard MP. Posterior urethral valves in Eastern Ontario - a 30 year perspective. Can J Urol. 2004 Apr;11(2):2210-5.

15. Kinsman SL, Johnston MV. Congenital anomalies of the central nervous system. In: Kliegman RM, Behrman RE, Jenson HB, Stanton BF, editors. *Nelson Textbook of Pediatrics*. Philadelphia, Pa: Saunders Elsevier; 2007. p. chap592.

16. Gearhart JP, Mathews R. Exstrophy-episadias complex: In: *Campbell-Walsh Urology*. Philadelphia, Pa: Saunders Elsevier; 2007. p. chapter19.

17. Elder JS. Anomalies of the bladder. In: Kliegman RM, Behrman RE, Jenson HB, Stanton BF, editors. *Nelson Textbook of Pediatrics*. Philadelphia, Pa: Saunders Elsevier; 2007. p. chap 541.

18. Wein AJ. Lower urinary tract dysfunction in neurologic injury and disease. In: Wein AJ, editor. Campbell-Walsh Urology.9th edition. Philadelphia, Pa: Saunders Elsevier; 2007.

19. Shamliyan TA, Kane RL, Wyman J ea. Systematic review: randomized, controlled trials of nonsurgical treatments for urinary incontinence in women. Ann Intern Med. 2008;148(6):459-73.

20. Holroyd-Leduc JM, Tannenbaum C, Thorpe KE ea. What type of urinary incontinence does this woman have? JAMA. 2008;299(12):1446-56.

21. Hanno PM. Painful bladder syndrome/ Intestinal cystisis and related disorders. In: Cambell-Walsh, Urology. Philadelphia, Pa: Saunders, an imprint of Elvesier; 2007.

22. Thrasher JB, Crawford ED. Current management of invasive and metastatic transitional cell carcinoma of the bladder. J Urol. 1993;149(5):957-72.

23. Housset M, Maulard C, Chretien Y ea. Combined radiation and chemotherapy for invasive transitional-cell carcinoma of the bladder: a prospective study. J Clin Oncol. 1993;11(11):2150-7.

24. Kachnic LA, Kaufman DS, Heney NM ea. Bladder preservation by combined modality therapy for invasive bladder cancer. J Clin Oncol. 1997;15(3):1022-9.

25. Raghavan D, Huben R. Management of bladder cancer. Curr Probl Cancer. 1995;19(1):1-64.

26. Thomas DF. Surgical treatment of urinary incontinence. Arch DIs Child. 1997;76:377-80.

27. Rao PK, Iverson AJ, Cespedes RD, and Sabanegh ES Jr. Augmentation Cystoplasty

. 2008.

28. Chun YW, Lim H, Webster TJ, Haberstroh KM. Nanostructured bladder tissue replacements. Wiley Interdisciplinary Reviews: Nanomedicine and Nanobiotechnology. 2011;3(2):134-45.

29. Cross WR, Thomas DFM, Southgate J. Tissue engineering and stem cell research in urology. British Journal of Urology International. 2003;92(2)::165-71.

30. Lima SVC, Araujo LAP, Vilar FO, Kummer CL, Lima EC. Nonsecretory intestinocystoplasty:a 10-year experience. journal of urology. 2004(171):2636-9,2639-40.

31. Hafez AT, Afshar K, Bagli DJ, Bahoric A, Aitken K, Smith CR, et al. Aerosal transfer of bladder urothelial and smooth muscle cells onto demucosalized colonic segments for porcine bladder augmentation in vivo: a 6 week experimental study. journal of urology. 2005(174):1663-7,1667-8.

32. Frazer M, Thomas DF, Pitt E, Harnden P, Trejdosiewicz L, and Southgate J. A surgical model of composite cystoplasty with cultured urothelial cells: a controlled study of gross outcome and urothelial phenotype. BJU international. 2004;93:609-16.

33. Dewan PA, Anderson P. Ureterocystoplasty: The latest developments. BJU international. 2008;88:744-51.

34. Free tissue transfer(n.d.) Gale Encyclopedia of Medicine [Internet].; (2008) [cited May 29 2011]. Available from: http://medical-dictionary.thefreedictionary.com/Free+tissue+transfer.

35. Schwenke-konig PSA, Hage JJ, and Kon M. Comparison of Rectus abdominis muscle and musculoperitoneal flap in closure of urinary bladder defects ina rat model. European journal of plastic surgery. 2004;27(5):233-237.

36. Savicky RS, Jackson AH. Use of a rectus abdominis muscle flap to repair urinary bladder and urethral defects in a dog. J Am Vet Med Assoc. 2009 Apr 15;234(8):1038-40.

37. Iijima K, Igawa Y, Imamura T, Moriizumi T, Nikaido T, Konishi I, et al. Transplantation of Preserved Human Amniotic Membrane for Bladder Augmentation in Rats. Tissue Engineering. 2007;13(3):513.

38. Badylak SF, Lantz GC, Coffey A, Geddes LA. Small intestinal submucosa as a large diameter vascular graft in the dog. journal of urology. 1989(155):2098-104.

39. Zhang Y, Kropp BP, Moore P, Cowan R, Furness PD 3rd, Kolligian ME, et al. Coculture of bladder urothelial and smooth muscle cells on small intestinal submucosa: potential applications for tissue engineering technology. journal of urology. 2000;164:928-935.

40. Vaught JD, Kropp BP, Sawyer BD, Rippy MK, Badylak SF, Shannon HE, et al. Detrusor regeneration in the rat using porcine small intestinal submucosal grafts: functional innervation and receptor expression. journal of urology. 1996;155:374-8.

41. Badylak S, Kropp B, McPherson T, Liang H, and Snyder P. Small intestional submucosa: a rapidly resorbed bioscaffold for augmentation cystoplasty in a dog model. Tissue Eng. 1998 Winter;4(4):379-87.

42. Kropp B, Cheng E, Lin H, and Zhang Y. Reliable and reproducible bladder regeneration using unseeded distal small intestinal submucosa. J Urol. 2004 Oct;172(4 Pt 2):1710-3.

43. Brown AL, Farhat W, Merguerian PA, Wilson GJ, Khoury AE, and Woodhouse KA. 22 Week Assessment of Bladder Acellular Matrix as a Bladder Augmentation Material in a Porcine Model. Biomaterials. 2002 May;23(10):2179-90.

44. Farhat WA, Chen J, Haig J, Antoon R, Litman J, Sherman C, et al. Porcine bladder acellular matrix (ACM): protein expression, mechanical properties. Biomed Mater. 2008 Jun;3(2):025015.

45. Roth C, Kropp B. Recent Advances in Urologic Tissue Engineering. Current urology reports. 2009:119-25.

46. Oberpenning F, Meng J, Yoo JJ, Atala A. De novo reconstitution of a functional mammalian urinary bladder by tissue engineering. nature biotechnology. 1998;17:149-155.

47. Eberli D, Filho LF, Atala A, Yoo JJ. Composite scaffolds for the engineering of hollow organs and tissues. Methods. 2009 2;47(2):109-15.

48. Rohman G, Pettit JJ, Isaure F, Cameron NR, and Southgate J. Influence of the physical properties of two-dimensional polyester substrates on the growth of normal human urothelial and urinary smooth muscle cells in vitro. Biomaterials. 2007 May;28(14):2264-74.

49. Baker SC, Rohman G, Southgate J, Cameron NR. The relationship between the mechanical properties and cell behaviour on PLGA and PCL scaffolds for bladder tissue engineering. biomaterials. 2009(30):1321-1328.

50. Dahms SE, Piechota HJ, Dahiya R, Lue TF, Tanagho EA. Composition and biomechanical properties of the bladder acellular matrix graft: comparative analysis in rat, pig and human. Br J Urol. 1998 Sep;82(3):411-9.

51. Zhang Y, Kropp BP, Ling HK, Cowan R, Cheng EY. Bladder Regeneration with Cell-Seeded Small Intestinal Submucosa. Tissue Engineering. 2004;10:181-187.

52. Drury JL, Mooney DJ. Hydrogels for tissue engineering: scaffold design variables and applications. Biomaterials. 2003;24:4337–4351.

53. French AC, Thompson AL, and Davis BG. High-purity discrete PEG-oligomer crystals allow structural insight. Angew Chem Int Ed Engl. 2009;48(7):1248-52.

54. Tessmar J.K, and Gopferich A.M. Customized PEG derived co-polymers for tissue engineering applications. Macromolecular Biosciences. 2007;7:23-39.

55. Adelow C, Segura T, Hubbell JA, and Frey P. The effect of enzymatically degradable poly(ethylene glycol) hydrogels on smooth muscle cell phenotype. Biomaterials. 2008;29(3):314-326.

56. Thapa A, Miller DC, Webster TJ, Haberstroh KM. Nanostructured polymers enhance bladder smooth muscle cell function. Biomaterials. 2003(24):2915–2926.

57. Pattison MA, Wurster S, Webster TJ, Haberstroh KM. Three-dimensional, nano-structured PLGA scaffolds for bladder tissue replacement applications. Biomaterials. 2005(26):2491–2500.

58. Chun YW, Lim H, Webster TJ, Haberstroh KM. Nanostructured bladder tissue replacements. Nanomedicine and Nanotechnology. 2010;3(2):134-145.

59. Kleinman HK, Philp D, and Hoffman MP. Role of the extracellular matrix in morphogenesis. Curr Opin Biotech. 2003;30:526–532.

60. Cooke MJ, Philips SR, Shah DSH, Athey D LJ, Przyborski SA. Enhanced cell attachment using a novel cell culture surface presenting functional domains from extracellular matrix proteins. Cytotechnology. 2008;56:71–79.

61. Long-Heise R, Ivanova J, Parekh A, Sacks MS. Generating elastin rich SIS-based smooth muscle constructs utilizing exogenous growth factors and cyclic mechanical stimulation. Tissue Engineering part A. 2009;15(12):3951-60.

62. Roby T, Olsen S, Nagatomi J. Effect of sustained tension on bladder smooth muscle cells in three-dimensional culture. Ann Biomed Eng. 2008 Oct;36(10):1744-51.

63. Zhang Y, Frimberger D, Cheng EY, Lin HK, and Kropp BP. Challenges in a larger bladder replacement with cell-seeded and unseeded small intestinal submucosa grafts in a subtotal cystectomy model. BJU Int. 2006 Nov;98(5):1100-5.

64. Wang Y, Kim HJ, Vunjak-Novakovic G, and Kaplan DL. Stem cell-based tissue engineering with silk biomaterials. Biomaterials. 2006 Dec;27(36):6064-82.

65. Lovett ML, Cannizzaro CM, Vunjak-Novakovic G, Kaplan DL. Gel Spinning of silk tubes for tissue engineering. biomaterials. 2008;29(35):4650-57.

66. Mauney JR, Cannon GM, Lovett ML, Gong EM, Vizio DD, Gomez P 3rd, et al. Evaluation of gel spun silk-based biomaterials in a murine model of bladder augmentation. biomaterials. 2011(32):808-818.

67. Jack GS, Zhang R, Lee M, Xu Y, Wu BM, and Rodriguez LV. Urinary bladder smooth muscle engineered from adipose stem cells and a three dimensional synthetic composite. Biomaterials. 2009 Jul;30(19):3259-70.

68. Li ST, editor. Biologic biomaterials : tissue derived biomaterials (Collagen) The Biomedical Engineering Handbook. Boca RAton ,FL: CRS Press; 1995.

69. Engelhardt EM, Stegberg E, Brown RA, Hubell JA, Wurm FM, Adam M, et al. compressed collagen gel: a novel scaffold for human bladder cells. journal of tissue engineering and regenerative medicine. 2010;4:123-130.

70. Cen L, Liu W, Cui L. Collagen tissue engineering :development of novel biomaterials and applications. pediatrics research. 2008;63:492-6.

71. Brown RA, Wiseman M, Chuo CB, Cheema U, and Nazhat SN. Ultrarapid Engineering of Biomimetic materials and tissues:Fabrication of Nano- And Microstructures by plastic compression. Advanced functional materials. 2005;15:1762-1770.

72. Engelhardt EM, Micol LA, Houis S, Wurm FM, Hillborn J, Hubbell JA, et al. A collagen-poly (lactic acid-co-ε-caprolactone) hybrid scaffold for application in bladder tissue regeneration. Biomaterials. 2011;32(16):3969-76.

73. Sivaraman S, Nagatomi J. Polymer-based scaffolds for urinary bladder tissue engineering. In: Shalaby SW, Burg KJ, Shalaby W, editors. Polymers for vascular and urogenital applications. Florida ,USA: CRC press; 2012. p. 175-200.

74. Joseph DB, Borer JG, De Filippo RE, Hodges SJ, McLorie GA. Autologous Cell Seeded Biodegradable Scaffold for Augmentation Cystoplasty: Phase II Study in Children and Adolescents with Spina Bifida. J Urol. 2014 5;191(5):1389-95.

75. Annor A, Tang M, Pui C, Ebersole G, Frisella M, Matthews B, et al. Effect of enzymatic degradation on the mechanical properties of biological scaffold materials. Surg Endosc. 2012;26(10):2767-78.

76. Lovett ML, Cannizzaro CM, Vunjak-Novakovic G, Kaplan DL. Gel spinning of silk tubes for tissue engineering. Biomaterials. 2008 12;29(35):4650-7.

77. DeKosky BJ, Detamore MS, Dormer NH, Gehrke SH, Ingavle GC, Lomakin J, et al. Hierarchically designed agarose and poly(ethylene glycol) interpenetrating network hydrogels for cartilage tissue engineering. Tissue Engineering, Part C: Methods. 2010 12; 2014/7;16:1533+.

78. Park Y, Lutolf M, Hubell J, Hunziker E, Wong M. Bovine primary chondrocyte culture in synthetic matrix mettalloproteinase-sensitive poly (ethylene glycol)- based hydrogels as a scaffold for cartilae repair. Tissue Engineering. 2004;10(3):515-521.

79. Brandl FP, Seitz AK, TeÃŸmar JKV, Blunk T, GÃ¶pferich AM. Enzymatically degradable poly(ethylene glycol) based hydrogels for adipose tissue engineering. Biomaterials. 2010 /5;31(14):3957-66.

80. Sosnik A, Sefton MA. Semi-Synthetic collagen/poloxamine matrices for tissue engineering. biomaterials. 2005(26):7425-35.

81. Kutty JK, Cho E, Soo Lee J, Vyavahare NR, Webb K. The effect of hyaluronic acid incorporation on fibroblast spreading and proliferation within PEG-diacrylate based semi-interpenetrating networks. Biomaterials. 2007 11;28(33):4928-38.

82. Cho E, Lee JS, Webb K. Formulation and characterization of poloxamine-based hydrogels as tissue sealants. Acta Biomaterialia. 2012(0):-.

83. Blumenkrantz N, Asboe-Hansen G. An assay for hydroxyproline and proline on one sample and a simplified method for hydroxyproline. Anal Biochem. 1975 /2;63(2):331-40.

84. Cho E, Lee JS, Webb K. Formulation and characterization of poloxamine-based hydrogels as tissue sealants. Acta Biomaterialia. 2012 7;8(6):2223-32.

85. Hiremath J, Vishalakshi B. Effect of Crosslinking on swelling behaviour of IPN hydrogels of Guar Gum & Polyacrylamide. Der Pharma Chemica,. 2012;4(3):946-955.

86. Suri S, Schmidt CE. Photopatterned collagen–hyaluronic acid interpenetrating polymer network hydrogels. Acta Biomaterialia. 2009 9;5(7):2385-97.

87. Donati I, Paoletti S. Material properties of alginates. In: Rehm B, editor. Alginates: Biology and Applications: Biology and Applications. Springer; 2009. p. 40.

88. Kim J, Kim IS, Cho TH, Kim HC, Yoon SJ, Choi J, et al. In vivo evaluation of MMP sensitive high-molecular weight HA-based hydrogels for bone tissue engineering. Journal of Biomedical Materials Research Part A. 2010;95A(3):673-81.

89. Shi Y, Vesely I. Characterization of statically loaded tissue-engineered mitral valve chordae tendineae. Journal of Biomedical Materials Research Part A. 2004;69A(1):26-39.

90. Venkatraman L, Ramamurthi R. Induced elastic matrix deposition within three-dimensional collagen scaffolds. Tissue Engineering part A. 2011;17(22):2879-2889.

91. Stevenson K, Kucich U, Whitbeck C, Levin R, Howard P. Functional changes in bladder tissue from type III collagen-deficient mice. Mol Cell Biochem. 2006;283(1-2):107-14.

92. Nagatomi J, Gloeckner DC, Chancellor M, deGroat W, Sacks M. Changes in the Biaxial Viscoelastic Response of the Urinary Bladder Following Spinal Cord Injury. Ann Biomed Eng. 2004;32(10):1409-19.

93. Ross JJ, Tranquillo RT. \ECM\ gene expression correlates with in vitro tissue growth and development in fibrin gel remodeled by neonatal smooth muscle cells. Matrix Biology. 2003;22(6):477.

94. Berglund JD, Mohseni MM, Nerem RM, Sambanis A. A biological hybrid model for collagen-based tissue engineered vascular constructs. Biomaterials. 2003 3;24(7):1241-54.

95. Grassl ED, Oegema TR, Tranquillo RT. A fibrin-based arterial media equivalent. Journal of Biomedical Materials Research Part A. 2003;66A(3):550-61.

96. Sant S, Iyer D, Gaharwar AK, Patel A, Khademhosseini A. Effect of biodegradation and de novo matrix synthesis on the mechanical properties of valvular interstitial cell-seeded polyglycerol sebacate–polycaprolactone scaffolds. Acta Biomaterialia. 2013 4;9(4):5963-73.

97. Hong Y, Guan J, Fujimoto KL, Hashizume R, Pelinescu AL, Wagner WR. Tailoring the degradation kinetics of poly(ester carbonate urethane)urea thermoplastic elastomers for tissue engineering scaffolds. Biomaterials. 2010 5;31(15):4249-58.

98. Sant S, Hwang CM, Lee S, Khademhosseini A. Hybrid PGS?PCL microfibrous scaffolds with improved mechanical and biological properties. Journal of Tissue Engineering and Regenerative Medicine. 2011;5(4):283-91.

99. Sant S, Iyer D, Gaharwar AK, Patel A, Khademhosseini A. Effect of biodegradation and de novo matrix synthesis on the mechanical properties of valvular interstitial cell-seeded polyglycerol sebacate–polycaprolactone scaffolds. Acta Biomaterialia. 2013 4;9(4):5963-73.

100. Courtney T, Sacks MS, Stankus J, Guan J, Wagner WR. Design and analysis of tissue engineering scaffolds that mimic soft tissue mechanical anisotropy. Biomaterials. 2006 7;27(19):3631-8.

101. Stankus JJ, Soletti L, Fujimoto K, Hong Y, Vorp DA, Wagner WR. Fabrication of cell microintegrated blood vessel constructs through electrohydrodynamic atomization. Biomaterials. 2007 6;28(17):2738-46.

102. Fujimoto KL, Tobita K, Merryman WD, Guan J, Momoi N, Stolz DB, et al. An Elastic, Biodegradable Cardiac Patch Induces Contractile Smooth Muscle and Improves Cardiac Remodeling and Function in Subacute Myocardial Infarction. J Am Coll Cardiol. 2007 6/12;49(23):2292-300.

103. Sant S, Khademhosseini A. Fabrication and Characterization of Tough Elastomeric Fibrous Scaffolds for Tissue Engineering Applications. Conference proceedings : ...Annual International Conference of the IEEE Engineering in Medicine and Biology Society.IEEE Engineering in Medicine and Biology Society.Conference. 2010;2010:3546-8.

104. Khurana I. Excretory system. In: Pathak R, Nasim S, editors. Essentials of medical physiology. ; 2008. p. 339.

105. Fujimoto KL, Tobita K, Merryman WD, Guan J, Momoi N, Stolz DB, et al. An Elastic, Biodegradable Cardiac Patch Induces Contractile Smooth Muscle and Improves Cardiac Remodeling and Function in Subacute Myocardial Infarction. J Am Coll Cardiol. 2007 6/12;49(23):2292-300.

106. Fujimoto KL, Guan J, Oshima H, Sakai T, Wagner WR. In Vivo Evaluation of a Porous, Elastic, Biodegradable Patch for Reconstructive Cardiac Procedures. Ann Thorac Surg. 2007 02/01;83(2):648-54.

107. Amoroso NJ, D'Amore A, Hong Y, Rivera CP, Sacks MS, Wagner WR. Microstructural manipulation of electrospun scaffolds for specific bending stiffness for heart valve tissue engineering. Acta Biomaterialia. 2012 12;8(12):4268-77.

108. Hashizume R, Fujimoto KL, Hong Y, Amoroso NJ, Tobita K, Miki T, et al. Morphological and mechanical characteristics of the reconstructed rat abdominal wall following use of a wet electrospun biodegradable polyurethane elastomer scaffold. Biomaterials. 2010 4;31(12):3253-65.

109. GLOECKNER DC, SACKS MS, FRASER MO, SOMOGYI GT, de GROAT WC, CHANCELLOR MB. Passive Biaxial Mechanical Properties of the Rat Bladder Wall After Spinal Cord Injury. J Urol. 2002 5;167(5):2247-52.

110. Sanders L, Stone R, Webb K, Mefford T, Nagatomi J. Mechanical characterization of a bifunctional Tetronic hydrogel adhesive for soft tissues. Journal of Biomedical Materials Research Part A. 2015;103(3):861-8.

111. A tissue engineering challenge. In: Fisher JP, Mikos AG, Bronzino J, editors. Tissue engineering. Taylor and Francis Group; 2007. p. 25-6.

112. Bai F, Wang Z, Lu J, Liu J, Chen G, Lv R, et al. The Correlation Between the Internal Structure and Vascularization of Controllable Porous Bioceramic Materials In Vivo: A Quantitative Study. Tissue Engineering Part A. December 2010;16(12):3791-3803.

113. Hubschmid U, Leong-Morgenthaler P, Dardare A, Ruault S, Frey P. In Vitro Growth of Human Urinary Tract Smooth Muscle Cells on Laminin and Collagen Type I-Coated Membranes under Static and Dynamic Conditions. Tissue Engineering. 2005;11(1-2):161-171.

114. Seltzer E, Tillinger M, Jayo MJ, Bertram TA. Role of biomechanical stimulation (cycling) in neo-bladder regeneration-translational basis for clinical outcomes. J Urol. 2009;181(4):282.

115. Heise R, Parekh A, Joyce E, Chancellor M, Sacks M. Strain history and TGF-β1 induce urinary bladder wall smooth muscle remodeling and elastogenesis. Biomechanics and Modeling in Mechanobiology. 2012;11(1-2):131-45.

116. Parekh A, Cigan AD, Wognum S, Heise RL, Chancellor MB, Sacks MS. Ex vivo deformations of the urinary bladder wall during whole bladder filling: Contributions of extracellular matrix and smooth muscle. J Biomech. 2010 6/18;43(9):1708-16.

117. Haberstroh KM, Kaefer M, DePaola N, Frommer SA, Bizios R. A Novel In-Vitro System for the Simultaneous Exposure of Bladder Smooth Muscle Cells to Mechanical Strain and Sustained Hydrostatic Pressure. Journal of Biomechanical Engineering. 2002 March 29;124(2):208-13.

118. Srouji S, Kizhner T, Suss-Tobi E, Livne E, Zussman E. 3-D Nanofibrous electrospun multilayered construct is an alternative ECM mimicking scaffold. J Mater Sci Mater Med. 2008;19(3):1249-55.

119. Sloff M, Simaioforidis V, de Vries R, Oosterwijk E, Feitz W. Tissue Engineering of the Bladder—Reality or Myth? A Systematic Review. J Urol. 2014 10;192(4):1035-42.

120. Kim JH, Lee HJ, Song YS. Treatment of Bladder Dysfunction Using Stem Cell or Tissue Engineering Technique. Korean J Urol. 2014 /4/;55(4):228-38.

121. Seth A, Chung YG, Gil ES, Tu D, Franck D, Di Vizio D, et al. The performance of silk scaffolds in a rat model of augmentation cystoplasty. Biomaterials. 2013 7;34(20):4758-65.

122. Sivaraman S, Ostendorff R, Fleishman B, Nagatomi J. Tetronic®-based composite hydrogel scaffolds seeded with rat bladder smooth muscle cells for urinary bladder tissue engineering applications. Journal of Biomaterials Science, Polymer Edition. 2015 02/11; 2015/04;26(3):196-210.

123. Lei Y, Grover A, Sinha A, Vyavahare N. Efficacy of Reversal of Aortic Calcification by Chelating Agents. Calcif Tissue Int. 2013;93(5):426-35.